DOCTORAL DISSERTATION

Construction of a dual display phage and its applications on real-time label-free biosensing platforms

Doctoral dissertation submitted to obtain the degree of
Doctor of Biomedical Science, to be defended by

Kaushik Rajaram

Promoter: Prof. Dr Luc Michiels
Co-promoter: Prof. Dr Veerle Somers

universiteit
►►hasselt | BIOMED
BIOMEDISCH
ONDERZOEKSINSTITUUT

Members of the jury

Prof. dr. I. Lambrichts, Universiteit Hasselt, Diepenbeek, Belgium, chairman

Prof. dr. L. Michiels, Universiteit Hasselt, Diepenbeek, Belgium, promoter
Prof. dr. V. Somers, Universiteit Hasselt, Diepenbeek, Belgium, copromoter

Prof. dr. M. Ameloot, Universiteit Hasselt, Diepenbeek, Belgium
Prof. dr. W. Guedens, Universiteit Hasselt, Diepenbeek, Belgium
Prof. dr. P. Wagner, Katholieke Universiteit, Leuven, Belgium
Prof. dr. P. Dubruel, Universiteit Gent, Gent, Belgium
Prof. dr. B. Van Grinsven, Universiteit Maastricht, Maastricht, The Netherlands
dr. V. Vermeeren, Universiteit Hasselt, Diepenbeek, Belgium
dr. K. Somers, Children's Cancer Institute, South Wales, Australia

Table of Contents

List of Figures

List of Tables

List of Abbreviations

ACPA   Anti-Cyclic Citrullinated Peptide Antibodies

AFM   Atomic Force Microscopy

Bp   Base Pairs

CB   Empty phage

CCP   Cyclic Citrullinated Peptide

cDNA   Complementary Deoxyribonucleic Acid

Cfu   Colony Forming Unit

CP   Unmodified M13cp helper plasmid (without SBP)

CR21   Single display phage displaying UH_RA.21

CVD   Chemical Vapour Deposition

DNA   Deoxyribonucleic Acid

EDC   1-ethyl-3-(3-dimethylaminopropyl) Carbodiimide

ELISA Enzyme Linked Immunosorbent Assay

FET   Field Effective Transistors

HRP   Horse Radish Peroxidase

HTM   Heat Transfer Method

IgG   Immunoglobulin

IL   Interleukin

MHC   Major Histocompatibility Complex

MPBS   Marvel PBS

mRNA   Messenger Ribonucleic Acid

NCD   Nanocrystalline Diamond

NHS   N-Hydroxysulfosuccinimide

PBS   Phosphate Buffered Saline

PCR   Polymerase Chain Reaction

PSPB   Unmodified phagemid (without UH_RA.21)

QCM-D Quartz Crystal Microbalance with Dissipation Monitoring

RA   Rheumatoid Arthritis

RF   Rheumatoid Factor

Rth   Heat Transfer Resistance

RU   Response Unit

SAS   Serological Antigen Selection

SB   Single display phage displaying SBP

SBP   Streptavidin Binding Protein

SPR   Surface Plasmon Resonance

SMCC   Sulfosuccinimidyl 4-(N- maleimidomethyl) cyclohexane-1-
            carboxylate

SR21   Dual display phage displaying SBP and UH_RA.21

ssDNA   Single Stranded Deoxyribonucleic Acid

STD   Standard

STD 21 Standard or conventional single display phage displaying UH_RA.21

STV   Streptavidin

TNF α   Tumour Necrosis Factor α

1

General introduction and aims

1.1 Introduction to biosensors

In recent years, biosensors have gained enormous attention in medicine and certainly in e-health and nanotechnology. There is indeed a growing interest in their application in tissue engineering, disease diagnosis and regenerative medicine (Hasan A et al, 2014). A biosensor is a biochemical analytical device in which a biologically derived ligand molecule is coupled to a physicochemical detector. The analyte that binds to the ligand will generate a readable detector signal that corresponds to the presence or even the concentration of the targeted analyte in the sample (Amanda et al, 2002; Garipcan B et al, 2011; Rapp BE et al, 2010 and Singh et al, 2013). The design and development of biosensors requires an interdisciplinary collaboration of researchers from different scientific fields such as biomedical sciences, chemistry, physics and engineering science. A typical biosensor consists of three important components including a bio-receptor molecule, a transducer and an output system with a detector and a readable monitor. The existing demand for a suitable biosensor is not restricted to disease diagnostics. It also extends to environmental monitoring, the detection of pathogens in food and even in tracing possible bioterrorism attacks (Mao C et al, 2009 and Hasan A et al, 2014). Furthermore, biosensors are also playing a crucial role in microfluidic tissue engineering models, where they are used to detect specific biological molecules within the miniaturized tissue constructs in real-time, at very low concentration levels using ultrasensitive sensing systems (Hasan A et al, 2014). A schematic representation of the working principles of biosensors is shown in Figure 1.1.

In the future, biosensors will become cost effective analytical tools used for acquiring critical diagnostic information for many disorders. This is already in use as a major diagnostic biosensor-based tool to monitor blood glucose concentrations in diabetic patients (Yoo EH et al, 2010). The successful wide spread use of biosensors will greatly benefit public health systems and the general public. The business opportunities for this rapid growing technological field are enormous especially if the novel systems and processes are becoming validated and standardized.

Bioreceptors   Transducers   Detectors
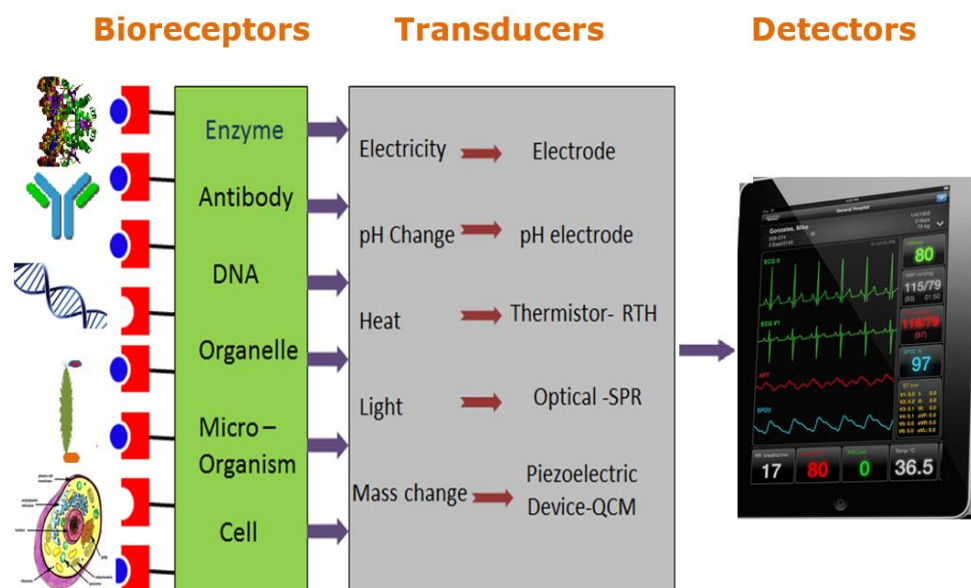
Figure 1.1 Schematic representation of a biosensor and its major components

Examples of the major components of biosensors in terms of bioreceptors and transducers are shown.

1.1.1 History of biosensor development

Most frequently biosensors are developed for medical applications (Turner et al, 2013), though the first biosensors, canary birds, were used in coal mines since 1911 to monitor the presence of the dangerous mine gas (Garipcan B et al, 2011). In 1962, Dr. Clark (University of Rochester, USA) made his first amperometric enzymatic biosensor for the detection of glucose (Yoo EH et al, 2010). These sensors were based on chemical sensing devices, such as glass electrodes for sensing the hydrogen ion concentration and oxygen electrodes. He has been considered as the father of the biosensor concept. After his historic milestone work, numerous studies were performed to monitor the interaction of biomolecules such as DNA, antibodies with their biological targets including enzymes, cells, viruses etc... on biosensor platforms.

Until the middle of the 1970s, the detection principle of enzyme sensors was largely based on the re-oxidation of hydrogen peroxide (H_2O_2) and these sensors

were known as the first generation enzymatic sensors. In the late 1970s, a second generation of enzymatic sensors was developed. These sensors make use of soluble electron mediators in the electrolyte to facilitate the mass transport between the electrode surface and the enzyme active site, thereby reducing the interference of non-specific analytes. Amperometric glucose biosensors work with this principle (Putzbach W et al, 2013). The third generation enzymatic sensor developed in the 1980s also came with electron mediators and enzymes but co-immobilized onto the electrode's surface instead of freely diffusing in the electrolyte. These sensors allow for repeated measurements and therefore minimize the biosensor cost. In 1983, Dr. Liedberg and his colleagues developed a technique in which real-time monitoring of affinity reactions was achieved using Surface Plasmon Resonance (SPR). This technology is still considered as a golden standard and high sensitive technique in biosensor applications. Nevertheless, in the recent era, nanotechnology and quantum dots based emerging novel biosensing principles and devices (such as metal nanoparticles based localized SPR- SoPRano technology of Pharma diagnostics, Belgium) have been described as being accurate, sensitive and reliable biosensors (Yogeswaran U et al, 2008 and Goshal S et al, 2010). The flowchart in Figure 1.2 summarizes the history of the development of biosensors in the last decades.
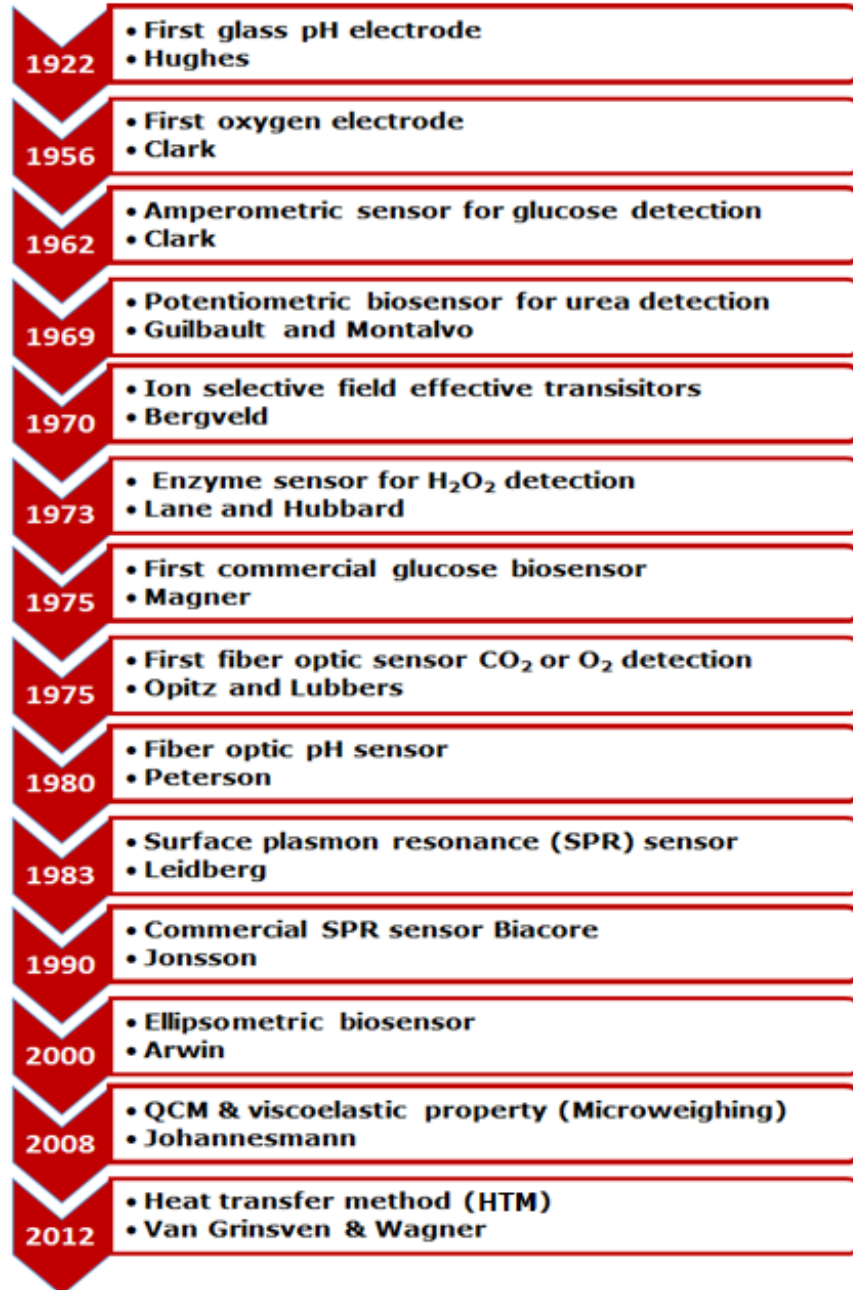
Figure 1.2 Historical overview of biosensor developments

Major advances in biosensor development in the last decades are shown in the time table.

1.1.2 Characteristics of a good biosensor

The following features are considered as the most important characteristics of an efficient biosensor device (Ivnitski et al, 1999).

Specificity or selectivity: Selectivity is defined as the extent to which a method can determine particular analytes in mixtures or matrices interference by other components. In this way a successful biosensor should provide a very specific interaction between the ligand and the analyte even in differentiating analogues and it should not react to admixtures and contaminants.

Sensitivity vs Detection limit: Sensitivity is the ability of a sensor to detect a target analyte (e.g.: an antibody/antigen), which is usually expressed as the minimum detectable concentration of the analyte. A biosensor should therefore be able to detect as low concentrations of target molecules as possible.

Response time: The time required to have a 95% response should be rapid and accurate. Results should be obtained within the timescale of the regular process/diagnosis.

Linearity: The values in a response curve from higher substrate concentration to a lower concentration should be linear.

Cost: It should be cheap to produce biosensors in large numbers using readily available raw materials.

Size: The sensing device should be sufficient small to allow for the construction of a portable device, eventually with a low maintenance cost. (Owen TW et al, 2007).

Reproducibility: Biosensors should have the ability of duplicating the entire experiment in the same conditions within acceptable drift or scatter in a series of observations or results.

Reliability: Is the overall consistency of a measurement in producing similar results under similar conditions.

The stability and sensitivity of a biosensor rely upon the biological ligand (bioreceptors) molecule and its coupling chemistry with the transducer's surface. Bioreceptor molecules can be nucleic acids, peptides, polysaccharides, antibodies (immuno sensor), tissues, cells, enzymes or microorganisms (Phage or virus sensors) (Figure 1.1). Peptides and nucleic acids are most frequently used as probes or ligands in biosensors (Dover JE et al, 2009). A logical classification of

biosensors can be made according to the type of the transducer and the sensing method that is used (Garipcan B et al, 2011).

1.2 Bioreceptor molecules and substrates used in biosensors

The immobilized bioreceptor molecules or biosensing components define the specificity and the type of biosensor. In a catalytic-based enzyme biosensor, enzymes recognize their substrate and convert them into a reaction product. In the affinity biosensors, recognition takes place via the formation of an affinity complex. Affinity-based biosensors in most cases make use of antibodies or single stranded DNA (ssDNA) as bioreceptor molecules and are called immunosensors or DNA biosensors respectively. Whole cells and viruses can also be used as bioreceptor molecules (Mao C et al, 2009).

Biosensors are also classified according to their usage, such as single use sensors, intermittent use (non-continuous and reusable) sensors and continuous use sensors. (Dover JE et al, 2009). The intermittent use sensors are currently being used in many labs and they have shown more accuracy and may have data storage facilities (Dover JE et al, 2009).

Many different substrate materials such as glass, polystyrene, carbon electrodes, gold and semiconductors like silicon and indium tin oxide (ITO) are traditionally used for the immobilization of bioreceptors in biosensor construction. Choosing a right substrate is a very important criteria in order to obtain a stable and high signal. Recently, nano crystalline diamond (NCD) has attracted many material researchers, because of its electronic and chemical properties. The intrinsic insulating property and chemical inertness of the diamond, prevents the degradation, upon contact with electrolyte solutions. Its high thermal and electrical conductivity, biocompatibility and low thermal expansion allows diamond in many *in-vivo* applications (Christiaens P et al, 2006). The detailed description of the different types of transducers are given in the latter section (section 1.6) of the introduction.

Table 1.1 Classification of biosensors based on the type of transducer

Type of transducer	Measured property
Electrochemical	Potentiometric, conductometric, impedometric, amperometric
Optical	Fluoresence, absorption, reflection, refraction
Mass based	Acoustic resonance frequency change
Thermal	Temperature change

1.3 Immobilization strategies used in biosensor development

The foremost important step in biosensor development is the immobilization of bioreceptor molecules onto a transducer surface. This should be firmly and at the same time keeping the bio recognition part active to bind the analytes (Putzbach W et al, 2013). This is due to the fact that most of the detection of target molecules and signal transduction usually must occur at a liquid-solid interface. There are a number of immobilization strategies that may be considered, including covalent coupling, adsorption and affinity binding. Each has its benefits and drawbacks, which should be considered in the context of the research objectives, reagent requirements and technician/laboratory expertise. Different approaches are briefly discussed in the following paragraphs.

1.3.1 Physical adsorption of bioreceptor molecules on biosensors

Non-covalent binding is frequently applied for the immobilization of macromolecules like nucleic acids and proteins on biosensor surfaces. Different types of non-covalent bonds are reported including hydrogen bonds, Van der Waals interaction and hydrophobic binding (Stoler E et al, 2015). The energy released in forming a non-covalent binding is about 5 KCal/ Mol and this is much less as compared to that of a covalent binding which is 100 Kcal/ Mol. Non-covalent bonds are also weaker as compared to covalent binding, since there is no electron sharing between the inter and intra molecules.

The hydrophobic binding of bioreceptors to the surface of a transducer results in a random disordered binding. Moreover bioreceptors are (partly) removed from

the surface even by mild or stringent washing steps which may create problems when developing biosensors (e.g. label free sensors). The random adsorption process may lead to the unavailability or inaccessibility of a portion of the biologically active parts and also conformational changes can decrease the specificity and the binding efficiency of the target (Nakanishi et al, 2008). These events may result in a significant loss of active binding sites for biomolecules on the surface, leading to a decrease in sensitivity and reproducibility of the resulting biosensor. Nevertheless, in some specific cases physical adsorption approaches also do yield a stable immobilized and well-oriented biomolecule layer. Physical adsorption/ non-covalent coupling can provide few advantages such as simplicity (by simply dipping the substrate in a protein solution) and possible reusability of the substrate (Redeker ES et al, 2013).

Several non-covalent approaches based on affinity interactions between biomolecules have also been used to obtain an oriented protein immobilization onto the sensor surfaces. This can be achieved using antigen / antibodies, avidin / biotin and other biological tags. (Redeker ES et al, 2013). Streptavidin (STV) and avidin are homotetrameric proteins, forming stoichiometric interactions with biotin and these bindings are considered to be the strongest site specific natural non-covalent bonds (Kim WJ et al, 2011; Nakanishi et al, 2008 and Bastings MMC et al, 2011). Both avidin and STV are sharing 30% of sequence similarity (Dudak FC et al, 2011). Avidin is isolated from chicken egg-white and streptavidin is secreted by the bacterium *Streptomyces avidinii* (Kim WJ et al, 2011) and the molecular weight of STV is about 60 kDa. Biotinylation can be achieved for any kind of target molecule using tags (Lamla T et al, 2003) that form an irreversible, extremely stable bonds over a wide range of pH, temperature and withstand typical washing procedures. Therefore STV-modified sensor chips are commercially available for the detection of biotinylated targets and these sensors are well known in the biosensor field.

1.3.2 Covalent coupling of bioreceptor molecules on biosensors
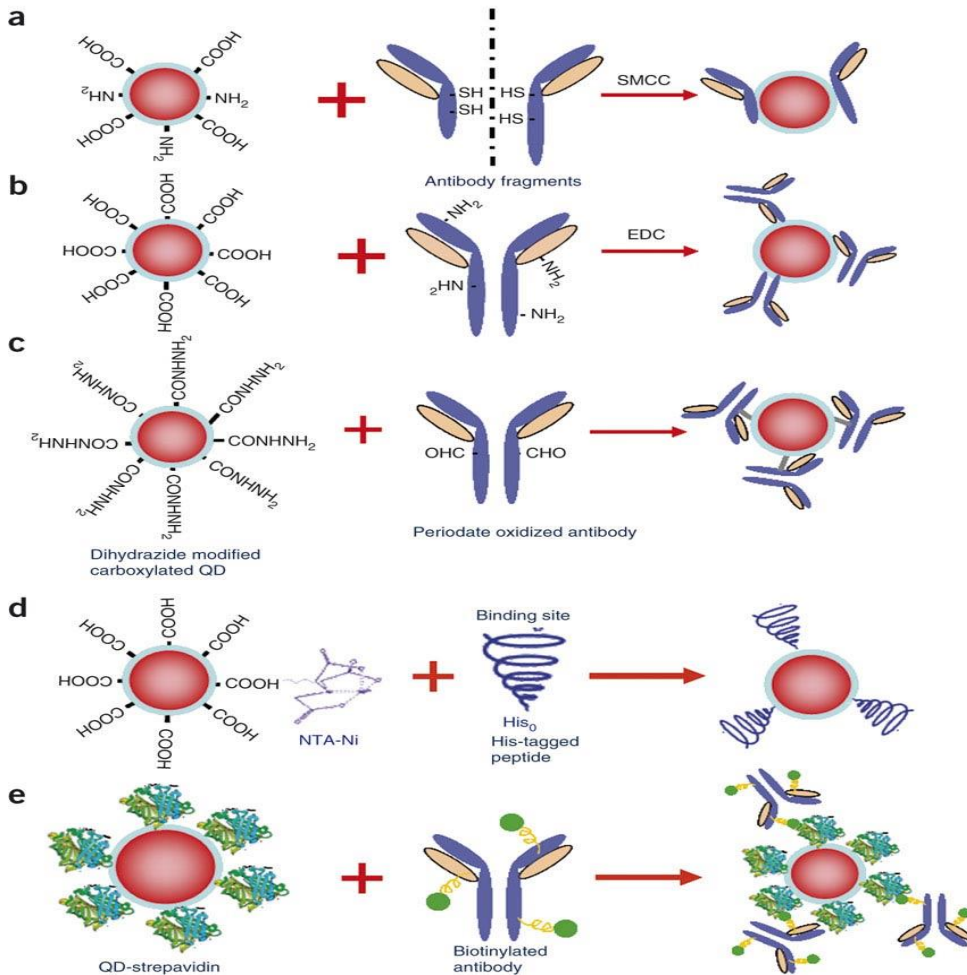
Figure 1.3 Various methods for conjugating antibodies with quantum dots (Xing Y et al, 2007).

Quantum dots (QD) are conjugated to antibody fragments via (a) disulphide reduction and sulfhydryl-amine coupling; (b) covalent coupling between carboxylic acid (-COOH) coated QDs and primary amines (-NH$_2$) on intact antibodies using EDAC as a catalyst; (c) site-directed conjugation via oxidized carbohydrate groups on the antibody Fc portion and covalent reactions with hydrazide-modified QDs; (d) conjugation of histidine-tagged peptides or antibodies to Ni-NTA modified QDs; and (e) noncovalent conjugation of streptavidin-coated QDs to biotinylated antibodies.

SMCC: Sulfosuccinimidyl 4-(N- maleimidomethyl) cyclohexane-1-carboxylate, EDC:1-Ethyl-3-(3-dimethylaminopropyl) carbodiimide

Covalent coupling is a more robust strategy for efficient and stable immobilization of two mutually reactive functional groups of the bioreceptor components and the transducer when compared to the physical adsorption. Covalent coupling is considered as the technique of choice in most biosensors. The conditions for immobilization by covalent binding are much more complicated and stringent than in the cases of physical adsorption and ionic binding. Therefore, it can also change the conformational structure and active center of the bioreceptors, resulting in loss of activity and/or changes of the substrate.

However, the binding force between the bioreceptor and substrate is so strong that no leakage of the bioreceptor occurs, even in the presence of substrate or solution of high ionic strength. The covalent coupling of bioreceptor molecules can be achieved by modifying the sensor with $-NH_2$, hydroxyl (OH), imidazole, carboxyl (-COOH) and thiol ($-SH$) etc... groups in order to attract ligand molecules, as reviewed in Redeker ES et al, 2013. This way carboxyl (-COOH) modified surfaces and $-SH$ modified gold surfaces are widely used. As an example various methods for bio-conjugation of antibodies on the surface of quantum dots are shown in figure 1.3.

There are several chemical compounds that could be exploited to modify or to bind to the available reactive group on the biomolecules either by activating groups that normally exhibit low reactivity in an aqueous environment (e.g. carbodiimide for binding to COOH groups), or by linking these compounds to groups that are simply not reactive one to the other (e.g. NH2 to NH2). Often spacers are used when binding biomolecules to the sensor surface. These spacers ensure that the biomolecules extend from the solid surface and this way potential steric hindrance is avoided (e.g. when coupling small molecules or oligonucleotides to surfaces). Linkers can also be used to simplify subsequent conjugation reactions (e.g. photo reactive groups) or to introduce cleavable reactive groups (Bangs laboratories INC, TechNote 205, USA).

Also Self-Assembled Monolayers (SAMs) are used to activate sensor surfaces. These are formed when surfactant molecules spontaneously are chemisorbed into a mono-layer on several solid substrates. This provides an interesting tool to

design the transducer's surface for different affinity assays (Ulman A, 1996). Two of the most widely studied SAMs systems are gold-alkyl thiolate monolayers typically used on gold surfaces and alkylsilane monolayers that are used on silica substrates or on indium tin oxide surfaces (Bhushan et al, 2005).

1.4 Filamentous phage and phage display systems used as bioreceptor molecules in biosensors

Among the different bioreceptor molecules whole phage displaying certain peptide receptors and synthetic peptide receptors as identified by phage displaying selection tools are getting popular these days due to their target specific antigen binding properties (Mao C et al, 2009). In this section the physiology of the M13 filamentous phage and its use in the phage display technology is discussed.

1.4.1 The physiology and structure of the M13 bacteriophage

It is almost one century since phage were discovered in the UK by Frederick W. Twort. Since then it is the most diversified organism studied (Tolba M et al, 2010). Phage that specifically infect prokaryotic cells (bacteria) are called bacteriophage (phage) (Bratkovic T, 2010). Phage usually have hollow heads and a cylindrical tail/body and do bind or infect Gram negative bacterial cells. There are hundreds of varieties of phage that exist and each type can infect certain strains of bacteria via the F pilus (Monjezi R et al, 2010). Compared to other viruses, phage have a rather simple genetic and structural organization that enables them to grow easily on a bacterial host.

Phage are made up of a protein coat and carry genetic material in the core, which may be DNA or RNA; either single stranded or double stranded. Phage have a net negative charge under neutral pH (Monjezi R et al, 2010). When bacteria get infected, phage inject their genetic material into the bacteria and the phage genome uses the host bacterial machinery to produce phage proteins and to release new phage particles. This way hundreds of progeny phage can be produced from a single infection even within half an hour. After infection, phage can proceed to a lytic cycle (killing the host cell releasing phage particles) or to a lysogenic cycle (without killing the host) (Mao C et al, 2009). A particular lysogenic

phage type called M13 filamentous phage is the mostly used in the high throughput phage display technology.

1.4.2 M13 based phage display technology

In the last decades of the 20th century Prof. George Smith introduced the phage display technique (Hwang I, 2014 and Scott JK et al, 1990). The term phage display itself explains the technology, a foreign peptide is displayed on the surface of a bacteriophage (Bratkovic T, 2010). Using this approach an efficient technique becomes available to select peptides with specific binding properties to desired targets. It turned out to be a technology with a high versatility. Peptides of interest are inserted at a location in the genome of the filamentous phage such that the encoded peptide is expressed or "displayed" on the surface of the filamentous phage as a fusion product of one of the phage coat proteins (Guo Y et al, 2010). Hence, a direct link between the phenotype and genotype is established (Kwasnikowski P et al, 2005). Figure 1.4 shows the genotype (arrangement of genes) and the phenotype (structure and displayed peptides) of a M13 phage.
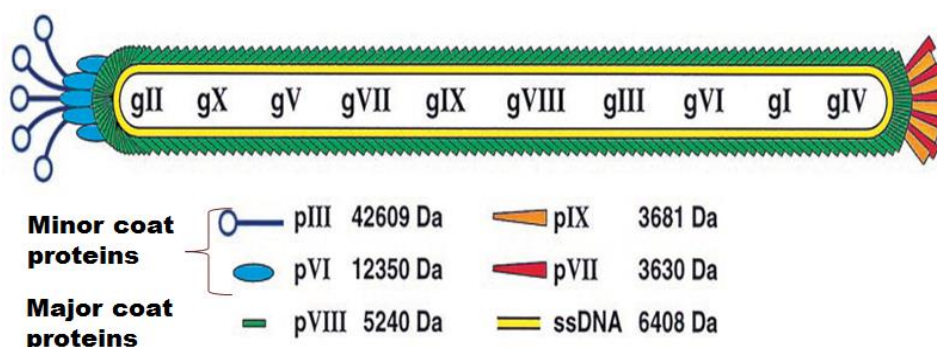
Figure 1.4 Link between the genotype and phenotype of a M13 filamentous phage (Goa C et al, 1999)

The arrangement of genes in the M13 genome is given and the corresponding proteins that are displayed on the surface of the phage are shown.

The capsid protein does not interfere with the displayed peptide, instead it serves as an anchor to display the inserted peptide to the outside and it even allows the peptide to behave freely as if it was in solution (Bratkovic T, 2010). Using this approach, 10^{10} variants of phage displaying a peptide library can be prepared from

a cDNA bank of any cell type. It is a key technique that enables the researcher to produce or to select antibody fragments or peptides binding to even highly infectious and / or toxic agents (Hengerer A et al 1999 and Chasteen L et al, 2006). Phage display also overcomes problems associated with the synthesis of small peptides or avoids the denaturation of natural small molecule ligands in unfavorable conditions. Moreover high affinity peptides can be produced without sacrificing animals (Hengerer A et al, 1999 and Dudak FC et al, 2011). The overall length of the bacteriophage depends on the size of the genome. On average a phage has 7400 nucleotides resulting in a length of about 800-900 nm and 6-7 nm width and the molecular weight is approximately 16300 kDa (Chen H et al, 2006).

The M13 phage genome contains eleven genes, including five coat protein genes, of which pVIII is called the major coat protein and it has 2700 copies present all over the phage (Hwang I, 2014; Kwasnikowski P et al, 2005 and Wang KC et al, 2009). At each end of the phage 5 copies of two coat proteins (pVII and pIX at one end and pIII and pVI at the other end) are displayed. The pVII and pIX proteins are necessary for the initiation of the phage assembly. pIII is the largest complex coat protein and it is used for the recognition and the infection of the host cell. All five coat proteins can be used for displaying peptides but pIII and pVIII are most often used because of the presence of a naturally occurring signal peptide that ensures an efficient peptide display. In all phage display protocols the desired peptide coding sequence is placed in frame between the coat protein coding sequence and the N terminal signal sequence. In contrast to the other coat proteins pVI has a carboxyl terminal facing towards the surface of the bacteriophage and therefore this gene is rather used for the construction of cDNA libraries (Wang KC et al, 2009). The N terminal display system should not contain in-frame stop codons which would abruptly end the display of the peptide of interest (Faix PH et al, 2004).

1.4.3 Vectors used in the phage display technology

There are two different types of vectors that are widely used in phage display, namely phage and phagemid vectors. When phage are genetically modified to display a protein of interest, all the resulting phage that are produced do display the protein of interest. The phage population produced from such a single clone result in a phenotypically and genotypically homogenous progeny phage. The disadvantage of the phage vector system is that it is prone to proteolysis and also deletion mutations occur, therefore the display of large proteins is not possible (Chasteen L et al, 2006; Bratkovic T, 2010). Phagemid is another type of vector that combines plasmid and phage properties. It contains the origin of replication (ori) of both the dsDNA (host) and the ssDNA (phage) (Sidhu SS, 2000; Hammers CM et al, 2013) allowing for the replication of both forms. Phagemids contain one or a few coat protein genes and the phage packaging signal, needed to insert the genome into the phage particle. Phagemids always need a coinfection of a helper phage, for the delivery of the other essential structural proteins needed to assemble a complete phage particle. Usually a helper phage genome does not have a (strong) packaging signal, hence, phagemids are packed preferentially into the progeny phage (Chasteen L et al, 2006). Due to the fact that helper phage provide structural proteins to make a complete phage, progeny phage are always heterogeneous in nature and display both wild type proteins and the protein of interest. This way only one copy of the protein of interest will be displayed and the remaining copies are wild type proteins coming from the helper phage. For this reason it is called a monovalent display system. In contrast to the phage system, the phagemid system does allow the display of larger proteins (Wang KC et al, 2009 and Bratkovic T, 2010).

A decade ago, Chasteen and co-workers (2006) introduced a new vector system in which the use of helper phage can be avoided and can be replaced by a helper plasmid. Helper plasmids contain all the 11 genes of a phage and allow the insertion of a DNA fragment encoding the protein of interest in any of the coat protein genes. During the production of phage particles in combination with phagemids, the helper plasmid provides only the proteins to the progeny phage but not the genetic material because the helper plasmid has no packaging signal. Hence, the genetic material packed in the progeny phage is only provided by the

phagemid. This results in a genetically pure phagemid system. This approach also makes multivalent display of a peptide of interest possible. Theoretically, if the helper plasmid is modified to display a protein of interest in one of the coat protein and if the same coat protein gene is missing in the phagemid, then the progeny phage will display the protein of interest in all of the displayed protein copies. The obtained titer values of produced phage using the helper plasmid approach are comparable to those produced with helper phage. The above concept is illustrated in figure 1.5.
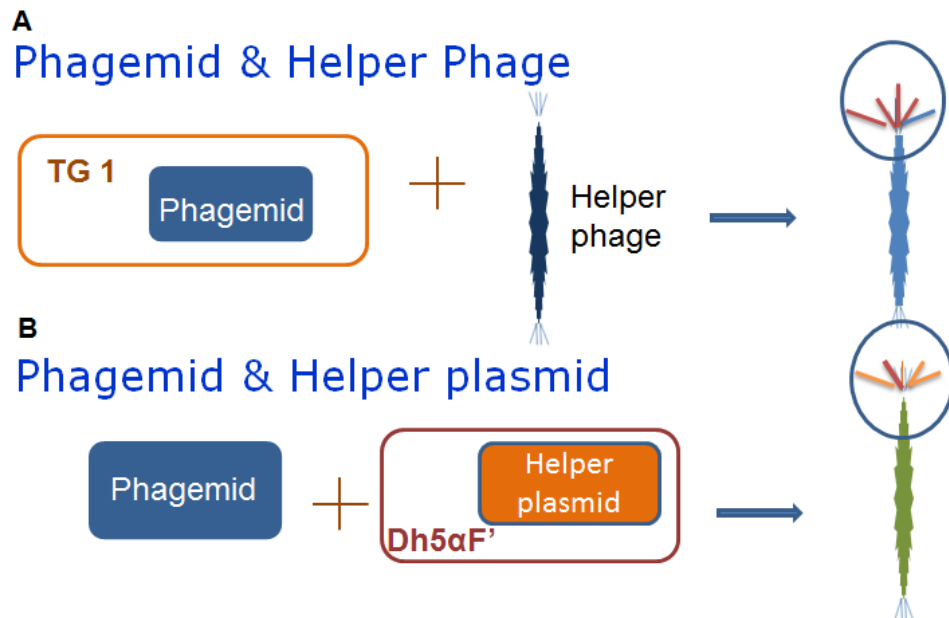
Figure 1.5 Different phage display vectors used in display strategies
A) A Phagemids and helper phage based system produces monovalent displaying phage.
B) A Phagemids and helper plasmid system produces multivalent displaying phage. Blue lines represent wild type coat proteins and brown lines represent fusion coat proteins displaying the protein of interest.

1.4.4 Strategies for the construction of a dual phage display system
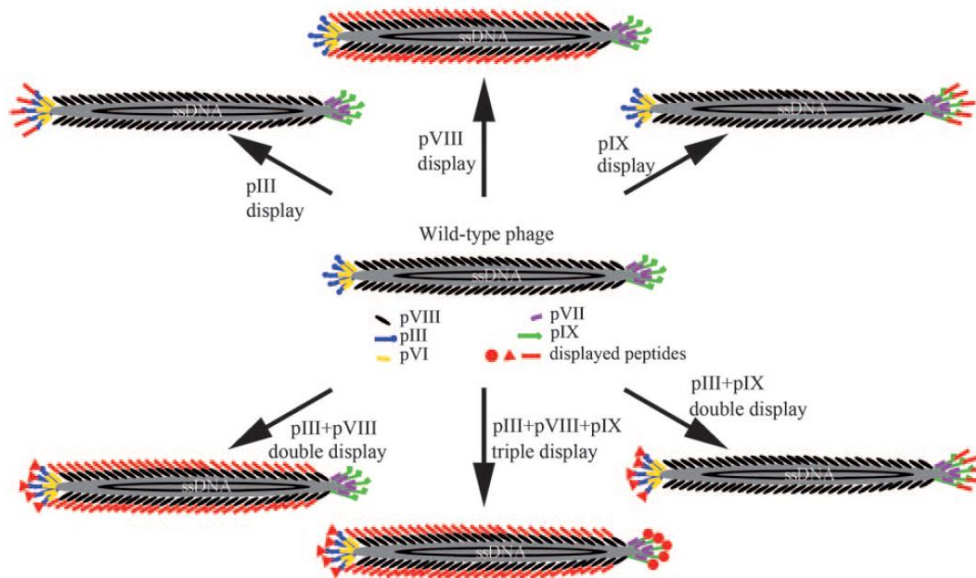
Figure 1.6 List of site specific genetic modifications of different coat protein genes of a M13 phage (Mao C et al, 2009)

A wild type M13 phage is shown in the center and the use of the different phage coat proteins to display peptides in different strategies (single, double and triple display) are shown in red.

Phage can also be modified to have multiple peptides displayed on the surface. Displaying two or three different proteins at one coat protein or at different coat proteins is called dual or triple display. These multiple display systems are possible by modifying different coat protein genes of the same phagemid or by combining different phagemids modified to display each of the peptides separately. Using this approach, it is possible to create more than one fusion protein per coat protein or two different proteins in two different coat proteins at the same time. In Figure 1.6, different possible display systems by modifying one or more coat protein genes are shown. Such multifunctional phage can be applied in different fields such as material sciences and in diagnostic biosensors. The display level of a fusion protein depends on the size of the protein and its sequence; e.g.: small peptides can be displayed in multiple copies but larger peptides are presented as

one copy (monovalent) per phage or even less (incomplete display). As stated before, pIII and pVIII are the coat proteins mostly used in phage display, due to the presence of natural signaling/leader peptides. However, by inserting the DNA code for a signaling peptide also other coat proteins can be used to display a protein of interest. A well-known leader peptide is pelB, a 28 amino acid peptide, which is usually placed in frame after the start codon of the coat protein gene of interest. This pelB helps in transferring the protein to the periplasm, where the packaging mechanism takes place and it also assists in the correct folding of the protein of interest.

As stated before, phage libraries are the key for the selection process termed biopanning (Koivunen E et al, 1999; Azzazy HME et al, 2002). Typically phage libraries contain approximately 10^{10} variants of peptides (Hammers CM et al, 2013). Biopanning is an iterative process in which a phage library is interacting with antigen coated wells to identify potential, even rare antigen binding clones in the phage library. DNA sequencing of the isolated clones results in the identification of the enriched peptides. These peptides can be used as recombinant or synthetic peptides in further diagnostic assays e.g. to detect the presence of their targeted ligands as biomarkers.

Customized phage libraries can be generated using cDNA from the targeted antigens present in tissues, organs or tumors. For example, in case of Rheumatoid Arthritis (RA), mRNA of synovial tissue has been extracted and a corresponding cDNA phage library was created. These libraries were applied in a modified high throughput biopanning process called Serological Antigen Selection (SAS) which is illustrated in figure 1.7. Using SAS affinity selections were performed with pooled patient body fluids thereby increasing the chances of selecting general disease specific immunoreactivities (Somers et al, 2009). In this approach, the above described cDNA phage display library constructed from RA synovial tissue was screened for antigen reactivity with autoantibodies present in pooled patient plasma (Somers et al, 2011). Next the phage-antibody complex is captured on a solid support coated with polyclonal anti-human IgG, and the bound phage complexes are eluted and amplified (in host bacteria) after multiple washing steps. By repeating positive and negative selection rounds a panel of biomarkers for RA

was identified (Somers K et al, 2011). Such a panel was also identified for Multiple Sclerosis (Somers K et al, 2009).

In this work, as a proof of principle/application, we will use one of the previously identified autoantigenic targets specific for the most common autoimmune disease called Rheumatoid Arthritis (RA) in a dual display phage construction approach.
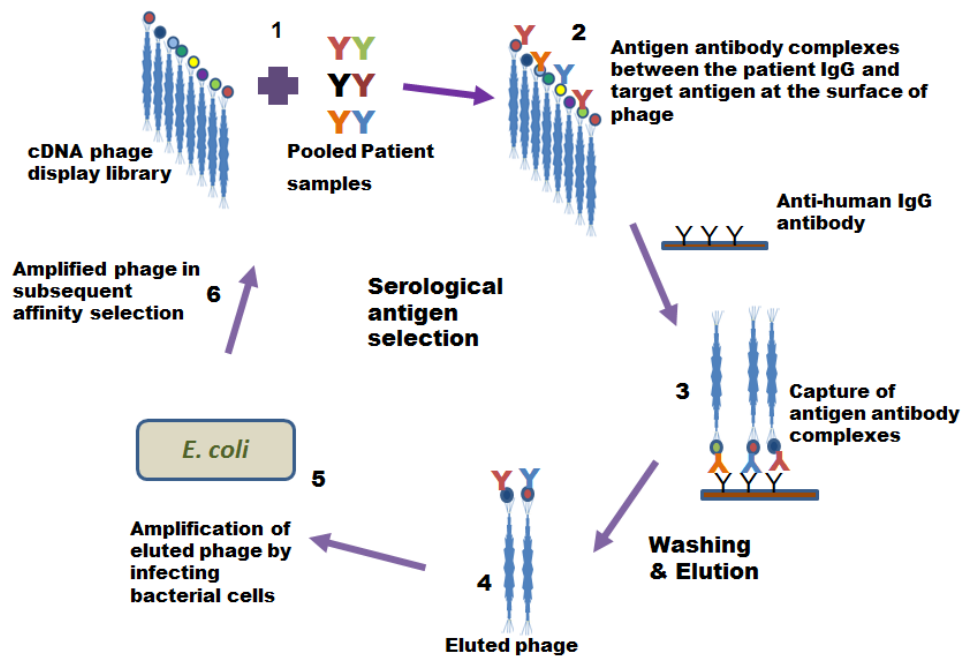
Figure 1.7 Identification of autoantibodies using the serological antigen selection process (Adapted from Somers K et al, 2011)

An affinity selection round is initiated by incubating phage displaying a cDNA library with pooled patient body fluids (1). During this incubation step, antigen–antibody complexes are formed between the auto antibodies present in the patient body fluids and their respective target antigens at the surface of the phage (2). These complexes are captured on a solid support by anti-human IgG capture antibodies (3). Bound phage are eluted (4), amplified through infection of host bacteria (5) and used as input in a subsequent affinity selection procedure (6). The succession of affinity selection and amplification of selected phage results in the enrichment of phage-displayed antigens targeted by patient IgG.

1.5 Introduction to autoimmune diseases

Autoimmunity is a disease that arises when our immune system fails to discriminate between self and non self (antigens).As a consequence our immune system triggers an immune response against own body cells or proteins. There are almost hundred different types of autoimmune diseases identified. The underlying cause and the etiology of autoimmune disorders are not yet completely understood. Some well-known examples are Multiple sclerosis, Rheumatoid arthritis (RA) and Type I diabetes (Rapp BE et al, 2010). RA is referred to as the most common autoimmune inflammatory disorder.

1.5.1   Introduction to Rheumatoid Arthritis

RA is considered to be the most common chronic inflammatory disorder (Somers K et al, 2009 and Aletaha D et al, 2010). The prevalence of RA in Northern European and North-America is estimated around 1% and women are more affected than men. Usually the disorder starts at the small joints in our body and later spreads to the other joints. It causes damage to the lining of the bones and joints which leads to the painful swelling of the synovial membranes and eventually ends in the erosion of bone (Lindstrom TM et al, 2010; Fattahi MJ et al, 2012). The inflammation is usually present on both sides (symmetrical or bilateral) of the body, which distinguishes RA from other types of arthritis. Figure 1.8 shows both healthy and RA affected joints.

RA also causes extra articular manifestations like the formation of rheumatoid nodules, anemia, cardio vascular problems, osteoporosis and lymphadenopathy. Though the etiology of RA is not completely known (Somers K et al, 2009), it is believed that the autoimmune attack of the synovium is probably the first trigger. Other factors like genetic (William et al, 2012), epigenetic (Martinez CB et al, 2012) hormonal (Nelson JL et al, 1997), immunological (Smolen JS et al, 2003) environmental (Albano SA et al, 2001) and infectious factors (Bennett JC, 2005) have also been described to have an impact on RA. Over time, all these elements may induce an immune response thereby worsening the condition by joint inflammation, and subsequent joint damage and destruction. The intercommunication between various Antigen Presenting Cells (APC) and T cells leads to the activation of B cells, which further differentiate to plasma cells and

cause the production of autoantibodies, such as Rheumatoid Factor (RF) and Anti-cyclic Citrullinated Peptide Antibodies (ACPA). During inflammation, arginine residues in proteins are converted to citrullinated peptides with the help of protein-arginine deiminase and if the formed citrullinated peptide is defective in shape, the immune system forms antibodies against it. In RA patients the thin synovial membrane usually gets inflamed and this also spreads into the pannus tissue (Smolen JS et al, 2003) due to the infiltration of immune cells such as T cells, plasma cells, B cells, mast cells and macrophages. In the long run this causes irreversible damage to the joint by invading into the cartilage, bone and sometimes even to the bone marrow.
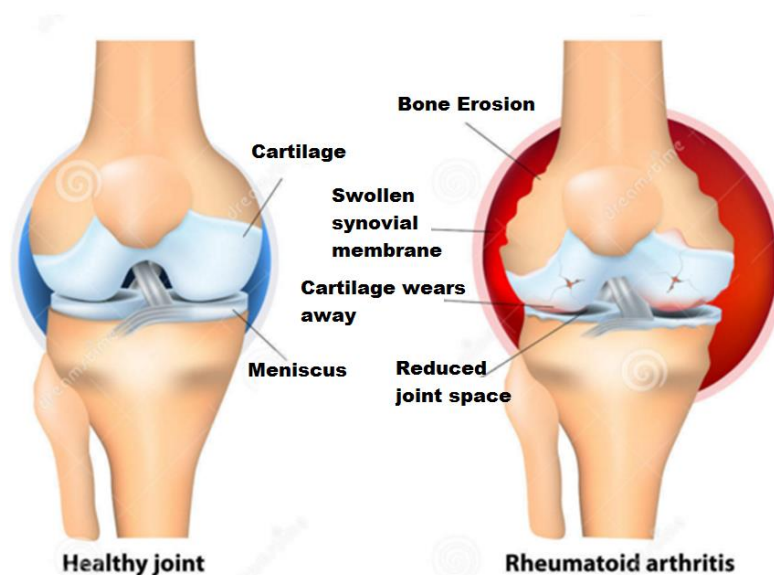
Figure 1.8 Appearance of healthy and RA joints (dreamstime.com)
The joint inflammation of RA causes swelling, pain, stiffness, and redness in the joints. The inflammation of rheumatoid disease can also occur in tissues around the joints, such as the tendons, ligaments and muscles. RA eventually causes bone erosion and cartilage damage too.

1.5.2 Biomarkers used in RA diagnostics

Biomarkers or signature molecules are substances that are present in body fluids or tissues that can be an indicator for the diseased state or the metabolites of a specific reaction or pharmacological response in an organism (Frank R et al,

2003). Finding a suitable highly specific biomarker is an important criterion for the diagnosis of a disease at an early stage and to assess or predict the severity of the disease and eventually to monitor the response to therapy. Early diagnosis of RA patients is a prerequisite but at present, it is not yet achieved. The inefficiency of the current diagnostic practice triggered the search for early diagnostic biomarkers for RA.

Table 1.2 RA auto-antigenic targets and their amino acid sequences

No	Autoantigenic Targets	RA Sensitivity in %	Amino acid sequences
1	UH-RA 1	10	EKRQEITTE* (9)
2	UH-RA 2	2	SISTS* (5)
3	UH-RA 7	3	SSQDV* (5)
4	UH-RA 9	4	RSCHHGCTFTEDQHWECGEDDAV* (23)
5	UH-RA 10	7	SNALENFVYNKFQQNNCVWPGAVAHACNPSTLRG* (34)
6	UH-RA 11	13	SSQPTIPIVGIIAGLVLFGAVITGAVVAAVMWRRKSSDRKG GSYSQAASSDSAQGSDVSLTACKV* (65)
7	UH-RA 13	2	QDSCQEN* (7)
8	UH-RA 14	12	KEELWRQ* (7)
9	UH-RA 15	5	DTIEVPEKDLVDKARQINIHNLSAFYDSELFRMNKFSHDLK RKMILQQF* (49)
10	UH-RA 16	5	RLLLSKGHSCYRPRRTGERKRKSVRGCIVDANLSVLNLVI VKKGE...................EQIAKRRRLSSLRASTSKSESSQK* (176)
11	UH-RA 17	3	AKRKEAGPLEVVVTTPAMWRSLGLALALCLLPSGGTESQ DQSSLCKQPPAWSIRDQDPMLNSNGSVTVVALLQAS* (76)
12	UH-RA 20	2	RGLHLPSGAPKDEPHSGMESTV* (22)
13	UH-RA 21	29	PGGFRGEFMLGKPDPKPEGKGLGSPYIE* (28)
14	UH-RA 22	2	FIGRGDKPTEPGDSWLSKIESQFNFKFAHRTL* (32)

RA auto-antigenic targets and their amino acid sequences identified using SAS technology, their sensitivity against serum autoantibody in the phage ELISA has been given. (Adapted from Somers K et al, 2011)

In most cases only one biomarker will not be enough for an efficient diagnosis, so a panel of biomarkers may be needed. Based on serological tests, RA can be

classified as seropositive RA (presence of RF and CCPs) and seronegative RA (absence of RF and CCPs). Both tests are usually combined in order to improve diagnostic efficiency. However, these tests become irrelevant in patients with seronegative RA, since they are negative for RF and ACPA antigens. Therefore, there is a need for suitable biomarkers to diagnose RA early in seronegative patients with greater sensitivity and specificity. Using the above described high throughput technique SAS, Prof. Somers and co-workers (2011) identified a panel of 14 biomarkers (Table 1.2) that show high potential for early RA diagnosis.

1.6 Phage based sensor models

Most of the phage based affinity tests are phage ELISA assays. The introduction of phage in biosensors is difficult to achieve due to the absence of specific immobilization procedures to attach phage onto sensor surfaces. Therefore the use of phage in biosensors is relatively new but emerging (Donavan KC et al, 2011). Synthetic peptides, which have been selected via phage display technology are also applied in different sensing platforms (Wu et al, 2011, Ayela C et al, 2007). In the table 1.3, few examples of phage probe based different transduction principles and their sensitivity have been given. Also it is important to note that, all the peptides cannot be synthesized chemically, due to the fact that possible incorrect folding occurs which leads to decreased binding ability to the target molecules. So, the phage displayed peptides are considered as a better alternative to the monoclonal antibodies in ease to produce, manipulation at the molecular level and resistant to environmental stresses (Dover JE et al, 2009).

The use of bacteriophage as a bioreceptor molecule in sensing assays was initially demonstrated by Petrenko et al, 2008. Both lytic phage and non-lytic filamentous phage have been used in sensing platforms. Lytic phage have been used in selective killing of bacterial pathogens and releasing the intracellular contents into the medium. Filamentous phage have been used in binding to different types of analytes such as peptides, proteins, antibodies. Phage can be mass cultivated by infecting bacterial cells and it is very cheap to produce those (Dover JE et al, 2009). Phage show stability against extreme conditions like high and low temperatures, pH variations, enzymatic activities and surfactants without losing bacterial infectivity (Arap, 2005). These properties make phage good candidate

receptor molecules in sensing devices. In the following section, different types of sensing platforms and different analytical methods that have been used in combination with the target specific phage display technology is briefly described.

Table 1.3 Different phage based sensor models and their sensitivity

Phage based sensor probe	Detection methods	LOD	Ref
Binding reaction between b-galactose binding landscape phage and b-galactose	SPR	1 pM	Nanduri. V et al, 2007
Affinity reaction between anti-pVIII antibody and M13 phage	QCM	10^6 PFU/ml	Dultsev. FN et al, 2001
M13 phage immobilized electrode in the binding of anti-M13 antibody	EIS, QCM	7 nM	Yang. LMC et al, 2008
M13 phage with a gene for alkaline phosphatase in the detection of E.coli	Amperometry	1 CFU/ml	Neufeld. T et al, 2005
branched polymers of maltose M13 phage displaying maltose-binding	QCM	20 phage	Uttenthaler. E et al , 2001
phage displaying morphine-binding peptide in the detection of morphine	FRET	5 ng/ml	Pulli. T et al, 2005
Binding reaction between phage based human scFv antibody and protein antigens	ELISA	Kd=220 pm–4 nm	Sheets. MD et al, 1998

Note: LOD- Limit of detection, EIS- Electrochemical impedance spectroscopy, SPR- Surface plasmon resonance, QCM- Quartz crystal microbalance, FRET- Fluorescence resonance energy transfer

1.6.1 Electrochemical biosensors

A biosensor that measures electrochemical properties of a biological system is called an electrochemical sensors. Electrochemical techniques are extensively used in biosensor applications because such sensors are easy to use, allow a rapid readout, are inexpensive to produce and have miniaturization potential (Mao C et al, 2009). Most of the electrochemical biosensors make use of enzymes to have a bio-catalytic activity that can be measured easily. Antibodies (Simon BP et al, 2011), recombinant antibody fragments (Byrne B et al, 2009), antigens and microorganisms (Jia J et al, 2002) are other types of bioreceptors that can be used in electrochemical sensors. Various types of electrochemical sensors have

been reported, measuring electric current, voltage, potential difference, impedance. Phage electrochemical sensors can be prepared by immobilizing them in a sensing electrode for the specific detection of target molecules in solution (Ionesco RE et al, 2007).

1.6.1.1 Amperometric sensors

Amperometric sensors mostly rely on the detection of ions in the solution. Signals are obtained as an electrical current caused by a redox reaction at a given constant voltage. This type of sensors are the oldest ones, explaining why a higher number of ready to use devices have been constructed. A three electrode setup is normally used in which a reference electrode measures the potential fluctuations and the current is measured between the working electrode and counter electrode (Prasek J et al, 2012). An amperometric readout is mostly used in enzymatic sensors and a current proportional to the concentration of the substrate is detected. Amperometric readout is giving a sensitive electrochemical sensing platform that is used in combination with immunosensing assays such as in pregnancy testing (human chorionic gonadotropin) and in the famous glucose sensors. Also in phage based amperometric sensors, electrochemically inert phage will lyse bacterial target cells thereby releasing intrinsic cellular marker enzymes that trigger the electrochemical signal. As an example Ionesco RE and coworkers (2007) immobilized functional T7 lytic phage, modified to display the West Nile virus antigen, on polypyrrole films. Using this approach the presence of West Nile virus specific antibody in serum, plasma, or cerebrospinal fluid was measured and West Nile virus infection of patients is detected.

1.6.1.2 Potentiometric sensor

A potentiometric sensor is a type of chemical sensor that determines the volumetric presence of a compound, based on the detection of ionic atoms or molecules in the compound that carry an electrical charge in the scenario of zero voltage. The accumulated charge potential between the working and the reference electrode can be measured by potentiometric devices. The presence of hydrogen ions is measured by a glass electrode that is attached to the reference electrode (same principle as for a pH electrode). Jia Y et al, 2007 successfully prepared a phage modified light-addressable potentiometric sensor for label-free detection of

cancer cells. In their sensor setup phage are covalently immobilized onto a silane-modified Si_3N_4 surface using glutaraldehyde. This sensor was used in the detection of human phosphatase of regenerating liver-3 (fatty liver grade 3). Measurements were done in the concentration range from 0.04 to 400 nM.

1.6.1.3 Conductometric sensors

Conductometry measures the electrical conductivity of an electrolyte or an element between the working and the reference electrode. Target molecules binding to immobilized capture molecules will induce a change in conductivity that can be measured. Electrochemical impedance measurements also belong to this group.

1.6.1.4 Impedimetric sensors

Electrochemical impedance spectroscopy (EIS) measures the dielectric properties of materials as a function of time. In this way electrochemical impedance spectroscopy explores the electrical behavior of a bioreceptor molecule as a function of an alternating current (AC) with a variable frequency. The electrical behavior is modeled by a suitable combination of Resistivity and Capacity circuits. The resistance of an AC potential is the impedance which is a more complex quantity than R because of a phase shift between the applied voltage and current (I). The use of electrochemical impedance spectroscopy as a transducer signal in biosensor applications is based on the fact that an interaction between a bioreceptor and its analyte recruited from the solution causes a change in the interfacial electron transfer kinetics between a redox probe in the solution and the electrode (Carvalho FC et al, 2014). The interference between the immobilized bioreceptor molecules and the current takes place in three different regions: inside the bioreceptor molecules, at the boundaries of the immobilization and on the surface of the electrode.

For a sinusoidal current, the given potential is according to **$U_t = U_0 \sin \omega t$**

U_t is the potential at time **t**, **U_0** is the amplitude of the signal

In a linear system, the response signal **I_t** is shifted in phase (**θ**) and has a different amplitude **I_0** (Figure 1.8).

$$\mathbf{I_t = I_0 \sin (\omega t + \theta)}$$

t: time
ω: angular frequency = $2\pi f$
f: frequency
ωt: phase angle
$\boldsymbol{\theta}$: phase shift
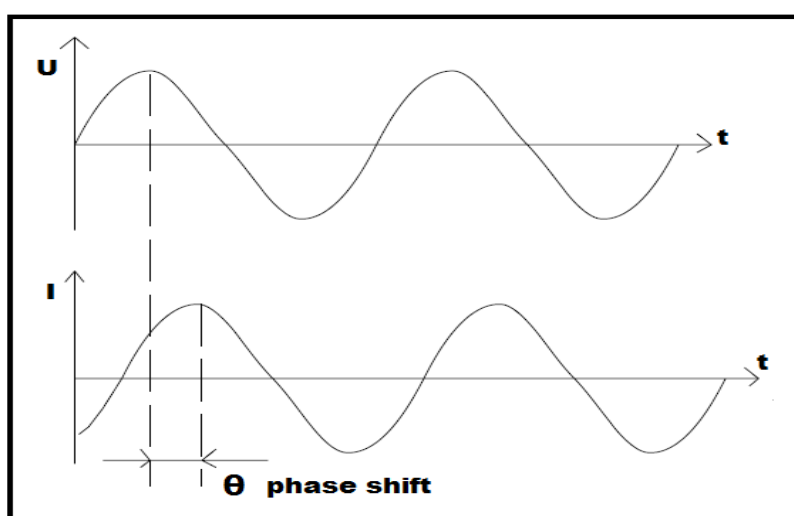
Figure 1.9 Electrochemical impedance spectroscopy

Sinusoidal current response in a linear system. In a linear (or pseudo-linear) system, the current response to a sinusoidal potential will be a sinusoid at the same frequency but shifted in phase (U is the given potential, I is the response signal and t is the time).

Finally the transducer signal of electrochemical impedance spectroscopy represents the electrochemical impediment of the redox probe caused by the target binding and it is measured by obtaining the charge transfer resistance from the electrochemical impedance spectroscopy spectra. Electrochemical impedance spectroscopy considered as a most suitable technique due to their high sensitivity and miniaturization within a multiplex capability (Carvalho FC et al, 2014).

Cheng MS et al, 2013 developed phage based impedimetric sensors to monitor bacterial infections. To achieve this, a monolayer of lipopolysaccharide specific antibodies was immobilized to capture the bacteria that are present and subsequently phage were added. Due to the phage infection the surface charge and the morphology of bacterial cell changes and the accumulation of redox probe, $Fe^{3-/4-}$ increases the electron transfer rate resulting in an impedimetric sensor signal.

1.6.2 Optical biosensors

In optical biosensors, the transduced output signal used is light. The biosensor can be made based on optical diffraction, absorption, fluorescence, refractive index or electrochemiluminescence. Optical sensors can be label free (direct) or with label (indirect).

1.6.2.1 Surface plasmon resonance
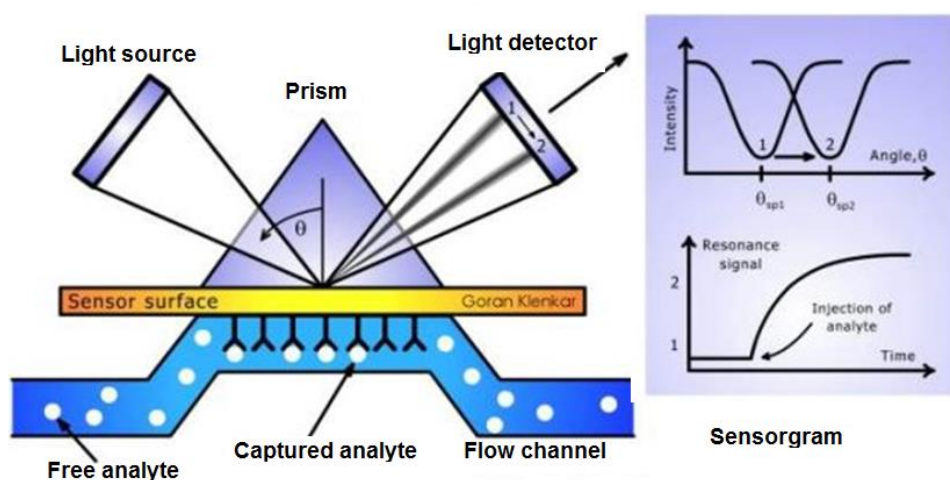
Figure 1.10 Working principle of surface plasmon resonance sensor (GE healthcare, Biacore, Sweden)

SPR occurs when surface plasmon waves are excited at a metal/liquid interface. Light is directed and reflected from, the side of the surface not in contact with sample, and SPR causes a reduction in the reflected light intensity (1 to 2 in the Figure) at a specific

combination of angle and -wavelength. The bio molecular binding events cause changes in the refractive index at the surface layer, which are detected as changes in the SPR signal.

Surface Plasmon Resonance (SPR), introduced in the early 80's, is a label free optical detection technique which measures a bio molecular interaction in real time and which is very popular and well known for its high sensitivity (Zhu et al, 2008). SPR has been widely used for different biological applications such as ligand receptor binding, binding properties of SAM, antibody-antigen binding (immune assays), DNA hybridization and protein DNA interactions (Amanda et al, 2002). Figure 1.10 represents a model SPR system.

Noble metals like gold and silver are known for their surface plasmons. SPR forms when a plain polarized light hits on an electrically conducting gold layer at the interface of a glass sensor with high Refractive Index (RI) and an external medium (gas or liquid) with low RI (Green RJ et al, 2000), creating minimum reflected light intensity at a particular angle. When a binding even happens on the surface, minimum angle changes, and it depends on the amount of samples bound on the surface. A small change in the interface results in a change in SPR signal and this can be accurately measured in real time. SPR analysis only requires a very small amount of sample and target detection limits down to the femtomolar range can be achieved (Sagle LB et al, 2011).

The reflected photons create an electric field and the plasmons create a comparable field that extends into the medium on either side of the film. This field is called an evanescent wave because the amplitude of the wave decreases exponentially with increasing distance from the interface surface, decaying over a distance of about one light wavelength. The wavelength of the evanescent field wave is the same as that of the incident light. The energy of the evanescent wave is dissipated by heat. The depth of the evanescent wave which could be useful for SPR measurements is within ~200 nm of the sensor surface and this explains the limitations in using bioreceptors which are more than 200 nm in size. And also important, the same interaction performed in close proximity to the sensor surface will have a three times higher response than if it occurs at distance of 200 nm

from the surface. Moreover small molecules of less than 200 D molecular weight require a higher ligand immobilization for their effective detection.

Lytic and lysogenic phage have been used in different SPR applications. Nanduri. V and coworkers (2007) used filamentous phage in detection of β galactosidase. They physically absorbed β galactosidase specific Ig40 phage in active flow cells and wild type phage in reference cells in SPREETA SPR sensors detected β galactosidase in a concentration down to 10^{-12} M.

1.6.3 Field effect transistor
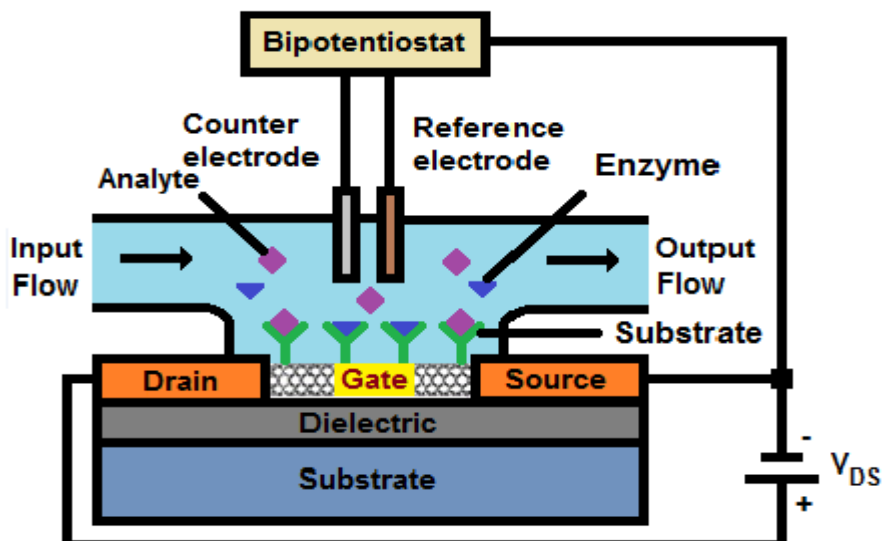
Figure 1.11 The working principle of field effective transistor sensors (Adapted from Bernal RV et al, 2012)

FET sensor's gate terminal is modified with a substrate containing an enzyme with the aim of detecting very low concentrations of analytes which are made flowing through it, therefore, a change in the drain-source current is presented due to the changing of charge density on the gate surface.

Field Effect Transistors (FET) are based on the change of the concentration of ions in a solution that will change the current in the transistor accordingly. It is also considered to be an emerging label free and real time sensor technology as it

measures the change of the ionic concentration in the electrolyte solution as a consequence of the bioreceptor molecules interaction on the working electrode. This technique is also referred to as BIO-FET sensors. BIO-FET sensors provide rapid and sensitive measurements, allow for portable instrumentation, can be produced at low cost (mass production) and can be used with a limited amount of sample. A basic FET is composed of 4 parts as shown in Figure 1.11, a drain, a source, a semiconducting body and a metal gate (Lee JO et al, 2008). The gate of a FET-type biosensor is usually replaced by a thin biofilm of bioreceptor molecules which are biologically specific for the target analyte. In response to the target molecules in solution, the bioreceptor modified gate's surface modulates the channel conductivity of the FET, which ultimately leads to a shift in the drain current.

Kim WJ et al, have used phage in single walled carbon nanotubes and polydiacetylene based FET for the detection of trinitrotoluene obtaining a 1 fM sensitivity. They observed a selective binding of trinitrotoluene by the phage displaying trinitrotoluene receptors but also a high selectivity was achieved for various trinitrotoluene like aromatic compounds such as dinitrotoluene, 2-nitrotoluene and 4-nitrotoulene.

1.6.4 Mass based biosensors for phage applications

Mass based biosensors measure the mass change that happens on the sensor surface following an immunological or biochemical interaction.

1.6.4.1 Phage based Quartz Crystal Microbalance biosensors

Quartz is one of the most abundant minerals on earth, it is very hard in nature and it is composed of a SiO_4 network. Quartz crystals belong to the kind of crystals that generate a piezo electric effect. The Greek word piezo means press, piezoelectricity means electricity generated due to pressure. The piezoelectric Quartz Crystal Microbalance (QCM) technology is a mass based biosensor and is often used in biosensor platforms. Such a QCM sensor can be used to evaluate the binding between the analyte to be detected and a sensing probe immobilized on the surface of the piezoelectric crystal. It is a label free approach that is

relatively inexpensive and it allows for rapid and simple sample preparation but nevertheless remains a high resolution mass based technique (Marx KA, 2002).

QCM crystals tend to oscillate at a particular frequency at a given voltage, this frequency alters when a mass is adsorbed on the QCM crystals and the relationship can easily be calculated using the Saurbrey's relationship formula (Rickert J et al, 1996, Dover JE et al, 2009). In addition to the fundamental frequency (called single harmonic; n=1, 5 MHz), other higher frequencies can be used as a readout e.g. 3rd (n=3, 15 MHz), 5th (n =5, 25 MHz)… 13th (n=13, 65 MHz) harmonics. Those are called the overtones and can be used in understanding the adlayers immobilized on the surface of the electrode.

Saurbrey's relationship formula:

$$\Delta m = \frac{-C.\Delta f}{n}$$ **(1)**

where C = 17.7 ng Hz^{-1} cm^{-2} for a 5 MHz quartz crystal, n is the overtone number (1st , 3rd , 5th … 13th), Δm is the mass change and Δf is the frequency change.

This equation can only be applied for rigid materials because soft materials can dissipate over the sensor leading to false calculations of the mass on the sensor surface. To cope with this problem, an advanced QCM called Quartz Crystal Microbalance with Dissipation monitoring (QCM D) can be used for analyzing viscoelastic soft materials that do not completely bind to the surface as explained in the next section.

Q-sense is a product of Biolin Scientific, a Swedish company that provides an analytic instrument based on the QCM-D technology (figure 1.12). In the QCM-D technology two important parameters are continuously measured to monitor the interaction of the bioreceptor and the target molecules: the frequency (related to mass/thickness) and the dissipation (related to rigidity). The resulting technique is measuring in real-time and can be used to monitor and characterize thin films on a surface in terms of adsorption, molecular interactions but also its structural

properties. When a substance is immobilized or adsorbed on the oscillating QCM sensor surface, hydrating water molecules will increase the mass and hence the signal response. In this regard a rigid surface will not or to a lesser extent be hydrated and therefore will not have a big energy dissipation. This can be calculated from the following formula,

$$\mathbf{D} = \frac{E_{lost}}{2n\,E_{stored}} \qquad \textbf{(2)}$$

where E_{lost} is the energy lost (dissipated) during one oscillation cycle, n is the overtone, E_{stored} is the total energy stored in the oscillator and D is the dissipation. As already mentioned above, in addition to the fundamental frequency, QCM-D allows to monitor several overtones and this allows us to study the structural properties of the layers that are attached to the surface in more detail.

Figure 1.12 Quartz crystal microbalance with dissipation monitoring from Q-sense (Courtesy Q Sense, Biolin Scientific, Sweden)

Indeed in contrast to the rigid surfaces as mentioned above soft biomaterials are elongating from the surface will hydrate fast which results in a high dissipation. Therefore by measuring the dissipation we can determine the rigidity or viscoelasticity and thus the structural properties of the used materials (Chen H et al, 2006). One drawback of using QCM may be that QCM is more prone to environmental perturbations (Wu J et al, 2011).

Phage have already been used in QCM sensors. However since phage are more resembling to soft material, oscillation will be suppressed due to the trapping of water inside the immobilized phage. Nevertheless, phage have been used in different QCM techniques, either as a direct probe or as analyte that binds to the attached specific probe molecule. Chen H et al, 2006 used phage displaying high frequency heptapeptides and they studied the phage binding capacity to SiO_2 and TiO_2 using a QCM D system. They have shown that phage displaying heptapeptides are binding with a high efficiency to SiO_2 and TiO_2 surfaces at a wide range of pH.

1.6.4.2 Phage based magnetoelastic biosensors

Magnetoelastic materials transduce or convert magnetic energy to mechanical energy and vice versa. In an applied magnetic field, the ME sensor surface undergoes oscillating shape changes (elongation and contraction) thereby inducing a mechanical vibration. Depending on the adsorbed mass on the resonator, the increased mass will decrease the resonant frequency and this change can be measured.

Magnetoelasticity appears when, upon the application of an external magnetic field, the shape of the material changes due to the superposition of its internal magnetic moments by spin–orbital coupling. For a planar material in a given AC field, the fundamental resonance frequency (f) of the longitudinal vibration caused by magnetostriction can be described as follows:

$$f = \frac{\sqrt{E}}{\rho(1-V)2L} \qquad (3)$$

where E, ρ, v, and L represent the elastic modulus, the density, Poisson's ratio and the length respectively (Johnson ML et al, 2008).

And the mass adsorbed over the sensor's surface that affects the resonance frequency can be obtained from the following formula:

$$\Delta f = \frac{-f_0 \, \Delta \mathbf{m}}{2 \, M} \qquad (4)$$

where Δf is the change in resonance frequency, Δm is the change in the sensor's mass due to the attached load, and M is the original mass of the sensor. The negative sign indicates that the frequency will shift to lower values upon the binding of mass over the sensor surface. Figure 1.13 shows a schematic representation of the working principle of a magnetoelastic sensor.
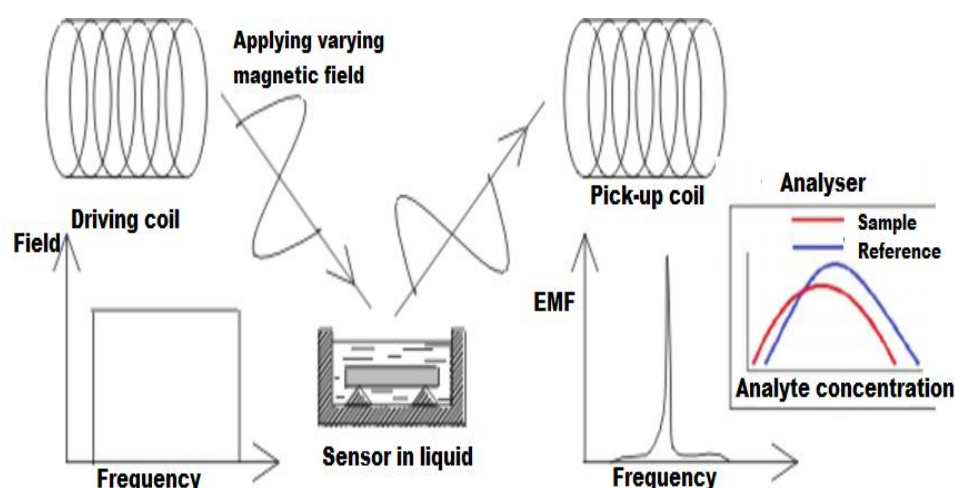
Figure 1.13 Working principle of a magnetoelastic biosensor (Adapted from department of chemical engineering, University of Patras, Greece)

In an alternating magnetic field, the magnetoelastic biosensor oscillates at its resonance frequency. When the physical parameter of the sensor changes due to the attachment of target molecules, it responds by altering the material properties of the magnetoelastic layer and thus its resonance frequency. Special electronics can be used to detect the resonance frequency and under suitable calibration, this physical parameter can be accurately measured.

Park MK and coworkers (2013) have developed a phage based ME sensor immobilized with filamentous E2 phage on an Au surface. The phage was genetically modified to specifically detect *Salmonella typhimurium* present on the surface of tomatoes. Using this approach they achieved a higher detection limit than could be achieved using sensitive quantitative PCR and this even without extracting the bacteria from the tomato.

1.6.5 Phage based Thermal Sensors- Heat Transfer Resistance

Recently, a real-time, label free sensing principle based on thermal resistance (R_{th}) or Heat Transfer Method (HTM) has been described by Van Grinsven and co-workers (2012). It is an interesting technique that relies on the morphological change of the bioreceptor molecule layer immobilized over the sensor surface upon the binding of its target. This change influences the efficiency of heat transfer through that biological layer and hence its thermal resistance.
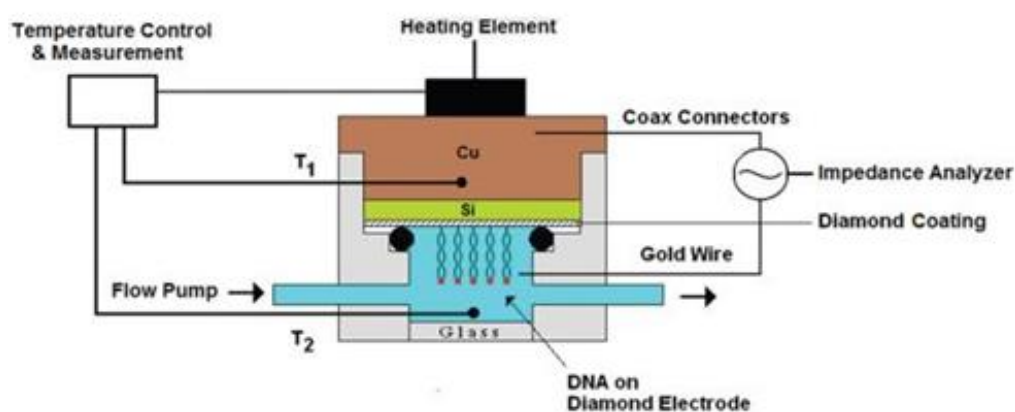
Figure 1.14 Working principle of an Rth sensor (Courtesy Van Grinsven et al, 2012)

In R_{th}, the temperatures T_1 from the copper and T_2 from the fluid are monitored and measured continuously. The difference between T_1 and T_2 depends on the quantity of analyte bound to the recognition element on the diamond surface. The R_{th} is deduced from the temperature difference, $T_1 - T_2$, and the input power from the heating element.

The R_{th} device is constructed using a diamond surface functioning as a working electrode. The diamond surface is in contact with a copper block at its back side, which serves as an electrical contact as well as a heat provider (figure 1.14). The top side of the diamond surface is functionalized with recognition elements and analyte is presented through the flow cell. A thermocouple is connected to the copper contact to measure, monitor and regulate temperature T_1 and to the liquid in the flow cell to monitor temperature T_2.

When heat is applied to the copper block, this heat is transferred through the diamond to the liquid in the flow cell above the diamond surface. The speed or

resistance to this heat transfer depends on the composition of the biological layer attached to the diamond surface and a difference in temperature between T_1 and T_2 is observed when biological material is present on the diamond surface that is acting as an insulating layer. When, applying a phage sample on Rth sensors, the thermal resistivity will be higher due the fact that the size of the phage is much larger as compared to other more abundant bioreceptor molecules.

1.7   Aim of the study and problem statement

The potential for diagnostic biosensors is rapidly growing due to their sensitivity, specificity and possible miniaturization. Developing such a biosensor with available potential biomarkers for a given disease is the first and critical step towards the disease diagnosis. In clinical applications, essential criteria such as speed and reliability can be achieved by reducing multistep processes and allowing real time measurements.

Phage display is a high throughput technique, in which the modification of one of its coat proteins results in the expression or display of the desired peptides on the phage protein coat. Bacteriophage have been used for displaying antibodies, biomarkers and peptides that show very specific interaction between the receptor molecule and its targets. However, there is a lack of a specific strategy to bring those phage displayed entities into different transducer platforms to address the need. Among the different types of phage, filamentous phage M13 has been used in most of the display processes and sensing platforms. Phage display was used in constructing cDNA libraries of interest, these phage libraries have been used for the selection of biomarkers displaying phage specific for a particular disease or disorder.

Once the selection of biomarkers displaying phage is achieved, phage ELISA is the technique mostly used to assess the quality of the selected biomarkers. For this horse radish peroxidase or other labels are needed in the assays. Phage assays were notorious for non-specific binding events, certainly when using complex samples like serum/ plasma which contains numerous proteins and antibodies. This results mostly in high signal to noise ratio and hence low sensitivity.

By considering the above problems, the main goal of this dissertation is to develop a phage sensor for the qualitative detection of Rheumatoid Arthritis (RA) biomarkers in patients' serum samples. Important objectives for this overall goal are (1) to develop a dual display phage system displaying a biomarker at one end and a capturing entity in the other end. (2) Finding a suitable capture entity which allows a selection process of displaying phage from complex samples and also supplies the possibility to attach phage firmly on a sensing platform. (3) Apply the resulting dual display phage systems, in high sensitive sensor platforms such as SPR, QCM and Rth to qualitatively assess the presence of that biomarker in a patient's sample. In order to achieve these striving objectives, milestones were set and following research questions were designed.

1) Can biotin like peptides serve as a good capturing peptide?
Streptavidin (STV) and biotin binding is the strongest non-covalent binding ever reported. It shows a high dissociation constant (KD) of about $\sim 10^{-15}$ M. Therefore biotin like streptavidin binding protein (SBP) could be a good option as a capturing protein. SBP contains a HPQ (His-Pro-Glu) motif which specifically binds to STV, its smaller size makes it easier to use in a fusion protein. Moreover the capturing peptide (SBP) will be flanked by restriction sites which allows the exchange of the capturing protein with other capturing structures in the future.

2) Can a dual display phage successfully be developed, by combining an RA biomarker displaying phagemid and a genetically fused capturing protein displaying system?
In order to achieve this, SBP will be introduced into a helper plasmid or in the traditional helper phage. Somers et al (2011), have identified a panel of biomarkers for RA using the serological antigen selection (SAS) technology as described before. One of the resulting autoantigenic targets from that study (RA21) is displayed in gene VI (gVI) of the phage. Because the RA21 biomarker is displayed at pVI of phage, SBP should be displayed either at the pVII or pIX of phage in order to provide an opposite displaying orientation. This approach also allows us to attach phage in a known orientation to a sensor surface as described below.

3) Can we achieve sample purification from complex sample mixtures using dual display phage?

One of the problems with phage assays on blood samples is the non-specific binding of different proteins to the sensor. To avoid this we will perform sample preparation by isolating a complex of dual display phage bound to autoantibodies from serum samples using STV coated magnetic beads. In this procedure the autoantigenic target displayed at one end of phage will bind with the serum autoantibody while the SBP in the other end will bind with STV coated magnetic beads. These phage complexes can subsequently be isolated form the patient serum by applying a magnetic field.

4) Will dual display and sample preparation provide more sensitivity as compared to the conventional single display system?

As stated before, the high signal to noise ratio is reducing the sensitivity of phage assays. We hypothesize that the above described sample purification in dual display phage assays will provide a higher sensitivity as compared to single display phage assays. It will reduce the background signal allowing a higher sensitivity towards the detection of the autoantibodies in patient samples.

The above four research questions are answered in chapter three.

5) Can dual display phage be applied in label free biosensing platforms to measure patient serum samples?

Similar to the sample purification approach, dual display phage with SBP introduced at one end of the phage in protein pVII and the autoantibody peptide RA21 at the other site in protein pVI will be used to immobilize onto the different sensor surfaces coated with STV. Our dual display system allows two types of approaches for the biosensor setup: either a phage probe based (STV-SBP) as described in chapter four or a phage complex based approach as reported in chapter five. STV coated biosensors that will be used are SPR and QCM to assess the binding of the phage. By studying the viscoelastic properties on QCM-D sensors, we can obtain more information about the phage binding characteristics. Also, the phage complex mediated assay onto a sensor surface will be carried out

in order to have a qualitative screening for autoantibodies in patient serum samples as discussed in chapter five for the different sensing platforms.

In SPR and QCM to assess the binding of phage. By studying the viscoelastic properties on QCM-D sensors, we can obtain more information about the phage binding characteristics. Also, the phage complex mediated assay on sensor surface will be carried out in order to qualitative screening for autoantibodies in the serum samples. And it has been discussed in the chapter five in different sensing platforms.

2

Materials and methods

This section gives an overview of the physiological reagents and chemicals, sensor setups and experimental procedures used in the following chapters.

2.1 Materials

MCPc helper plasmid with Chloramphenicol (Chlr) resistance in DH5αF' bacterial hosts was kindly provided by Prof. ARM. Bradbury´s lab (Las Alamos, USA). pspB RA21 phagemids and pspB empty phagemids with Amp resistance in TG1 bacterial hosts and positive control serum samples with different levels of RA-autoantibodies (highly positive, moderately positive, borderline positive) as well as negative control serum samples were produced in house. Helper phage with Kanamycin (Kan) resistance was purchased from GE healthcare (Diegem, Belgium). Ampicillin resistant IDTB vector containing SBP mini-gene gVII-SBP was purchased from IDT (Leuven, Belgium). All the restriction enzymes used were purchased from Takara Bio Inc (Japan). For plasmid and phagemid purification from host bacterial cells the Qiagen midi prep kit from Qiagen (Antwerp, Belgium) was used. Ready to use 2x YT broth and agar were supplied by BD (Erembodegem, Belgium) and LB broth and agar were supplied by Invitrogen (Ghent, Belgium). Streptavidin (SO677) was obtained from Sigma Aldrich, Belgium. Streptavidin coated magnetic beads were purchased from Invitrogen (Ghent, Belgium). Serum autoantibodies (UH_RA.21 antibody positive or positive control) and negative control (UH_RA.21 antibody negative) serum were produced in house. Au coated AT-cut quartz crystals (diameter 14 mm, thickness 0.3 mm, surface roughness 3 nm and resonant frequency 4.95 MHz QCM-D crystals) were purchased from Q-sense, Sweden. The EDC and NHS were bought from Thermo Scientific, West Palm Beach, USA. SPR chips (SA and CM 5) were purchased from GE Healthcare, Sweden.

2.2 gVII-SBP mini-gene cloning into the genome of the M13cp helper plasmid

Restriction enzymes SnaB I and Bsp1407 I were used to replace the gVII of the helper plasmid with the SBP minigene. 5 µl of ligation product was then transformed into a freshly prepared chemically competent DH5αF' bacterial strain, by subjecting the bacteria to a heat shock at 42 °C for 30 seconds, after which they were plated on LB agar plates with 15 µg/ml of the antibiotic Chlr and

incubated overnight at 37 °C. A negative control was also prepared by transforming unmodified M13cp to DH5αF' bacterial strain. DH5αF' cells already containing the Chlr-resistant M13cpSBP or M13cp helper plasmid were prepared to be competent and co-transformed with Amp-resistant phagemid pspB, either empty (pspB), or bearing the cDNA of the autoantigenic target RA21 fused to its pVI gene (pspB RA21), in the same way as with the helper plasmid. The newly co-transformed DH5αF' colonies were plated in 2x YT media containing 15 µg/ml of Chlr and 100 µg/ml of Amp.

2.3 Colony PCR and sequencing

Positive colonies of helper plasmid transformed with SBP minigene were grown in antibiotic selective plates and were used in colony PCR using the forward primer 5'-AAT GTT CCG TTA GTT CG-3' and reverse primer 5'-CCA TTA AAC GGG TAA AAT AC-3' (Eurogentec; Seraing, Belgium). The primer sets used for phagemids were gVI forward primer 5'-TTA CCC TCT GAC TTT GTT CA-3' and the pUC 19 reverse primer 5'-CGC CAG GGT TTT CCC AGT CAC GAC-3'. The thermocycling conditions included an initial denaturation at 95 °C for 7 min, followed by 30 cycles comprising of a 30 s denaturation step at 95 °C, a 30 s annealing step at 55 °C, and a 4 min elongation step at 72 °C, and one final elongation step carried out at 72 °C for 10 min. The PCR products obtained, have been used without any further purification in sequencing with the forward primers mentioned above using ABI PRISM Genetic Analyser 310 (Applied Biosystems (Warrington, UK)). The sequences were analyzed using Chromas software version 2.13 and with DNAMAN version 7.0.

2.4 Phage production

Dual (SBP and RA21) and single (SBP or UH_RA.21) display phage were produced from the double transformed DH5αF' bacterial cells. A single colony was picked and grown until they attained an exponential growth rate in 2x YT medium containing 15 µg/ml of Chlr and 100 µg/ml of Amp. Then, 4 ml of exponentially growing cells were transferred into 50 ml of fresh 2x YT broth medium with both antibiotics. Subsequently, they were incubated in a shaking incubator at 200 rpm for 16 to 18 hours at 31 °C. Afterwards, all the bacterial cells were removed by centrifuging at 4000 rpm, and the supernatant was treated with 20% 6000 MW

PEG (Merck (Darmstadt, Germany)) in 2.5 M NaCl and kept on ice for 1 hour. White phage pellets were collected by centrifugation at 4000 rpm for 20 min and were washed with 1x PBS buffer. Four different phage types were prepared using helper plasmid and phagemid: SR 21 are phage displaying SBP and UH-RA.21 (dual display phage), SB are SBP displaying phage (single display), CR 21 are UH-RA.21 displaying phage (single display) and CB are non-displayer or empty phage.

In addition to produce a positive control phage called Std 21, TG1 bacterial cells bearing the phagemid pspB RA21 were grown up to the exponential phase and 10 ml of exponentially grown cells were infected with 5 µl of M13KO7 helper phage for 30 min in a 37 °C water bath. The culture was then incubated in a shaking incubator for 10 min at 100 rpm at the same temperature. The infected cell culture was added to fresh 2x YT medium containing 100 µg/ml Amp and 40 µg/ml Kan and incubated overnight at 30 °C. After the phage production, the amount of phage was tittered using the PR phage titration kit (Progen, Biotechnik GmbH; Germany). The absorbance values of phage samples were extrapolated with the standard graph made from the absorbance values of the known phage standards from the kit.

2.5 Phage ELISA

In order to check the SBP phage display, ELISA micro titer plates (Greiner Bio-One BVBA, Wemmel, Belgium) were coated overnight with 5 µg/ml anti-pVIII antibodies. For the detection of the RA21 phage display and dual expression at the phage surface, ELISA micro titer plates were coated overnight with 10 µg/ml anti-human IgG antibodies (Dako, Denmark) as shown in table 2.1. Afterwards, the plates were washed twice with 1x PBS buffer. The wells were blocked with 5% Marvel skim milk powder (Chivers, Dublin Ireland) in 1x PBS buffer (MPBS) for 2 hours at 37 °C while shaking. After blocking, the plates were washed three times with 1x PBS buffer containing 0.1% of tween 20 (PBST) and once with 1x PBS buffer. All the phage samples were diluted to 10^{12} colony forming units (CFU)/ml in 5% MPBS. In order to confirm the RA21 and dual expression, 100 µl of 1x 10^{12} CFU/ml of phage in 5% MPBS was first pre-incubated with 100 µl of 100-fold in 5% MPBS diluted RA patient sera having different levels of anti-RA21 autoantibodies (highly positive, moderately positive, borderline positive, and

negative (healthy control)) at 37 °C for 30 min under static conditions and for 30 min while shaking at 100 rpm. For the evaluation of dual expression using magnetic beads, 1 µl of 10 µg/µl (3-6 x 10^6) streptavidin coated magnetic beads (Invitrogen (Ghent, Belgium) were added to the phage serum mixture and incubated again at 37 °C for 30 min while shaking.

Table 2.1 Components used in phage ELISA protocols

Target assay	Coating antibody	Sample	Detection antibody / entity
SBP	Anti M13	Phage	Streptavidin HRP
UH-RA.21	Anti human IgG	Pre-incubated phage and serum	Anti M13 HRP
Dual display	Anti human IgG	Pre-incubated phage serum and streptavidin bead	Anti M13 HRP

Different protocols were used in phage ELISA experiments for the evaluation of SBP displaying, UH-RA.21 displaying phages and autoantibody screening.

The phage-serum-bead complexes were isolated using a magnet, washed twice with 5% MPBS to remove unbound phage or remaining serum, re-suspended in 5% MPBS and further used in a phage ELISA. The same phage-serum-bead complexes in 1x PBS buffer (no blocker) were also used in biosensing platforms in chapter five.

For the evaluation of SBP display on phage, 100 µl of pure 10^{12} CFU/ml phage was added to the ELISA wells. For the confirmation of RA21 expression, 100 µl of the pre-incubated phage and serum samples were added to the wells. In the dual expression ELISA, 100 µl of the pre-incubated phage/serum/bead complex was added to the ELISA wells. All ELISA wells were incubated for 1 hour under static conditions and for 30 min. while shaking at 37 °C. After washing the plates as described above, 0.83 µg/ml of a streptavidin-HRP conjugate was added for the

detection of SBP and incubated for 1 hour at RT while shaking. In the RA21 and dual expression experiments, polyclonal anti-M13 antibodies conjugated with HRP from the phage titration kit were added as secondary antibodies. After washing, ready-to-use TMB and H_2O_2 (Thermo Scientific (Erembodegem, Belgium) was used as a substrate solution for HRP, inducing a color reaction and 2 M H_2SO_4 was used as a stop solution. The ELISA plates were measured at a wavelength of 450 nm to get the absorbance values.

2.6 Dot Blotting

Different 5 µl spots containing 10^{13} CFU/ml of phage were applied to a Whatman nitrocellulose membrane filter paper (Whatman GMBH, Germany). The spots were allowed to dry for 15 min and then the surface was blocked with 5% MPBS buffer for 15 min. After rinsing 2 times in 1x PBS buffer, the nitrocellulose filter paper was treated with 0.83 µg/ml of streptavidin-HRP for 1 hour at RT while shaking. The paper was washed 3 times with 1x PBS buffer containing 0.5% Triton™ X-100 and twice with 1x PBS buffer. Finally, fresh DAB and H_2O_2 (Thermo Scientific, Erembodegem, Belgium) solution was added to develop the colored spots.

2.7 Atomic Force Microscopy (AFM)

Phage stocks were diluted with Milli-Q (MQ) water to a concentration of 10^{11} cfu /ml in order to reduce the salt concentration and to avoid crystal formation. 100 µl of the phage sample was placed on a 1 cm^2 silicon wafer, incubated at RT for 1 h, and then washed twice with MQ water. The wafer was allowed to air-dry for a few minutes and was kept at 4 °C overnight. The AFM used was NX 10 (Park Systems, Suwon, Korea). Non-contact mode was employed in this study with a rectangular silicon tip at a frequency of 300 kHz. The cantilever has a force constant of 25 to 70 N/m and a spring constant of 40 N/m. The XEI Park Systems software 2.0 was used for image acquisition.

2.8 Biosensing platforms

2.8.1 Characterization of SBP display in phage and immobilization onto STV functionalized sensing platforms

2.8.1.1 Phage immobilization on STV surfaces of Quartz crystal microbalance with dissipation monitoring (QCM-D)

The Au-coated quartz sensors were cleaned with a 5:1:1 mixture of Milli-Q water (conductivity of 0.055 S cm^{-1} at 25 °C) ammonia and hydrogen peroxide, and were UV-ozone treated with a Digital PSD series UV-ozone system from Novascan for 15 min, followed by rinsing in Milli-Q water and drying with N$_2$. For all the measurements, we have used QCM-D on a Q-sense E4 instrument (Gothenburg, Sweden) to monitor the frequency shift Δf and the dissipation change ΔD. The changes in Δf and in ΔD were monitored at three different overtones (from 3rd to 7th) in a continuous flow mode with a rate of 100 μl/min over plain Au coated QCM-D sensors. All measurements were performed at 20 °C.

The procedure carried out for each type of phage can be summarized as follows. After a baseline in 1x PBS buffer was established in plain Au crystal or in biotinylated crystals, 25 µg/ml of STV in 1x PBS buffer was injected until saturation was observed. 1x PBS buffer was flushed to remove unbound STV from the surface and to check the stability of the adsorbed layer. Then, 1x10^{11} CFU/ ml of phage samples were injected for 20 minutes and flushed with 1x PBS once more to remove the unbound phage from the crystals.

2.8.1.2 Phage immobilization on STV surfaces for Surface Plasmon Resonance (SPR)

All four phage samples have been diluted to 1x10^{11} CFU per ml in 1x PBS buffer and the predesigned immobilization protocols have been used while keeping 1x PBS as running buffer with a flow rate of 12 µl/min and the flow duration as 500 seconds. Flow cell 1 (FC 1) was immobilized with CR21, FC 2 with SR21, FC 3 with CB and FC 4 with SB phage. The immobilization response values were monitored for all four phage preparations. SA chips of Biacore are 3-D chips containing a dextran matrix pre-immobilized with STV. The affinity binding of dual displaying phage to STV was monitored on these BIACORE streptavidin-functionalised chips

(SA sensor chips, GE Health care, Belgium). SPR measurements were performed on a Biacore T200 instrument (GE Healthcare, Uppsala, Sweden) in PBS running buffer at constant temperature of 25°C.

2.8.2 Screening of autoantibodies in patient serum samples
2.8.2.1 QCM-D

For the screening of autoantibodies present in patient serum samples, first, anti-human IgG was immobilized on the sensing platform by introducing 10 µg/ml anti-human IgG in 1x PBS buffer over plain Au coated QCM-D sensors with a flow rate of 100 µl/min while the temperature was kept constant at 25°C. After saturation of the sensor surface, unbound anti-human IgG were removed by flushing the system with 1x PBS buffer. Next, phage complexes (positive and negative as described before) were introduced with a flow rate of 100 µl/min in the corresponding cells and subsequently rinsed with 1x PBS after saturation was completed.

2.8.2.2 SPR

A CM5 chip of Biacore was covalently immobilized with 1 µg/ml concentration of Anti human IgG using an amine coupling (10 mM EDC (1-ethyl-3-(3-dimethylaminopropyl) carbodiimide) and 10 mM NHS (N-hydroxysulfosuccinimide)) strategy as instructed by the manufacturer in a pre-designed program of the SPR Biacore T200 system. Ethanolamine was used as blocking agent and 1 x PBS used as a running buffer throughout the experiment. Both negative and positive complexes has been flushed alternatively for 300 sec. Finally the chip was regenerated using 2.25 pH glycine HCl.

2.8.2.3 Thermal Resistance (Rth)

Equal amounts (50 mg/ml) of EDC and NHS were dissolved in 25 mM MES buffer. The Wide Band Gap Materials (WBGM) group at the Institute for Materials Research (Prof. Dr. Ken Haenen, IMO, UHasselt), provided us with synthetic Nano Crystalline Diamond (NCD). Boron (B)-doped NCD was prepared using chemical vapour deposition (CVD), hydrogenated and functionalized with 10-undecanoic fatty acid via photochemical attachment as is shown in figure 2.1. Of the EDC-NHS mix, 100 µl was applied onto such a 10-undecanoic acid-functionalized NCD

sample and incubated for 30 min at RT before washing once with 25 mM MES buffer. Subsequently, 1 µg/ml of polyclonal rabbit anti-human IgG was added and allowed to incubate for 1 h. This was blocked with 100 mM ethanolamine for 30 min. at RT. The autoantibody/phage/magnetic bead complex was incubated on the NCD surface for 90 min. at 37 °C and then rinsed twice with 100 mM MES buffer. At this stage, the functionalized NCD samples were mounted into the Rth setup. The sensor cell used for the Rth measurements, displayed in figure 1.14, was initially developed and constructed by the Biosensor group at IMO. The functionalized NCD sample was mounted into the Rth setup by attaching it with its silicon backside to a copper block via silver paste. An O-ring was placed on the
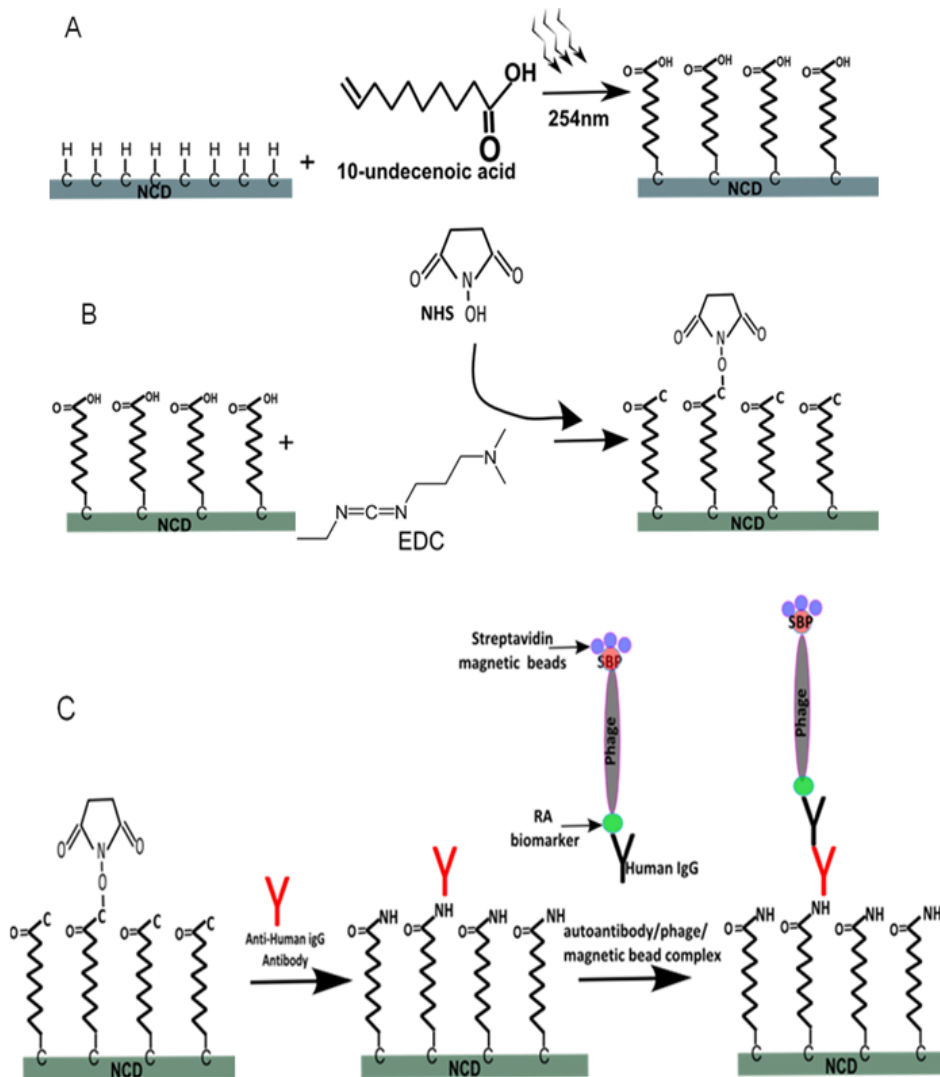
Figure 2.1 Bio-conjugation of an antibody to an NCD surface

A) The hydrogenated NCD was covered with 10-undecanoic acid and irradiated with UV light to form carboxyl groups on the NCD surface. B) Carboxylate (COOH) reacts with NHS in the presence of EDC forming a semi stable NHS ester which reacts with primary amine to form amide crosslink. C) With the help of amide crosslink, the antibody is covalently coupled to the NCD surface, allowing the capture of the autoantibody/phage/magnetic bead complex.

functionalized side of the NCD surface to mark the sensing area and the system was closed to form a flow cell. 1× PBS buffer was flowed through the setup at a rate of 325 µl/min. To observe how stably the phage complex is bound on the anti-human IgG coated NCD surface. Heat is regulated by applying a potential of 0 to 10 V to the copper block, which has a resistance (R) of 22.2 Ω.

The temperature is measured at two locations: in the copper block (T1) and in the liquid (T2). The temperature of the copper block (T1) was fixed at 40 °C. When analytes are present on the NCD surface, they insulate the NCD surface, and an increase in Rth is observed from the copper block (T1) to the liquid in the flow cell (T2) as compared to the Rth of a naked NCD sample. The Rth was calculated as follows:

$$Rth = (T1 - T2)/P$$

Where T1 is the temperature of the copper block, T2 is the temperature in the liquid and P is the power of the system needed to control the temperature.

The power (P) was calculated as follows:

$$Power = V^2/R$$

Where V is the applied voltage and R is the resistance of the device, which is 22.2 Ω.

2.9 Evaluation of phage capturing on NCD using Light microscopy

The difference in surface of NCD incubated with positive complex and negative complex was evaluated with the aid of Axio Zoom V.16 fluorescence microscope from Carl Zeiss Microscopy GmbH, Germany. Images were collected using the Zen software (blue edition) version 1.0.1.0, also from Carl Zeiss Microscopy GmbH.

2.10 Statistical analysis

Statistical analysis was performed using a GraphPad InStat version 3.1. Non-parametric ANOVA (Kruskall-Wallis testing) and Dunn's multiple comparison tests were used to compare the reactivity against the serum samples with the different

levels of anti-UH-RA.21 positivity. The levels of statistical significance were as follows: a P-value of <0.05 (*), a P-value of <0.01 (**), and a P-value of <0.001 (***).

3

Construction of a dual display phage and phage ELISA based screening for autoantibodies

Based on:

Construction of helper plasmid mediated dual-display phage for autoantibody screening in serum

Kaushik Rajaram, Veronique Vermeeren, Klaartje Somers[†], Veerle Somers, Luc Michiels

Biomedical Research Institute, Hasselt University, Martelarenlaan 42, 3500 Hasselt, Belgium.

[†]Complix NV, BioVille, Agoralaan building A-bis, 3590 Diepenbeek, Belgium

3.1 Abstract

M13 filamentous bacteriophage has been used in displaying disease specific antibodies, biomarkers and peptides. One of the major drawbacks of using phage in diagnostic assays is the aspecific adsorption of proteins leading to a high background signal and decreasing sensitivity. To deal with this, we developed a genetically pure, exchangeable dual display phage system in which biomarkers and streptavidin binding protein (SBP) are displayed at opposite ends of the phage. This approach allows for sample purification, using streptavidin (STV) coated magnetic beads resulting in a higher sensitivity of signal detection in assays. Our dual display cassette system approach also allows for easy exchange of both the anchor protein (SBP) and the displayed biomarker. The presented principle is applied for the detection of antibody reactivity against UH-RA.21 which is a good candidate biomarker for rheumatoid arthritis (RA). The applicability of dual display phage preparation using a helper plasmid system is demonstrated and its increased sensitivity in phage ELISA assays using positive control and negative control serum samples are shown.

3.2 Introduction

Phage display has taken its stand in the era of molecular biology in the last two decades by displaying a large number of proteins, antibodies, amino acids, etc... on the surface of phage (Reynolds F et al, 2011; Soendergaard M et al, 2011). There were different *in-vitro* display techniques has been reported over the years such us, bacterial and yeast surface display (Daugherty PS, 2007), mRNA display (Amstutz P et al, 2001), ribosomal display (Mattheakis LC et al, 1994) etc... Though, phage display technique hold its stand firmly and still used as an *in-vitro* display platform in many industries and research labs. The non-lytic M13 filamentous phage is a single-stranded (ss) DNA virus that infects a number of gram-negative bacteria. A phage particle consists of a long cylindrical protein structure, 800-900 nm in length and 6.5 nm in diameter. Phage are considered as bio-macromolecules with a molecular weight of approximately 16000 KD (Mu Y et al, 2005). It has one major coat protein, pVIII, that surrounds the entire phage body with 2700 copies, and each end has two minor coat proteins (pVII, pIX and pVI, pIII), each present in 3-5 copies. All these coat proteins contribute to the stability of the phage (Sidhu SS, 2001; Sidhu SS, 2000; Arap MA, 2005). The phage genome carries the genes for these five coat proteins and the genes for the proteins involved in phage replication. Phage display involves the fusion of a foreign peptide or protein with a minor or major coat protein of the phage through genetic recombination of the phage genome with the cDNA of the insert, resulting in the phage particle displaying the peptide or protein fused to the coat protein, and also possessing the gene of the protein insert, providing a direct link between the phenotype and the genotype (Dover et al. 2011). The size of the phage is rely upon its size of the genome, bigger DNA makes bigger phage.

Between the two popular vector systems, using a phagemid vector system to produce functional phage particles is better than using a phage vector, showing a good display level of the fusion protein, and being genetically more stable in displaying larger proteins (Sidhu SS, 2001). However, a phagemid vector carries only the gene for the coat protein to which the cDNA of the protein of interest is fused. So, after transformation of the bacterial host with phagemid, it needs a co-infection from a helper phage to provide the native genes for all the other structural proteins to make a complete and functional phage. The genome of the

helper phage lacks a packaging signal, so the genome of the phagemid vector will preferentially get packaged into the new phage particles, retaining the link between the phenotype and the genotype of the phage (Qi H et al, 2012; Bratkovic T, 2010). Chasteen L and coworkers proposed a different vector system as an alternative to the use of helper phage, making use of helper plasmids, providing multivalent display and genetically pure phage (Chaseteen L et al, 2006). As with the helper plasmid/phagemid vector system, phage produced by this method contains only the genome of the phagemids.

Protein aggregation and lack of protein transfer to the bacterial periplasm is often observed and results in failure of phage display. This problem can be addressed by the introduction of a leader peptide or signaling peptide into the fusion protein. However, the correct folding can be compromised due to the secretion of the phage from the host (Velappan N et al, 2010). Therefore coat proteins pVIII and pIII are commonly used for protein display because those genes contain N-terminal periplasm-directing signal sequences. By introducing such a signal sequence between the N-terminus of pVII or pIX and the cDNA of the protein of interest, it becomes possible to develop a stable display system using those coat proteins as well (Georgieva Y et al, 2012 and Loset GA et al, 2011). There is a persisting demand for suitable disease related biomarkers as indicators for diseases, like proteins, peptides, metabolites, and antibodies (Vithayathil et al, 2011). The capability to display disease-specific proteins on a phage surface could be a big advantage in the field of diagnostics. Phage can be directly used as a probe when it is modified to display disease-related antigens on its surface (Kierny MR et al. 2011). Also, problems associated with synthesizing small molecules can be overcome by phage display (Dudak FC et al. 2011). This would involve the phage in the development of diagnostic biosensors, functioning as a receptor, attached to an electrode or transducer surface. Increasing attention has been drawn towards the use of phage as a receptor molecule in different applications, due to its inherent stability and resistance to denaturation in unfavorable conditions, unlike DNA and antibodies. It can sustain higher temperatures of up to 70°C and pH variations from 2.5 to 12 (Arap MA, 2005 and Mao C et al, 2009).

Phage production is also cost-effective, in contrast to the production of monoclonal antibodies. They can be produced in sufficient numbers by just infecting a bacterial host. Phage based assays are mostly performed in an ELISA format, however if complex substances such as serum are used in detecting targets, this approach lacks sensitivity due to aspecific binding of interfering serum components increasing the background signal (Roy MD, 2008). The same problem can be expected in the above mentioned biosensor setups. Therefore sample preparation should also be taken into account when setting up such assays.

The design of a dual display system, where phage display both a biomarker and a capturing protein allows for such a sample preparation. In the presented approach the dual display phage will display a biomarker fused to pVI at one end and an anchoring SBP fused to pVII at the other end of the phage. SBP will be binding to STV-coated magnetic beads allowing a magnetic capturing of the phage. As a proof of principle, a candidate biomarker for Rheumatoid Arthritis (RA) UH-R.A21 (Somers K et al, 2011; Somers V et al, 2005) is used to screen for the presence of autoantibody reactivity in the serum of RA patients in comparison to basic ELISA procedures.

3.3 Results

3.3.1 Construction of the M13cpSBP helper plasmid
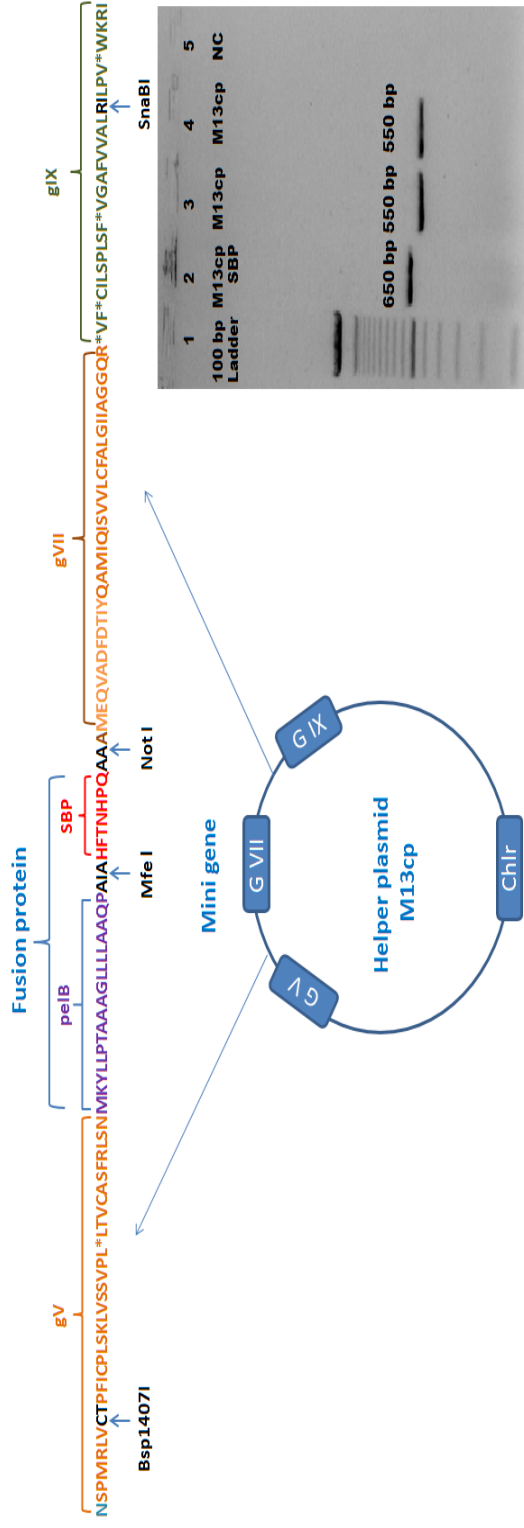
Figure 3.1 Construction of the helper plasmid M13cpSBP

A minigene was constructed in which PelB (purple) and SBP (red) coding sequences are inserted upstream of the gVII gene of wild-type M13cp phage DNA. The SBP sequence is flanked by the restriction sites Not I and Mfe I. The entire gVII-SBP minigene is located between gV and gIX and is contained between the restriction sites SnaBI and Bsp1407I. Figure 3.1 insert-A 1 % agarose gel demonstrates the successful insertion of SBP and PelB into gVII of M13cp. Lane 1, 100 bp ladder; lane 2, recombinant M13cpSBP construct; lanes 3 and 4, wild-type M13cp; and lane 5, negative control. Sequencing of the M13cpSBP confirmed the in-frame insertion of the SBP and pelB sequences as shown in the presented sequence

Displaying proteins, such as SBP in this case, on pVII is feasible but only if the cDNA of the insert is placed between the gVII start codon and a signaling or a leader peptide (Loset GA et al. 2011; Kierny MR et al. 2011). Figure 3.1 shows the design and construction of the helper plasmid M13cpSBP. The most common signaling peptide PelB is used to ensure the correct folding of SBP and its transport to the bacterial membrane, and eventually to the phage surface (Kwasnikowski P et al, 2005). A predesigned SBP minigene consisting of the cDNA of the signaling peptide sequence PelB and the cDNA of SBP is inserted upstream of the start codon of gVII of the helper plasmid M13cp (Figure 3.1). This SBP minigene was designed between two restriction sites SnaB I and Bsp1407 I which allows easy insertion into the gVII of the wild type helper plasmid M13cp. In addition to this, the coding sequence of the anchor peptide SBP itself is flanked with two different restriction sites Not I and Mfe I, which makes SBP easily interchangeable with another type of anchoring peptide. The resulting SBP modified helper plasmid was termed M13cpSBP, and it was transformed into a DH5αF' bacterial host. As a negative control unmodified helper plasmid M13cp was also transformed. After transformation, successful insertion of the SBP mini-gene into the helper plasmid M13cp was confirmed by colony PCR and sequencing. Figure 3.1 insert shows the ~100 bp longer fragment of M13cpSBP (lane 2) as compared to unmodified M13cp (lane 3-4) the sequence of the resulting construct shown in Figure 3.1 was confirmed by sequencing analysis.

3.3.2 M13cpSBP and wild type phage production

In order to produce phage particles, a helper plasmid always needs support from a phagemid, since a helper plasmid lacks a packaging mechanism. So, Dh5αF' cells bearing either modified M13cpSBP or unmodified M13cp helper plasmid were cotransformed with pspB carrying UH-RA.21 and pspB phagemids (Somers K et al, 2011) without insert (empty phagemid) and plated on 2x YT plates containing Chloramphenicol (Chlr) and Ampicillin (Amp).
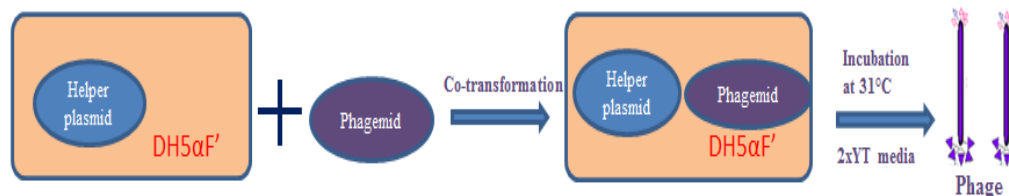
Figure 3.2 Dual display phage production

Graphical representation of the cotransformation and resulting phage preparation DH5αF′ host bacteria, containing the M13cpSBP or M13cp helper plasmid, were cotransformed with UH-RA.21 autoantigenic target bearing or empty phagemid. Bacteria containing both plasmids were grown in 2×YT medium to produce phage particles.

These antibiotics are used to select bacteria containing both helper plasmid (with and without SBP) and phagemid (with and without UH-RA.21). A schematic overview of the cotransformation and phage production procedure is shown in Figure 3.2. Chlr and Amp resistant cells were subjected to colony PCR and the resulting products were analyzed by gel electrophoresis (Figure 3.3 A). The colony PCR products show the additional 600 bp in the SR21 phage (lanes 2-4) corresponding to the UH-RA.21 marker, as compared to the SB phage (lane 5-7). Sequencing analysis (Figure 3.3 B) confirmed the sequences of RA21 (Somers K et al, 2011). One of the confirmed positive SR21 colonies containing the two targets SBP and RA21 was selected for phage production in 2x YT medium. This helper plasmid mediated phage production leads to genetically pure phage, because the M13cp helper plasmid does not have any packaging signal and delivers only proteins. The phagemid genome, carrying the gVI displayed UH_RA.21 cDNA is preferably packed into each phage (Chasteen L et al, 2006). Titer values of all the phage particles produced range from 1x 10^{13} to 5.5 x 10^{13} CFU/ml.
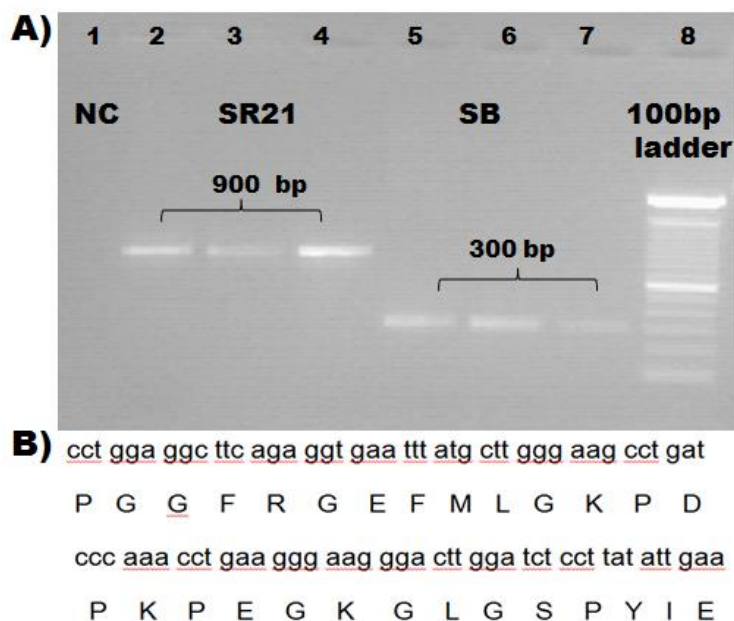
Figure 3.3 Cotransformation of DH5αF' cells with pspB phagemids

1 % agarose gel demonstrating the difference of ~600 nucleotides, corresponding to the 28 amino acids of the UH-RA.21 marker and the linker sequences between the dual-display phage SR21 (lanes 2, 3, and 4) and the single-display phage SB (5, 6, and 7). Lane 1 shows the result of the colony PCR for RA21 performed on DH5αF' bacteria cotransformed with native pspB. B) Sequence analysis confirms the in-frame sequences of RA21 and its translation product is shown.

This way four different phage samples were prepared using this approach as is summarized in Table 2.1. The standard positive control phage (Std21) which has been used previously in conventional phage ELISA protocols (Somers K et al, 2011), is prepared differently by infecting a bacterial host containing UH_RA.21 in pspB phagemids with helper phage M13, result in phage displaying RA21 at pVI of the phage and contains other wild type proteins from helper phage M13.

Table 3.1 Phage titration assay

Name of the phage	Displayed protein	Titer in CFU in 10^{13}
SR21	SBP and RA21	2.4
SB	SBP	2.1
CR21	RA21	1.7
CB	----	3.1
Std21	RA21	5.3

The first four phage are the different types of phage produced using phagemid and helper plasmid system. Std21 is the conventional phage prepared and used as a positive control in phage ELISA.

3.3.3 Dual display phage size determination using AFM
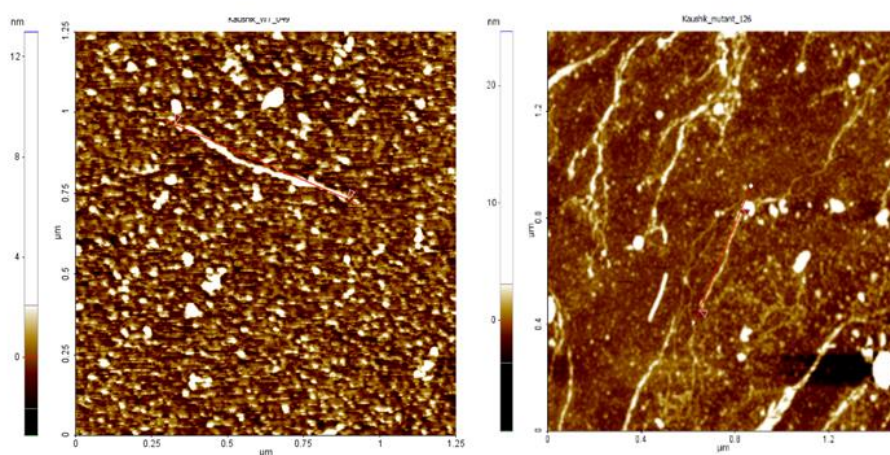
Figure 3.4 AFM images to characterize phage size

A) AFM image of phage produced by infection of the Dh5αF' bacteria with helper phage, showing a length of 623 nm and a diameter of 2.14 nm. B) AFM image of phage produced by transformation of the Dh5αF' bacteria with M13cp helper plasmid, showing a length of 429 nm and a diameter of 1.43 nm.

Phage were produced as described in Materials and Methods and titrated using the Progen PR phage titration kit. Considering that the genome of the phagemid only contains the biomarker-gVI fusion and that the genome inside the resulting phage determines its size, the size of phage produced through cotransformation of Dh5αF' bacteria with helper plasmid and phagemid is quite small and provides a direct link between the genotype and phenotype. On the other hand when helper phage are used instead of helper plasmid, some helper phage genomes are also packaged. Therefore the resulting phage particles consists of a mixture of both phagemid and helper phage genome containing phage.

In order to get some more insight, AFM experiments have been carried out on phage produced either by infection of Dh5αF' bacteria with helper phage and compared with phage produced using M13cp helper plasmids. Differences were observed in both length and diameter of the resulting phage. Phage produced using helper phage have a length of 623 nm and a diameter of 2.14 nm (Figure 3.4 A) while those produced by M13cp helper plasmid had a length of 429 nm and a diameter of 1.43 nm (Figure 3.4 B).

The standard length of phage in literature varies between 700-800 nm depending on their genome size and they have a fixed diameter of 6.5 nm. Phage that are produced by infection of bacteria with helper phage did show a length close to the standard phage but its diameter is much smaller than that of the phage reported in literature. This reduction may be due to the way phage were prepared for AFM analyis. The AFM samples need to be air-dried, which may have caused the phage to shrink. On the other hand, we observed that phage produced by the cotransformation of bacteria with M13cp helper plasmid had a much smaller size in terms of diameter and length as compared to phage produced by infection with the helper phage. On top of the genetic purity of the produced phage, the smaller size of the produced phage could be exploited on sensing platforms, taking advantage of the smaller size to increase the immobilization density, and hence, the sensitivity.

3.3.4 Evaluation of SBP expression

Theoretically, phage SR21 and SB should display SBP on all five copies of the coat protein pVII of the phage particle, due to the lack of native gVII in the pspB phagemid. Moreover, SBP can be displayed at a higher local concentration due to the small size of pVII and the tightly packed system (Kwasnikowski P et al, 2005). This is evident from the immediate strong colour formation in a dot blotting experiment, as shown in Figure 3.5 A.
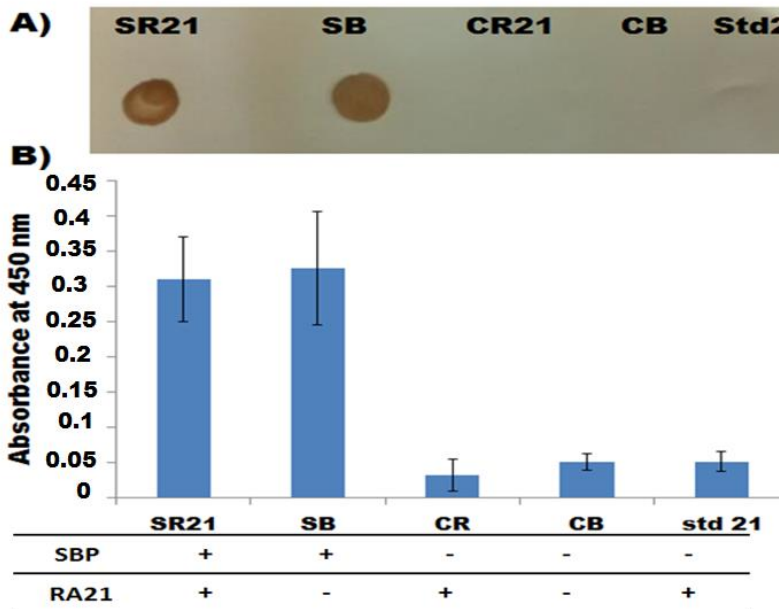
Figure 3.5 Expression of SBP in pVII in displaying phage

Expression of SBP in pVII in displaying phage. The expression of SBP was analyzed in four types of phage (SR21, SB, CR, and CB) produced through the helper plasmid/phagemid system and compared to phage (Std21) produced through the helper phage/phagemid system. A Dot blot shows the four types of phage and the Std21 phage on a nitrocellulose paper, using a SBP-dependent color reaction. B) Phage ELISA on anti-pVIII-coated plates, treated with the four types of phage and the Std21 phage, and detected with a STV-conjugated HRP and a TMB-dependent color reaction.

Among the five different phage preparations, the dual display phage SR21 and one of the single display phage, SB, are positive while the other phage types remain negative. This was confirmed in a phage ELISA format, as shown in Figure

3.5 B, in which SR21 and SB show a six fold absorbance compared to the negative phage CR21 and CB. As a control in both experiments, phage produced from the cotransformation of DH5αF' with SBP-negative helper phage and pspB carrying RA21, referred to as Std21, were also checked for SBP expression, and were found to be negative for SBP expression.

3.3.5 Screening of RA patient sera using UH-RA.21 displaying phage
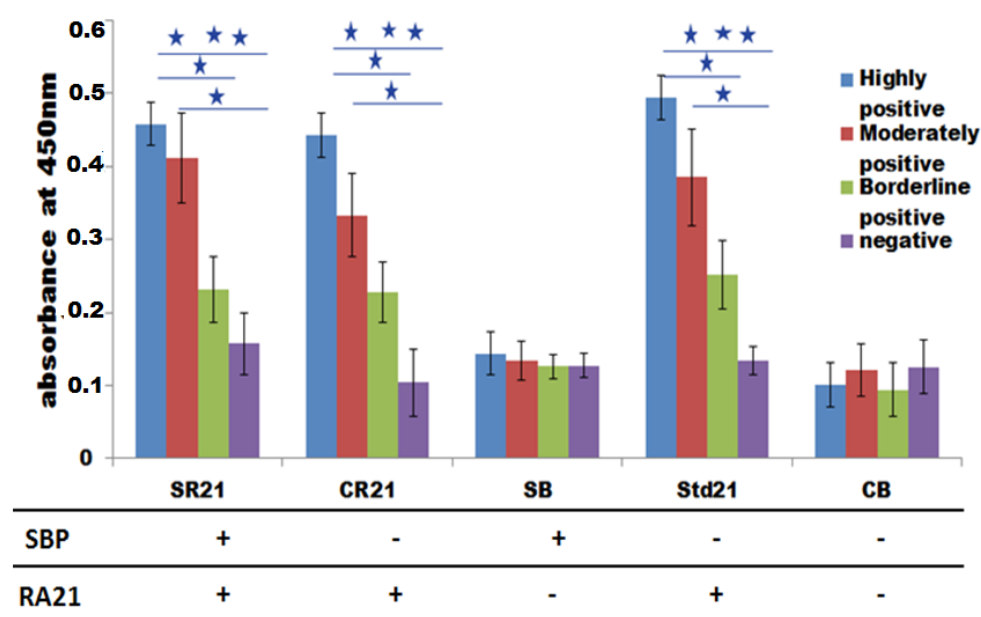
Figure 3.6 Evaluation of UH_RA.21 Display in phage ELISA

RA patient sera were screened for the presence of autoantibodies with RA21 displaying phage preparations. All four types of phage (SR21, CR21, SB, and CB) were produced through the helper plasmid/phagemid system as compared to phage (Std21) produced through the helper phage/phagemid system by phage ELISA. The four types of phage and the Std21 phage were pre-incubated with serum that was highly positive (blue), moderately positive (red), borderline positive (green), and negative (violet) for antibody reacting against UH-RA.21 and captured onto anti-human IgG-coated ELISA plates. The statistical comparison of the phage ELISA results among the sera with different levels of autoantibody positivity has been given in the form of stars (*/**/***) which corresponds to the approximate P values of $P<0.05$ (significant), $P<0.01$ (good significant), and $P<0.001$ (excellent significant) respectively. This experiment was carried out three times, with each condition in duplicate.

As a proof of concept we have used one of most promising RA autoantigenic targets RA21 which was displayed on pVI of the filamentous phage M13 (Somers K et al, 2009; Somers K et al, 2011). The expression of RA21 was evaluated in phage ELISA using sera from RA patients who were classified according to the amount of autoantibodies present in their serum (either highly positive, moderately positive, or borderline positive), and serum from healthy controls who are negative for anti-RA21 autoantibodies. These sera were allowed to react with the 5 types of phage displaying UH-RA.21 (SR21, CR21, Std21) or not displaying (SB, CB) UH-RA.21. Autoantibodies and phage complexes were captured onto anti-human IgG-coated ELISA plates. Anti-M13 (anti-pVIII) polyclonal antibodies conjugated with HRP were used as detection antibodies in a sandwich ELISA protocol.

Figure 3.6 shows the ELISA results of the Std21 phage preparations, which is used in a standard phage ELISA protocol to the single (CR21) and the dual display phage (SR21). Both CR21 and SR21 show high levels of absorbance in the phage ELISA when treated with serum from highly, moderately and borderline positive patients for anti-RA21 autoantibodies. This is comparable to the standard ELISA procedure using Std21 phage. All three phage types (SR21, CR21 and Std21) however, were not able to distinguish the borderline positive sera from the negative control sera significantly. Nevertheless, our dual display phage system did not interrupt the display of UH-RA.21 and performs well in phage ELISA, comparable to Std21 phage used up to now. This confirms the expression of the UH-RA.21 marker in our phage preparations.

3.3.6 Screening RA patients sera for UH-RA.21 autoantiodies after sample purification based on dual display phage

The five types of phage were again pre-incubated with the sera from RA patients containing different levels of antiUH_RA.21 antibody positive (highly positive, moderately positive and borderline positive) and with anti-UH_RA21-negative sera from negative controls, to allow recognition of the displayed RA21. The phage with and without bound serum autoantibodies were subsequently isolated with STV-coated magnetic beads, binding to the displayed SBP. These complexes of
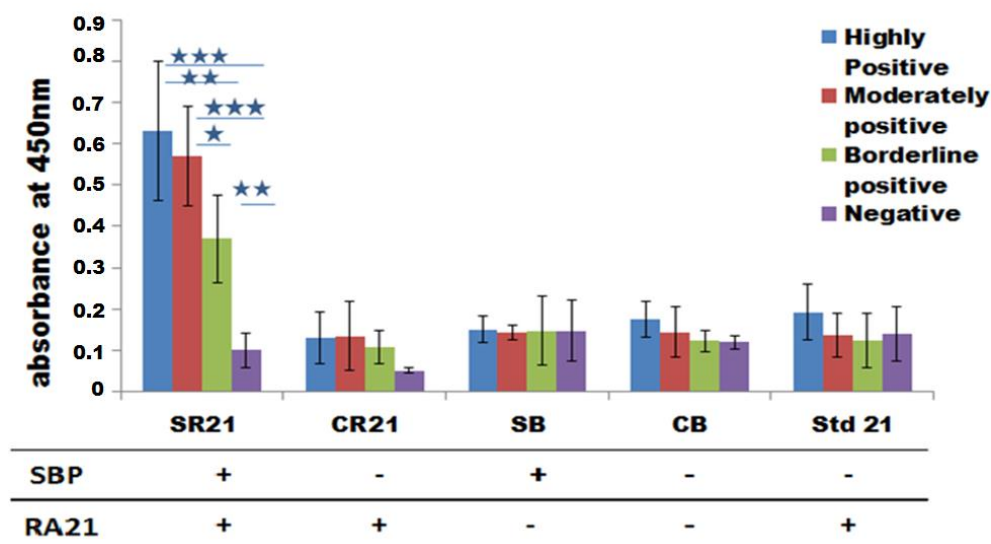
Figure 3.7 Screening for autoantibodies using phage complex in ELISA
Screening RA patients' sera for UH-RA.21 autoantibodies after sample purification based on dual-display phage: All four types of phage (SR21, CR21, SB, and CB) produced through the helper plasmid/phagemid system, as compared to phage produced through the helper phage (Std21) system by phage ELISA. The four types of phage and the Std21 phage were pre-incubated with serum that was highly positive (blue), moderately positive (red), borderline positive (green), and negative (violet) for anti-UH-RA.21, and isolated with STV-coated magnetic beads. The resulting complexes were captured onto anti-human IgG-coated ELISA plates. The statistical comparison of the phage ELISA results among the sera with different levels of autoantibody positivity is shown in which */**/*** which corresponds to approximate P values of $P<0.05$ (significant), $P<0.01$ (good significant), and $P<0.001$ (excellent significant), respectively. These experiments were carried out three times, with each condition in duplicate

phage and serum autoantibodies captured on STV-coated magnetic beads were then added to anti-human IgG-coated ELISA plates, and detected with anti-M13 antibodies conjugated with HRP. All phage displaying SBP are bound to and isolated by the magnetic beads. However, of those, only the one displaying RA21 will bind to the microtiter plate through an anti-RA21/anti-human IgG complex, and generate a colour reaction. Figure 3.7 shows very clear that dual display phage SR21 which is pre-incubated with the positive sera can specifically bind to the autoantibodies in the serum with its pVI-displayed UH-RA.21 autoantigenic target and also to the STV-coated magnetic beads by its pVII-displayed SBP at

the same time, and generate a positive ELISA result. This dual display system allows magnetic capture of phage complex and allows to specific selection of dual display phage in assays, that gives higher sensitivity. Moreover, the absorbance values for the borderline positive sera still increased significantly as compared to the negative serum. In other words, using a dual display phage system, a higher sensitivity is reached in RA diagnosis, allowing the detection of an additional group of patients, displaying only low amounts of anti UH-RA.21 autoantibodies. Since these patients could still be in an early stage of the disease, this could have tremendous impact on prognosis.

3.4 Discussion

In previous work, (Somers K et al. 2009; Somers K et al. 2011) have identified a panel of 14 autoantigenic targets for RA in a pVI-displayed cDNA library using SAS technology. One of these 14 biomarkers, UH_RA.21 shows a high sensitivity to detect early RA patients who are rheumatoid factor negative (RF-) and anti cyclic citrullinated peptide (ACCP-) negative (Somers K et al, 2009). This biomarker was chosen as a proof of principle target in this study. In order to increase the assay sensitivity, we introduced a short SBP peptide (HFNTHPQ) into the gene VII (gVII) of the helper plasmid, which contains a His-pro-glu (HPQ) motif that allows strong STV binding (Dudak FC et al, 2011; Kwasnikowski P et al, 2005; Chen et al. 2004). It is a very strong natural non-covalent coupling with a dissociation constant of $\sim$ 2.5 x 10^8 M (Chen et al, 2004). In this report, we have demonstrated a novel approach to produce dual display phage, displaying a disease-related biomarker for screening at one end of the phage, and an anchor peptide for attachment to a sensing platform at the other end, for an easy, rapid and cost-effective way of diagnosis. In order to achieve this, cotransformation of bacterial host cells with a phagemid vector providing the autoantigenic target UH-RA.21 and with helper plasmid, providing the anchoring peptide SBP was performed. This SBP was fused with a leader peptide pelB, at the pVII of helper plasmid M13cp. The resultant phage displayed the autoantigenic target UH-RA.21 at one end and SBP at the other end.

Moreover, AFM studies showed that our phage are actually smaller than standard phage. The size of our phage was about 429 nm in length in diameter compared

to that of standard phage which has a length of 700-800 nm. The reduced size is due to the M13cp helper plasmid we used in our phage system and not helper phage to produce phage particles. Four different types of phage displaying, both UH-RA21 and SBP (SR21), either UH-RA.21 (CR21) or SBP (SB), and non-displaying (CB) produced by co-transforming helper plasmids bearing bacterial cells with phagemid. And the conventional positive control phage Std21 is produced via helper phage and phagemid system (Std21) was used to compare the efficiency of different RA21 displaying phage. The SBP end of a phage will allow to capture the phage in a well-oriented fashion on a STV-functionalized sensor surface by forming strong affinity bonds or on magnetic beads allowing for the isolation of autoantibodies from the serum of a patient. At the same time, the other end of the phage is readily available to screen for the autoantibodies in the patient's material.

Phage ELISA and dot blotting has been used in characterizing the display of SBP, and the results confirms the clear expression of SBP in both SR21 and SB phage from few fold higher absorbance compared to the other phage samples in ELISA and immediate strong color formation in dot blotting. Phage ELISA was also used to characterize the displaying capacity of UH_RA.21 in three phage samples RA21, CR21 and in standard positive control phage Std21. As in standard ELISA procedures all show higher absorbance in phage ELISA with the positive control serum samples. Though it is not significantly discriminating the borderline positive serum from negative control significantly.

However, using our novel dual display approach sample purification process could be achieved to isolate autoantibodies in the serum, selectively by the phage displaying UH-RA.21 and SBP. In addition, it was shown that the optimal use of dual display phage in the screening for anti-RA21 autoantibodies in patient sera is resulting in an increased assay sensitivity. Even patients that are borderline positive for the presence of autoantibodies, and that could not be discriminated from healthy controls using regular phage ELISA approaches, show a significant increase in absorbance, and can be clearly discriminated from healthy controls.

3.5 Conclusion

In summary, dual display phage displaying STV specific capturing peptide SBT at one end of the phage (pVII) and RA specific autoantigenic UH-RA.21 at the other end (pVI) of a filamentous bacteriophage have constructed using helper plasmid and phagemid based system. Thus produced dual display phage's size is smaller than the conventional phage due to the lack of genome from helper plasmid. Both peptide's display were characterized using phage ELISA protocols. Dual display phage allows pre-concentration of sample by allowing specific isolation of target autoantibodies from a complex serum samples with the negative control samples. Moreover, this system is designed as a cassette- setup to allow the exchange of SBP with any other anchoring peptide and UH-RA.21 with any other biomarker depending on varying needs. These dual display phage could be used as a bioreceptor on different sensing platforms, in order to achieve rapid, label-free and highly specific diagnosis of RA and other diseases possible.

4

Immobilization of phage on sensing platforms

4.1 Abstract

The display of a protein of interest using phage display technology could be achieved by cloning the gene codes for this protein in any of the coat proteins of an M13 filamentous phage. This way, disease specific biomarkers, antibodies, tags and other biologically important target molecules could be displayed on the surface of the bacteriophage. These desired protein displaying phage should be introduced onto a sensing platform in order to develop rapid and high sensitive assays. Phage do need a specific strategy to immobilize them on a sensing surface. The well-known, strongest ever affinity binding, streptavidin (STV) -biotin entity is considered to be a good model for many sensing platforms and in affinity assays. In order to apply this strategy in our dual phage display, phage were modified to display streptavidin binding protein (SBP) on its pVII coat protein. The resulting STV binding phages have a likely vertical oriented immobilization onto STV surfaces and thereby protruding the biomarker counterpart displayed on the pVI coat protein in the solution above. This way, more phage can be attached on the sensor surface as compared to a horizontal orientated immobilization strategy. The immobilization of the constructed dual display phage onto a sensor surface has been monitored in real-time using the QCM-D sensing platform and is compared with the different phage types (both SBP displayers and non-displayers) prepared previously in chapter 3 and the immobilization kinetics has been analyzed. As a complementary biosensor platform phage were also immobilized on SPR sensor chips to monitor the binding properties of phage to STV functionalized surfaces. The results of both approaches QCM and SPR prove that our concept of dual display phage is successful and that these phage act as stable probes attached onto the different sensing platforms while protruding the displayed biomarkers in the solution above readily available for the screening of patient samples for the presence of the target, in this case autoantibodies against the RA marker UH-RA21.

4.2 Introduction

The sensitivity and selectivity of a biosensor rely largely upon the quality of bioreceptor molecules that are used. The most commonly used bioreceptors are antibodies, nucleic acids, proteins, whole cells or microorganisms such as phage or bacteria (Turner. APF, 2000). Bacteriophage could be versatile bioreceptors in the development of diagnostic biosensors, due to their intrinsic properties such as their high thermal and chemical stability and robustness (Arap MA, 2005; Mao C et al, 2009 and Singh A et al, 2013). Phage could be used to display different types of peptides, proteins and antibody libraries in order to be employed in the affinity selection of target specific phage particles (Arap MA, 2005; Mao C et al, 2009; Tolba M, 2010; Reynolds F et al, 2011; Soendegaard M et al, 2011 and Petrenko VA et al, 2008). Phage can be directly used as a probe when they are modified to display disease related antigens on their surface (Kierny MR et al, 2012). Phage production is also cost effective, they can be produced in sufficient numbers by infecting a bacterial host. Up to now, most of the bio-recognition assays rely upon antibodies that need multistep processing and labelling of the sample (Wu J et al, 2010). Phage based short peptides have advantages such as stability, easy to produce and inexpensive over complex affinity scaffolds such as antibodies (Iqbal SS et al, 2000; Luong JH et al, 2008; Luppa PB et al, 2001 and Marquette CA et al, 2006). Therefore phage based biomarkers are good candidates to be functionalized on sensing platforms to achieve real-time, label-free and high sensitivity assays. However, a few drawbacks on bacteriophage based assays still have to be addressed such as the nonspecific adsorption of proteins leading to a high background signal and hence a decreased sensitivity. Therefore most of the phage-based assays are limited to an ELISA format.

Current advances in biosensor development are providing the possibility for immobilizing bioreceptor molecules in a site directed pattern while retaining their intact structure and native biological function (Nakanishi K et al, 2008). The covalent coupling of bioreceptors or a STV-biotin based affinity binding are the methods of choice for an optimal immobilization of phage or bioreceptor molecules. Moreover, biotin/ STV functionalized sensor chips are commercially available, making it easily available. As recently reported, the oriented

immobilization of bacteriophage on a sensing platform resulted in a higher sensitivity in the detection of autoantibodies in serum samples (Tolba M, 2010).

The STV and biotin interaction has become a universal molecular system in many interdisciplinary fields and it is used frequently mainly due to its high affinity and specificity, its fast on-rate and its resistance to heat and pH and its high stability with a dissociation constant of Kd=10^{-15} M (Santala V et al, 2004; Su X et al, 2005), which is known as the highest in biochemistry. STV is a tetrameric protein secreted by bacterium *Streptomyces avidinii.* Its molecular weight is approximately 52.8 KD with a near neutral isoelectric point and each of its four identical subunits can bind with one biotin molecule. The STV–biotin interaction is used in variety of applications including: the sensitive detection of target molecules, labeling, immobilization and purification of proteins, supramolecular protein complex formation and the study of protein–protein interactions in living cells (Sorenson AE et al, 2015).

The stoichiometric interaction between STV and biotin allows one subunit of STV to bind one biotin molecule. STV forms a monolayer on the surface of the transducer and rapidly binds the biotin or biotinylated tag containing target molecules (Park JW et al, 2005; Kim WJ et al, 2011). This biotinylation can be achieved using different biotin tags (Lamla et al, 2004) or by the introduction of a genetic element encoding a biotin peptide in phage, bacteria or in other display models. These recombinant biotin like entities are called Streptavidin Binding Proteins (SBP), and different kinds and sizes of SBP were reported previously (Santala V et al, 2004). SBPs contain a His-Pro-Glu (HPQ) motif somewhere in the amino acid sequence. This HPQ motif specifically binds to the STV molecule. Recombinant SBPs in proteins are more effective in assays as compared to biotinylation of proteins using enzymes or other approaches. Random biotinylation may occur that alters the binding properties of antibodies and protein structures (Santala V et al, 2004). In order to express SBP on phage the use of smaller SBP peptides is most efficient.

In this chapter, we are addressing the immobilization techniques that could be used in making dual display phage as a probe for sensing platforms. There are

different sensing platforms currently in use, among them SPR and QCM –D are considered as high sensitive technologies. In this chapter the immobilization of dual display phage onto STV functionalised SPR and QCM-D sensors is studied. Different phage samples such as SBP displayers and non SBP displayers as prepared previously in chapter three (Rajaram et al, 2014) were compared on STV modified Au coated QCM-D sensors and on STV functionalized SPR chips. The kinetics of the immobilization process has been analysed from the QCM-D results.

4.3 Results

4.3.1 Immobilization of dual display phage on QCM-D sensor platforms

4.3.1.1 Immobilization of phage on plain Au crystal surfaces of QCM-D

QCM-D is an acoustic surface sensitive technique based on the inverse piezoelectric effect, in which, application of an AC voltage over the sensor electrodes causes the piezoelectric quartz crystal to oscillate at its acoustic resonance frequency. The adsorption of sample is reflected as a shift in the resonance frequency (Δf) and the energy dissipation factor (ΔD). The former is related to mass changes over the sensor surface (Sauerbrey G, 1959) while the latter accounts for the energy dissipation due to the presence of the adsorbed layer (Hook F et al, 1998). Figure 4.1 A and C represents the Δf and ΔD responses, upon 25 µg/ml STV adsorption with the flow rate of 100 µl/min (kept constant throughout the experiment) and subsequent binding of $1x10^{11}$ CFU/ml of SBP displaying phage SR 21 (positive) and the Figure 4.1 B and D shows the same for non SBP displaying phage CR 21 (negative). The concentration of STV and the flow rate used was according to the supplier's instructions given for biotinylated crystals. Upon binding of STV, Δf decreases to ~ −20 Hz, indicating the physical adsorption of an STV layer onto the Au coated QCM crystal's surface.

Subsequent introduction of the SBP displaying phage (SR21) into the system caused larger shifts in both Δf and ΔD. The Δf response decreases to ~ −160 Hz for overtone 3, reflecting the binding event of SBP displaying phage SR21. In addition, the increases in ΔD (~150 Hz for the overtone 3) indicated that the adsorbed SBP displayed phage layer is very dissipative. No significant changes in the level of Δf and ΔD was detected after introducing the negative sample (non SBP displaying phage CR21) to the systems (Figure 4.1 B and D). It also

destabilized the STV layer, and removed adsorbed STV partially (~25 %), as concluded from the increase (decrease) in Δf (ΔD) response. Table 4.1 shows the Δf and ΔD values of all different phage used upon STV adsorption and phage binding for the overtone 3.

Table 4.1 Δf and ΔD values upon phage binding

Phage type	Frequency change Δf Overtone 3 in Hz		Dissipation change ΔD Overtone 3 in Hz	
	Upon STV adsorption	Upon phage binding	Upon STV adsorption	Upon phage binding
CR21	-22	-9	1	-2
SR21	-22	-163	1	150
CB	-22	-26	1	2
SB	-22	-138	1	144

The Δf and ΔD values shown are obtained for the adsorption of STV on the plain Au coated QCM-D surfaces and the subsequent binding of the phage types as indicated to the STV coated surfaces.
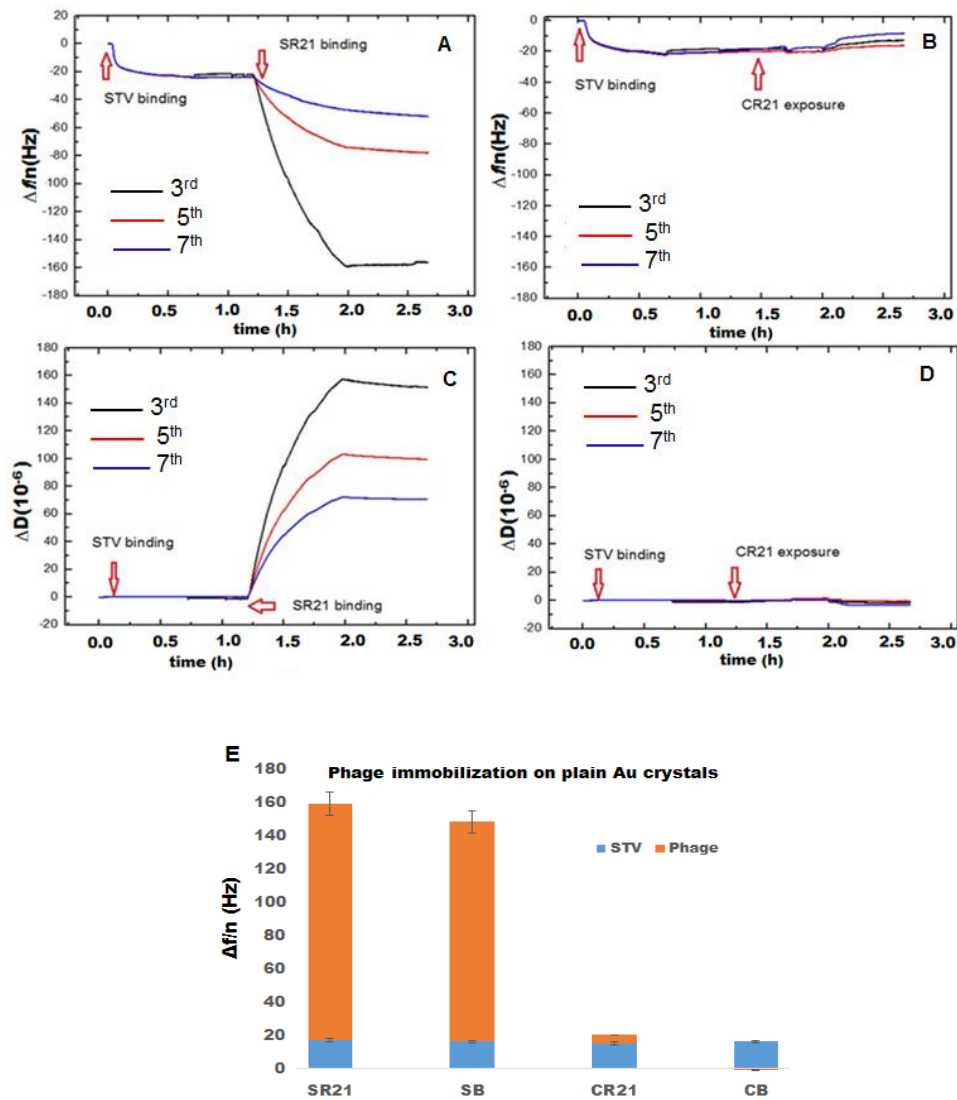
Figure 4.1 Phage immobilization on plain Au crystals of QCM-D

Characterization of STV adsorption and subsequent binding of SBP displaying phage SR21 (A and C) and non SBP displaying CR21 (B and D) to the plain Au coated QCM-D sensors. The results obtained for 3 different overtones (3rd, 5th and 7th) are shown. The bar chart (E) represents the Δf values upon the physisorption of streptavidin to the different plain Au crystals (blue) and the binding of different phage samples to the STV layer (orange) as measured for overtone 3 in two typical experiments.

4.3.1.2 Phage immobilization on biotinylated sensor surfaces of QCM-D
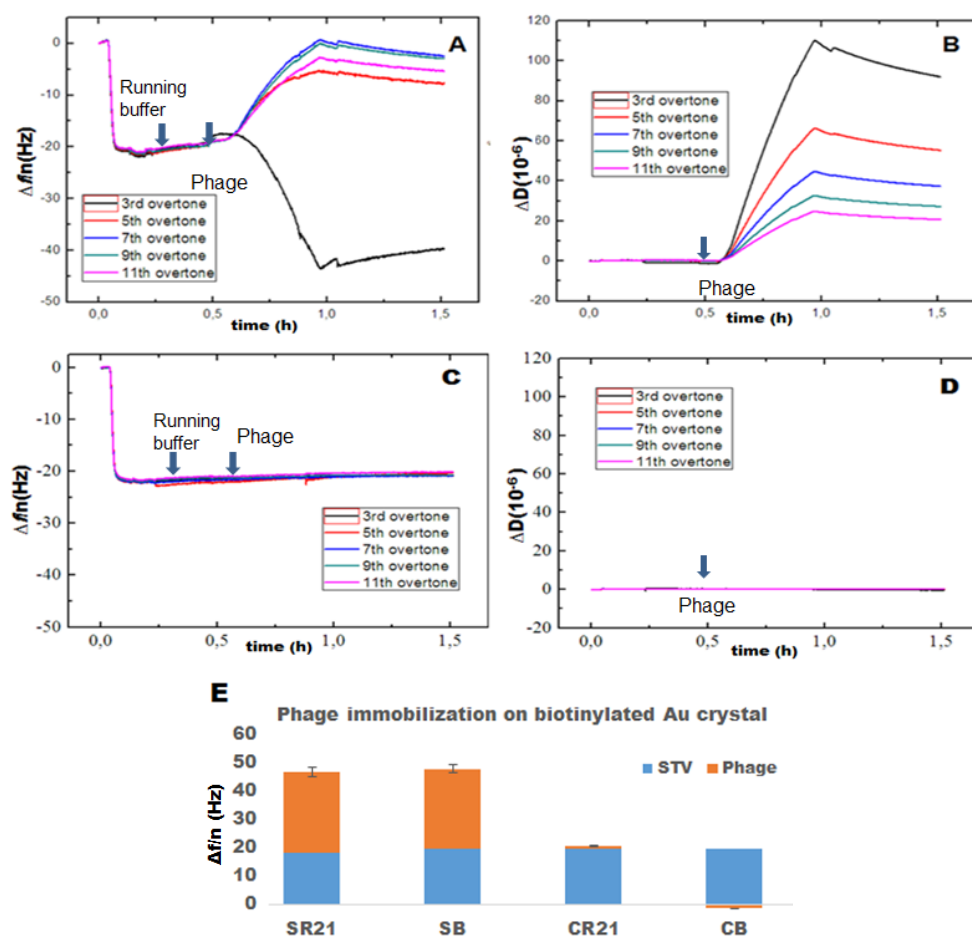
Figure 4.2 Phage immobilization on biotinylated Au crystals of QCM-D

Figures A and B show changes in frequency (Δf) and dissipation (ΔD) respectively upon binding of 25 μg of STV followed by binding of 10^{11} CFU of SR 21 phage on biotinylated Au crystals. Figures C and D show the Δf and ΔD respectively upon binding of the STV and non SBP displaying CR 21 phage on the biotinylated Au crystals. These experiments were performed in duplo and the same pattern was observed for other phage samples (SB- SBP displayer and CB- non SBP displayer). The bar chart (E) represents the Δf values upon the binding of streptavidin to the different biotinylated Au crystals (blue) and the subsequent binding of phage samples to the STV layer (orange) for the overtone 3 for two typical experiments.

If the same experiment is performed on biotinylated Au crystals (Figure 4.2), the binding of STV occurs in all different crystals is completed very rapidly (~60 sec) and uniform as compared to the plain Au crystals (~300 sec) with a Δf of 22. Flushing with running buffer suggests that the biotin and STV complexes were not stable since it seems as if they are slowly removed from the surface. After phage binding, the obtained Δf was lower for the biotinylated crystals than for the plain Au crystals. The 1st and 3rd overtones do behave as expected but the other overtones showed unusual results. Indeed for the overtones 5 to 11 the Δf shows a gain in frequency instead of decrease in frequency. On the other hand the observed dissipation pattern was as expected in all the overtones. The final washing steps also removed some (~5%) of the bound phage from the surface.

4.3.2 Phage immobilization on STV functionalized SPR chips (SA)
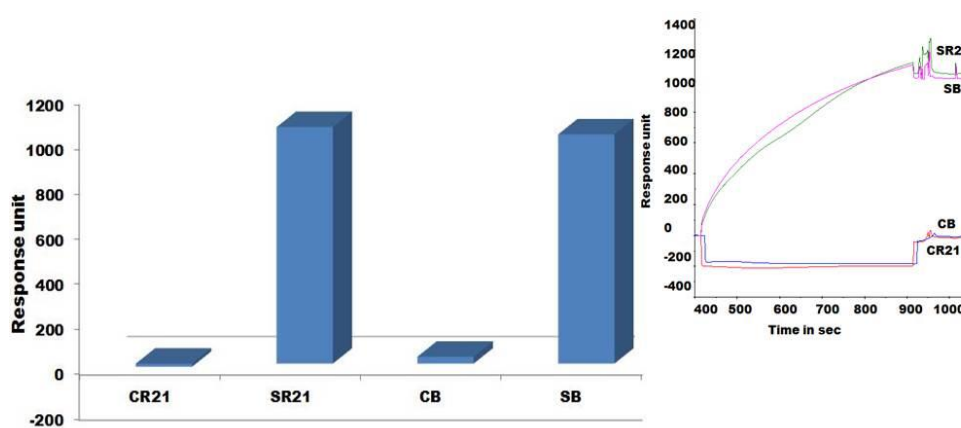
Figure 4.3 Phage immobilization on SA SPR chips

The SBP displaying phage (SR21 and SB) binds to the STV surface of SA chip and non SBP displaying phage (CR21, CB) shows no binding pattern. Figure 4.3 insert shows the real time binding curves, and SBP displayers show high stability when flushing with buffer while the negatives revert back to the base line due to the buffer effect.

The physical principle behind SPR is based on the change of optical properties of the medium upon sample adsorption, which translates in a shift in the reflectivity *vs* angle dip (Liedberg B et al, 1983 and Rich RL et al, 2007). STV can form affinity binding with biotin or with SBP, and one can expect it to happen very rapid (Swann

MJ et al, 2004 and Lin Z et al, 2008). Since STV and SBP binding are mostly irreversible, the chips cannot be reused or regenerated. 1×10^{11} CFU/ml of phage samples were introduced over the corresponding FC's of a SA chip (STV functionalized 3D chips) of SPR Biacore, at a flow rate of 12 μl/min and the binding response was immediately observed. Figure 4.3 represents the specific binding response of different phage on the surface of SA chip, as expected higher responses of binding affinity and stability were observed with the positive samples (SR21 and SB) in compared to both negative samples (CR21 and CB) and the insert Figure shows the real time binding curves. SBP displayers show high stability when flushing buffer while the negatives back to the base line from the buffer effect.

4.4 Discussion

Gervais and co-workers (2007) have reported a 15 times higher response when using STV mediated attachment of capsid biotinylated phage onto a gold electrode as compared to the physical adsorption of wild type phage.

Indeed STV and biotin are popular for the intrinsic affinity binding properties and therefore are often used in sensor platforms and biochemical assays as a substrate, ligand, or tags. Both biotin tags and SBP are available in different sizes and with high affinity towards STV. In this study four types of phage produced previously (chapter 3) have been used. Two phage samples are displaying SBP (SR21 and SB) and the other two phage do not display SBP (CR21 and CB). The phage display SBP at pVII of the bacteriophage in a multivalent display system, meaning that all five copies of pVII are expected to display SBP. Hence, the binding of these SBP displaying phage to the STV surface should happen rapidly. Since the pVII coat protein is situated at one end of the phage, immobilization of these phage onto an STV functionalized sensor surface phage most likely results in a vertical conformation which is very useful for binding as many phage as possible and which could result in higher sensitivity phage based assays. According to Roy MD and coworkers (2008) relaxation and reorientation happens upon binding of the phage to the sensor surface which could limit the detailed study on binding parameters.

In this study the display of SBP in phage samples has been evaluated on different sensing platforms such as QCM-D and SPR. In QCM-D, STV layers were formed by physically adsorbing 25 µg/ml STV on plain Au coated crystals. On these plain Au coated QCM crystals, the STV layer is quite rigid, as can be deducted from the observation that $\Delta D \sim 0$ and from the fact that the overtones in both Δf and ΔD do overlap (see Figure 4.1).
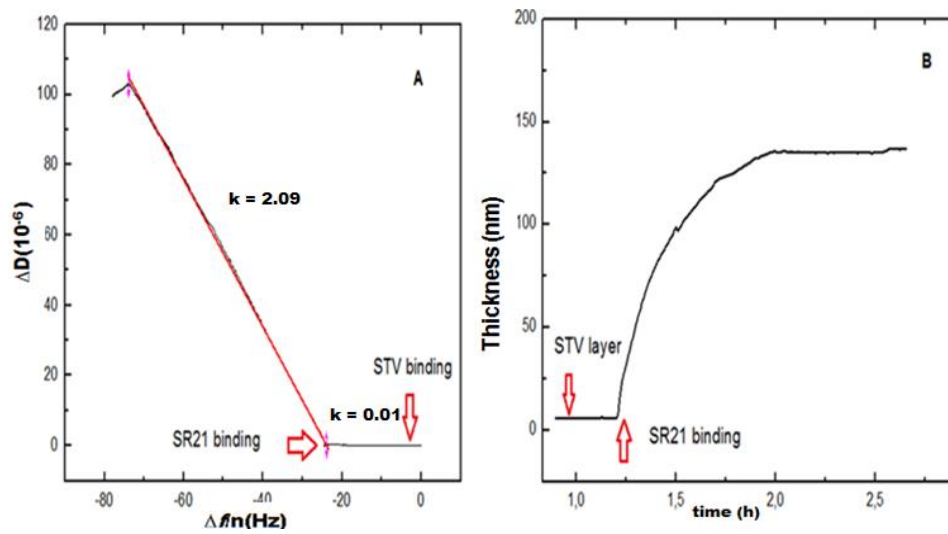
Figure 4.4 Rate of phage adsorption and measuring the thickness of the attached phage layer on QCM-D sensor chips

(A) $\Delta D - \Delta f$ plots showing the adsorption of STV (black solid line) and SBP displaying phage SR 21 (red solid line) for overtone number 3. (B) An effective thickness of the SBP displaying phage SR 21 layer was estimated using a Voigt based model.
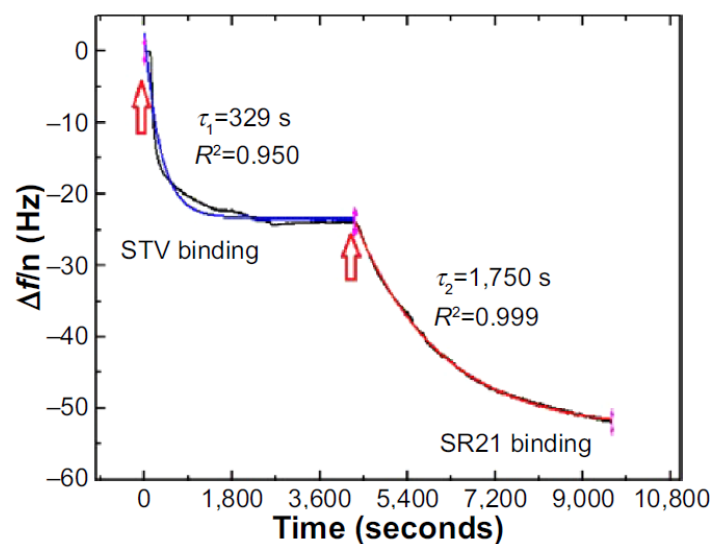
Figure 4.5 Kinetics of STV and phage binding on QCM-D sensor chips
The adsorption of STV to Au coated QCM-D sensors and the subsequent binding of SBP displaying phage SR 21 is shown. τ is time constant and R is the correlation coefficient.

Flushing with PBS buffer did not change the level of Δf and ΔD indicating that the STV layer was quite stable. The $\Delta D - \Delta f$ plot shown in Figure 4.4 A, eliminates time as an explicit adsorption parameter and therefore provides insight into the viscoelastic nature of the formed adlayers (Sandberg T et al, 2009). More specifically the slope of the line between the initial and final point of adsorption, $k_{D-f} = \Delta D/\Delta f$ scales differently with different adlayer conformations. This means that rigid and compact layers yield low k_{D-f} values, whereas bulky and diffuse layers yield high k_{D-f} values (Sandberg T et al, 2008).

If this is applied to our measurements as shown in figure 4.4 A, different slopes are observed upon STV and subsequently SBP displaying phage adsorption onto the plain Au crystals. Indeed adsorption of STV yields a $k_{D-f} = -0.01$, while adsorption of SBP displaying phage $k_{D-f} = -2.09$. As anticipated before, the STV layer is a rigid and compact layer, while the phage is a soft biomolecule in a vertical conformation that permits trapping of water molecules thus showing large energy dissipation. Furthermore, the effective thickness before and after phage addition was calculated using the Voigt based model consisting of an elastic

element (spring) in parallel with a viscous element (dashpot) (Voinova MV et al, 1997 and Losada-Pérez P et al, 2014). The data of several overtones (3rd to 7th) were fitted using the software Qtools (Q-Sense AB, Sweden) keeping the density and the viscosity of the fluid as fixed parameters at 1.0 g cm^{-3} and 1 mPa s respectively. The obtained values should be taken as an approximation, since we ignore the density of the STV and dual display phage layers. However, the significant increase in thickness (figure 4.4 B) upon phage binding is due to the most likely vertical configuration of the phage. Also the speed of adsorption of the two processes can be addressed, the Δf responses of the separate events were fitted to a single exponential decay:

$$\Delta f = \Delta f_0 + Ae^{-t/\tau}, \qquad (5)$$

where A is the amplitude and τ is the time constant. As shown in figure 4.5 the adsorption of STV onto the Au coated QCM-D sensors is fast ($\tau \sim 329$ seconds), while the SBP displaying phage is bound more gradual and slower ($\tau \sim 1750$ seconds). Also the other two phage samples the SBP single displaying phage SB and negative phage CB behave in the same way as their positive and negative counter parts SR21 phage and CR21 phage respectively. Analogous experiments were performed using biotinylated QCM crystal and again STV shows very rapid (~ 60 sec) binding but immediately biotin started to remove from the surface upon flushing with running buffer. The resulting equilibrium between the binding of phage and the removal of the STV-biotin complex could explain the observed unstable measurements. Therefore we can conclude that biotinylated chips do not suit our phage based assays.

The commercial BIACORE SPR SA chips are 3 dimensional chips consisting of a carboxymethylated dextran matrix pre-functionalized with STV. It is famous for its high binding capacity, reproducibility, high chemical resistance and it can be used for broad range of applications. Again 1x10^{11} CFU/ml of our different phage samples were applied to different channels of the SPR SA chip and the observed response was gradual and stable. The SPR response was much higher for the SBP

positive samples SR21 and SB (~1000 RU) as compared to the SBP negative phage samples CR21 and CB (~10 RU) (see figure 4.3). The SPR based experiments do not allow kinetics studies, because these are only possible for the binding analysis protocols. Moreover SPR is a highly sensitive technique in which a small change in buffer (e.g. during sample preparation) can cause a change in response. Due to that, our negative control (non-SBP displayers) have shown an initial drop in response and then back to the baseline while flushing with running buffer.

From these results it is clear that SBP displaying phage such as SR21 and SB did specifically bind to STV functionalized surfaces of both QCM-D and SPR sensor chips. The SBP displaying phage do have a vertical orientation on the sensor surface as has been determined from the layer thickness in QCM-D after the phage binding. Although, SBP displaying phage did bind to STV functionalized biotinylated Au crystals, the results could not be taken further due to the unusual Δf curves obtained upon the phage binding. According to Olsen EV et al (2006), immobilization of phage using the edges of the bacteriophage leads to the attachment of a dense population of phage than the oblique orientation and this author has estimated a surface occupation of a single phage of 7.85×10^{-17} m^2.

Complimentary to QCM-D the highly sensitive SPR system was also used for the characterization of dual display phage and the ability to display SBP as well as possible immobilization on STV functionalized BIACORE chips. From the results shown in figure 4.3 it is clear that the binding of phage to the STV surface occurred with the high response as compared to the negative controls. A difference of about 1000 RU was observed for the SBP displaying phage. Tolba and coworkers (2010) have reported that the oriented immobilization of biotinylated phage onto STV coated magnetic beads behaved as an effective bio-sorbent capable of capturing up to 25-30% host cells. Likewise, our dual display phage also could behave as an effective biocapturing probe when immobilized on sensing platform in a vertical orientation.

4.5 Conclusion

In this part of the study, dual display phage immobilization has been carried out using two different high sensitive sensor platforms QCM-D and SPR. In QCM-D, plain/ biotinylated QCM crystals were functionalized with STV first and then subsequently treated with CR21, SR21, CB and SB phage as previously prepared in chapter 3. Among these four phage samples SBP displaying phage SR21 and SB show high affinity for STV while the two other non SBP displaying phage did not. SBP displaying phage also show high dissipation values and QCM-D thickness measurements did reveal a likely vertical orientation of phage on the sensor surface. The same binding pattern was also obtained using SPR sensor chips.

Using biotinylated QCM crystals, biotin and STV complexes were formed fast and stable, but aberrant properties were observed upon phage binding. The results obtained with QCM crystals and SPR clearly show that dual display phage form a specific binding with STV surfaces and that a very stable phage layer is formed on the sensor surface which can be used as biocapturing probes in screening targets.

5

Real-time and label-free screening of autoantibodies using sensing platforms

Kaushik Rajaram, Patricia Losada-Perez, Veronique Vermeeren, Baharak Hosseinkhani, Patrick Wagner, Veerle Somers, Luc Michiels.

5.1 Abstract

Over the last three decades, phage display technology has been used in the display of target specific biomarkers, peptides, antibodies etc. Phage display based assays are mostly limited to the phage ELISA, which is notorious for its high background signal and laborious methodology. These problems have been recently overcome by designing a dual display phage with two different end functionalities, namely STV binding protein at one end and a Rheumatoid Arthritis specific autoantigenic target at the other end. Using these dual display phage, a much higher sensitivity in screening specificities of autoantibodies in complex serum sample has been detected compared to single display phage system on phage ELISA. Herein, we aimed to develop a novel, rapid and sensitive dual display phage to detect autoantibodies presence in serum samples using quartz crystal microbalance with dissipation monitoring (QCM-D), surface plasmon resonance (SPR) and Heat transfer resistance (Rth) as sensing platforms. Screening for autoantibodies using anti-human IgG modified surfaces and the dual display phage with STV magnetic bead complexes allowed to isolate the target entities from complex mixtures and to achieve a large response as compared to negative control samples. Among these three types of sensing platforms QCM-D behaved as a more reliable, reproducible sensing platform for phage based assays. This novel dual display strategy can be a potential alternative to the time consuming phage ELISA protocols for the qualitative analysis of serum autoantibodies and can be taken as a departure point to ultimately achieve a point of care diagnostic system.

5.2 Introduction

Current demands in clinical research aim at the rapid screening of potential therapeutic and diagnostic targets (Hof D et al, 2006). For the last few decades, there are many biomarkers that have been identified and used in many different disease diagnostics. Biosensors are devices, designed for the rapid detection of the presence of those identified biomarkers in patients samples even at a very low concentration, this in contrast to conventional ELISA and other immunological assays (Saerens D et al, 2008). Biosensors consume less time and reagents. Biosensors provide an advanced platform for biomarker analysis with the advantages of offering multi-analyte testing capability (Tothill IE, 2007). It is also considered as less expensive (Rapp BE et al, 2010), convenient, portable and even can be taken to the point of care analysis (Owen TW et al, 2007). Biosensors, in which an antibody antigen based reaction is used to detect the target are called immunosensors and they rely on antibodies as the bioreceptor recognition element need multistep purification and labeling (Wu J et al, 2011). These antibodies probes/analytes should be prepared in such a way to deliver high stability, high specificity in a complex medium. Antibodies require a lot of time to develop which significantly increase the cost and they are highly fragile and cannot be reused (Wu J et al, 2011 and Olsen EV et al,, 2005). When detecting antibodies or antigens in a complex medium such as serum as an analyte, the sensitivity could be compromised due to the presence of different types of other nonspecific antibodies, proteins (blood components) etc.. all of which can aspecifically bind to the transducer surface. Since, antibodies and proteins are highly complex, both chemically and structuraly, it can create unpredictable issues on the sensor surface. It is often difficult to generate a biosensor strategy with these biomolecules (Saerens D et al, 2008).

In order to address these issues of blood components in the sample, different strategies has been exploited, among these, the selection of target specific peptides from a phage display library through biopanning has been widely reported. Though these phage can be used as a target specific probes in sensing platforms, the non phage bound synthetic peptides have been reported rarely (Wu J et al, 2011). It may be due to the complexity in synthesizing these peptides providing correct folding while retaining the recognition part available for the

specific binding. So the phage sensor probe or phage mediated sensor is the way of choice for those target specific peptides that can not be synthesized chemically. Moreover, phage sensors show good durability, reusability, stability, standardization and can be produced at a low cost, making them a good antibody substitute (Olsen EV et al, 2006). Phage are thermostable and do retain detectable binding ability for more than 6 weeks at 63° C or 3 days at 76° C. The activation energy of phage degradation was determined to be 1.34×10^5 J/mol (Nanduri V et al, 2007). Some reports already describe the used of phage as a probe in sensing techniques such as SPR (Nanduri V et al, 2007 and Balasubramanian S et al, 2007), QCM (Nanduri V et al, 2007), Magneto elastic sensors (Lakshmanan RS et al, 2007; Wan J et al, 2007 and Huang S et al, 2008), light addressable potentiometric sensor (phage LAPS) (Jia Y et al, 2007) and in CMOS (Yao L, 2008).

There are different types of signal transduction methods currently in use, each of them has its positive points and weaknesses (Haes AJ et al, 2002). The QCM transducers are called reasonably simple, convenient to use and can detect rapidly and in real time responses as compared to other transducers in direct affinity sensing (Rickert J et al, 1996 and Pedura Hewa TM et al, 2009). The QCM-D version (D for dissipation) gives extra information and can be used to study the viscoelastic properties of the adlayers on the sensorsurface. SPR sensors are currently considered as the method of choice in many affinity biosensing application because of its high senstivity and Biacore is the most common SPR device available (Ayela C et al, 2007). SPR detects the change in refractive index of the solution in proximity to a gold sensor surface using optical phenomenon (Laricchia-Robbio L et al, 2004). A third sensing platform is using a heath transfer method (HTM) based on the heath transfer resistance (Rth) of the transducer. HTM or Rth is an interesting technique and has been applied in different types of sensing applications such as DNA mutation studies (Vangrisnven B. et al, 2012), the detection of cells and small organic molecules (Bers K et al, 2014 and Peeters et al, 2013) and lipid phase transitions (Losada-Perez P et al, 2014) . This technique uses limited hardware including two temperature sensors, a heat source and an automated flow pump unit.

There are approximately 80 autoimmune diseases that have been identified including the very common Reumathoid Arthritis (RA). In contrast to other diseases in which large numbers of DNA, peptide or protein markers can be identified, autoimmune diseases mostly are identified by the presence of autoantibodies (Rapp BE et al, 2010).

In this chapter we describe the screening of autoantibodies present in the serum of patients suffering form RA using SPR, QCM and Rth biosensing platforms. To achieve this we will exploit our dual display phage system developed as described in chapter 3. The proposed approach is analogous to the successful ELISA setup in chapter 3. Phage complexes are made of autoantibodies captured by biomarker expressing dual display phage that are bound via the SBP expressed tag to STV coated magnetic beads. This step provides a sample purification free from the complex serum samples and did also increase the sensitivity of the phage ELISA (chapter 3). The same strategy is used in biosensing platforms. Our proposed novel dual display approach makes it possible to use phage in biosensing platforms as an alternative for phage ELISA assays in qualitatively screening for autoantibodies in patient serum samples.

5.3 Results
5.3.1 Screening for autoantibodies in patient serum using QCM-D
The presence of autoantibodies in serum was detected based on their bio interface characterization (Δf and ΔD) on QCM-D. Figure 5.1 shows the Δf and ΔD responses upon anti-human IgG (10 µg/ml) adsorption and subsequent binding of a dual display positive complex (dual display phage, positive control serum and STV coated magnetic beads) and negative complex (dual display phage, negative control serum and STV coated magnetic beads). In the first step, the adsorption value of anti-human IgG on Au coated sensors yielded $\Delta f \sim -30$ Hz and $\Delta D \sim 0.75 \cdot 10^{-6}$. The small ΔD value indicates that the layer of anti-human IgG is quite rigid and in addition to this, during the washing step with PBS buffer, Δf and ΔD values remained the same as became clear from the different overtones lying very close to each other. Although it is physical adsorption, as shown in figure 5.1, the binding of anti-human IgG (the first layer) was uniform in all Au crystals.
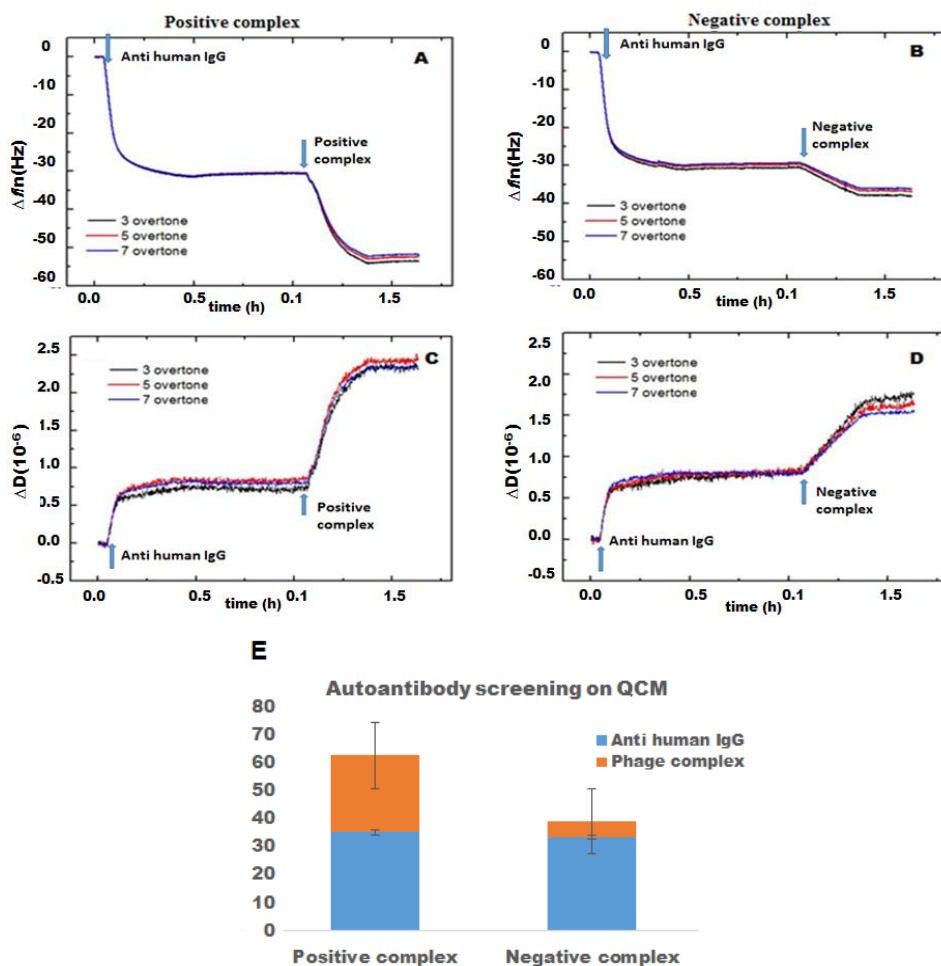
Figure 5.1 Autoantibody screening of patient samples on QCM-D

Characterization of anti-human IgG adsorption and subsequent binding of positive phage complex (left column) and negative phage complex (right column) to the Au coated QCM-D sensors. The bar chart (E) represents the Δf values upon the binding of anti-human IgG to the plain Au crystals (blue) and the subsequent binding of phage complexes (orange) to the anti-human IgG layer for the overtone 3 for two different experiments.

Subsequent introduction of the positive phage complex (with bound autoantibody) using a flow rate of 100 µl/min through the system, Δf and ΔD were considerably shifted. The Δf response changed in absolute value $\sim$ 25 Hz, while ΔD increased up to $\sim$ 2·10^{-6}. When the negative complex (with no autoantibody) was added, Δf decreased $\sim$ 5 Hz and ΔD increased to $\sim$ 0.75 ·10^{-6}. The positive phage complex

showed a larger Δf response than the negative phage complex, indicating the larger mass binding to the IgG layer. This reflecting the specific binding between of the phage bound autoantibodies to the anti-human IgG adsorbed surfaces. The display of the autoantigenic target on the phage pVI using the phagemid system will allow approximately 10% of the phage to display the target in contrast to the SBP display using a helper plasmid system, which allows the display of SBP in all phage (Woo MK et al, 2011). Hence, the Δf decrease is much lower as compared to the phage immobilization in chapter four (see figure 4.1). The binding of the negative complex was considered as a nonspecific binding, since the surface was not blocked.

Figure 5.2 shows the $\Delta D - \Delta f$ plots with the different slopes k_{D-f} upon anti-human IgG and phage addition stages. The low k_{D-f} values obtained with the formation of anti-human IgG layer in Au crystals used for the positive and negative complexes are similar for both experiments ($k_{D-f} \sim -0.03$) and also indicate that the anti-human IgG layer is rigid. The subsequent phage binding represented higher values for both the positive and negative complexes (figure 5.2 A and B). An effective thickness obtained using the Voigt-based model reflects a significant increase in thickness upon phage binding (see Figure 5.2 C and 5.2 D). Unlike binding of SBP displaying phage on STV surfaces (see chapter 4), where the phage conformation at the surface was vertical resulting in a large ΔD and k_{D-f} values, the binding of phage to anti-human IgG (figure 5.2 C and D) via the autoantigenic target (UH_RA.21) result in lower ΔD, k_{D-f} and thickness values.

These difference can be related to their conformation on the surface where the phage adopts a vertical configuration onto an STV layer, i.e. a flexible conformation that can be largely deformed during the shear oscillation, whereas in the case of phage bound to the anti-human IgG layer, the phage complex is more rigid and does not accommodate vertically due to the presence of a heavy magnetic bead on the opposite end.

Also the kinetics of the binding processes can be measured as shown in figure 5.3. The time constants obtained by fitting the Δf data to Equation 1 indicates that IgG adsorption onto Au surface is a fast process (τ ~180 seconds) as compared to the

phage complex. In addition, the subsequent binding of the positive complex to anti-human IgG was achieved faster (τ ~393 seconds) than did the nonspecific binding of the negative complex (τ ~713 seconds).
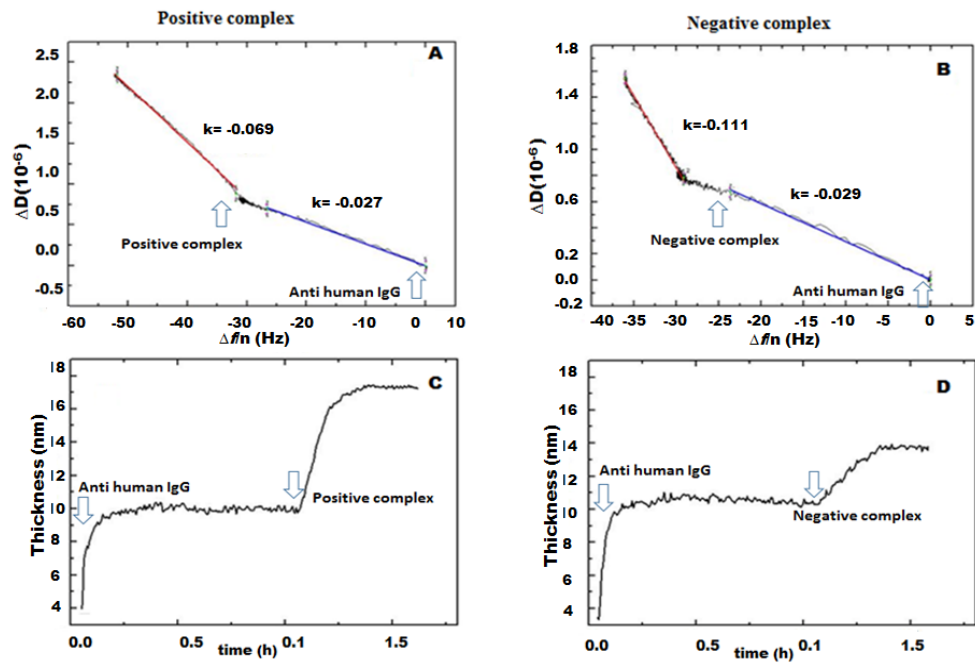
Figure 5.2 Binding rate of IgG and phage complexes and measurement of the thickness of the phage layers

$\Delta D - \Delta f$ plots for overtone 7 are shown for IgG adsorption (blue solid lines in A and B) and subsequent binding of positive phage complex (A) and the negative complex (B) (red solid lines). (C) and (D) show the estimated thickness of the positive complex and the negative complex layers respectively.
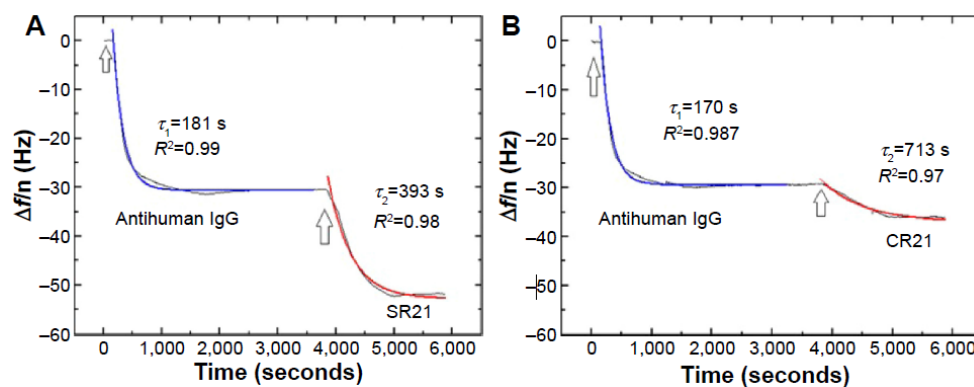
Figure 5.3 Kinetics of the phage complexes binding to Anti IgG coated sensors

The kinetics of the adsorption of IgG to Au coated QCM-D sensors and subsequent binding of positive phage complex SR 21 (A) and negative complex (B) for overtone 7 is shown. τ is time constant and R is correlation coefficient.

5.3.2 Screening for autoantibodies using SPR

An SPR CM5 chip has four flow cells (FC) that contain a three dimensional dextran matrix functionalized with carboxyl groups. Anti-human IgG is covalently immobilized on the SPR CM5 chip using an EDC-NHS based amine coupling protocol followed by a blocking step using ethanolamine. After pH scouting of the sodium acetate binding buffer, optimal antibody immobilization was achieved at pH 4.5. A similar immobilization efficiency of anti-human IgG (1 µg/ml) has been observed in all four FCs at a flow rate of 10 µl/min for 1500 sec, an average response of 659 RU was observed.

After IgG immobilization, a negative complex (without RA21 autoantibody) was analysed first followed by a positive complex (with RA21 autoantibodies) at the same flow rate and within the same time frame. This alternate cycle was repeated three times. In each cycle, the positive complex binds more to the anti-human IgG immobilized surfaces due to the specific binding between the anti-human IgG and the autoantibody in the positive complex. From the large phage complexes we would have expected a large response. But the observed average difference between the positive and negative is only 5 RU.

Table 5.1 Immobilization levels of anti-human IgG on a CM5 SPR chip

Amine coupling in Flow cells (FC)	Response bound (Ligand) in RU
FC 1	663
FC 2	634
FC 3	689
FC 4	651

The amine coupling protocol for the immobilization of 1 μg/ml concentration of anti-human IgG at a flow rate of 10 μl/min for 1500 sec was performed on four FCs of an SPR chip CM 5. The bound IgG is measured in response units (RU).
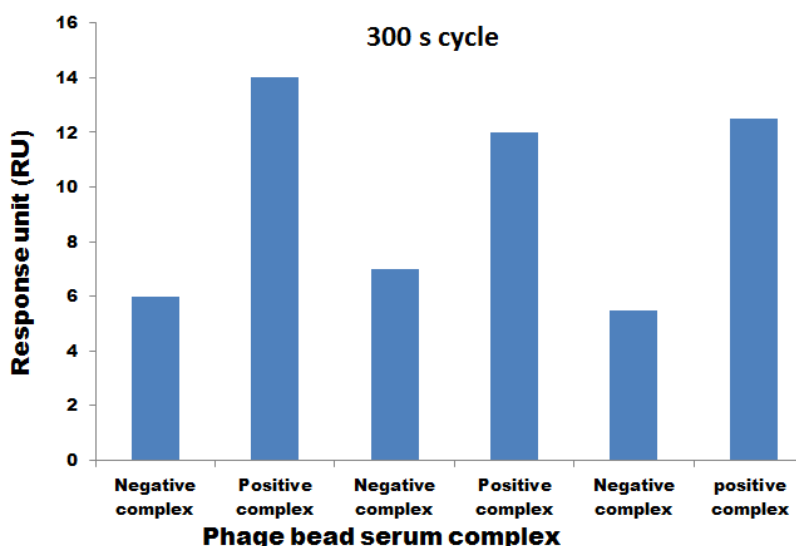
Figure 5.4 Autoantibody screening of patient samples using SPR chips

The alternating SPR measurements of manual binding of the negative complex (no autoantibodies) and positive complex (with autoantibodies) for 300 seconds on the anti human IgG immobilized surface of a CM5 chip on Biacore T200 SPR is shown.

5.3.3 Autoantibody screening using an Rth biosensing platform

Besides QCM and SPR also thermal resistance is an interesting and possible biosensing platform, this platforms makes use of NCD as a transducer. At first we investigated if the dual display phage could also be used on NCD coated chips. For this reason NCD surfaces were immobilized with anti-human IgG using an EDC/NHS covalent coupling chemistry. In order to evaluate the suitability of the

NCD to allow the capture of phage complexes by covalently attached antibodies, an ELISA-based colour reaction was performed using an anti M13-HRP conjugate to detect the presence of the dual display phage. As shown in Figure 5.5, the positive complex gives a 3 times higher optical density (Figure 5.5) than the negative complex. This is as expected because only the dual display phage specifically bound to the anti-human IgG via the serum autoantibodies on the displayed UH_RA.21 biomarker (autoantigenic target). These results indicate that the phage remains functional on NCD sensor platforms.
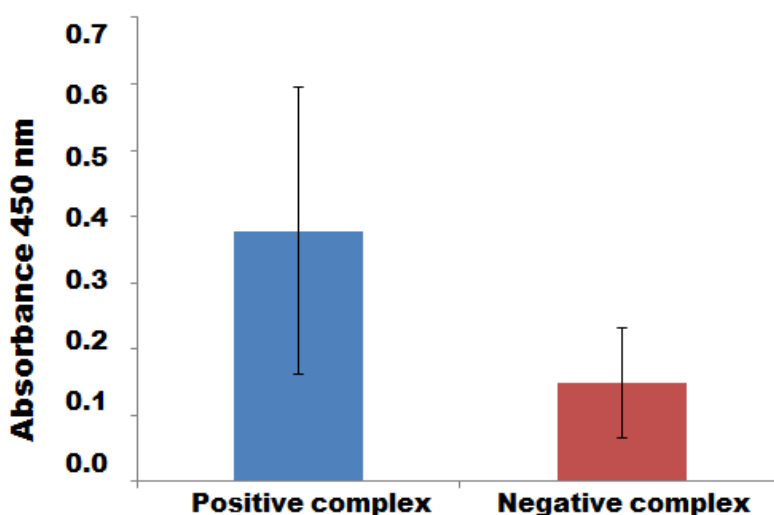
Figure 5.5 Phage ELISA on NCD

NCD samples were covalently coupled with anti-human IgG using EDC/NHS chemistry and then positive complex (with autoantibodies) and negative complex (no autoantibodies) were incubated on the corresponding NCDs for 90 mins. After multiple washing steps using MES buffer, anti M13-HRP conjugate was added as a secondary antibody. Absorbances are measured at 450 nm. This experiment was repeated at least three times.
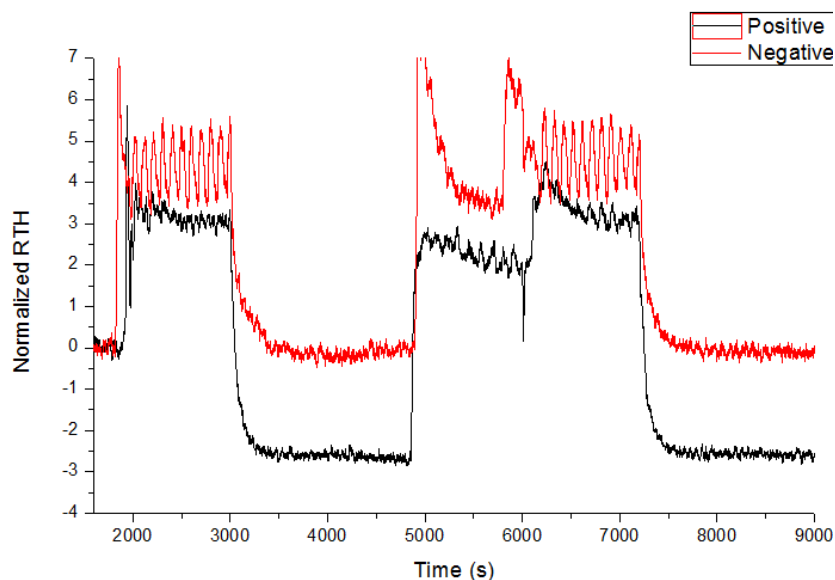
Figure 5.6 Autoantibody screening using Rth

Anti-human IgG-immobilized NCD samples, were exposed to either positive complexes (with autoantibody; red line), or negative complexes (no autoantibody; black line). Flusing was done with 1x PBS running buffer at a flow rate of 325 µl/min for 30 mins. The normalized Rth results are shown.

In the following step it was investigated whether we could detect phage complexes on NCD using the label free Rth read out method. Therefore NCD samples were again immobilized with anti-human IgG and treated with the positive or negative complexes as described earlier. These loaded NCD surfaces were mounted onto the Rth setup as described in chapter two untill a stable Rth value is reached (t = 1500 s). The initial Rth values remained the same for both NCD samples that was exposed to either the positive complex or the negative complex. After this the NCD surfaces were washed by flushing $1 \times$ PBS over the surface (t = 0 s) at 325 µl/min for about 30 minutes, and this resulted in a decrease of Rth values for the negative complex treated NCD. The fairly constant Rth of positive complex treated NCD (Figure 5.6) could be a result of the increased specificity of dual displaying SBP-RA 21 phage by making a phage complex during sample preparation. The negative complex does not have RA autoantibodies, so normally it can not bind to anti-human IgG on the NCD surface. Flushing with running buffer will therefore

result in the removal of the sedimented or unspecifically bound negative complexes as is was observed in the decrease in Rth values in Figure 5.6. At the begining of each 1 × PBS rinse, the Rth goes up. This is due to the temperature shift of the 1 × PBS (25° C) that enters the flow cell which has a temperature of 37°C. This temperature shift of the liquid in the flow cell (T2) is causing a higher difference between the copper temperature (T1) set at 40°C and T2. The bigger the difference of T1 and T2, the higher the Rth going by the formula giving in materials and method, paragraph 2.12.
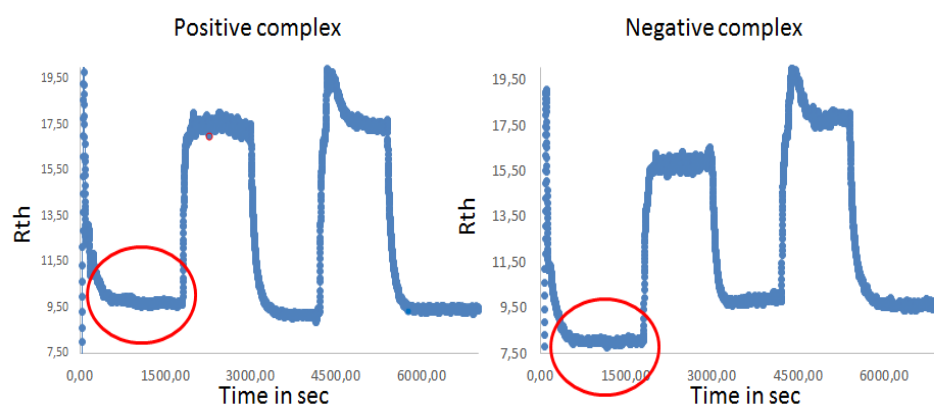
Figure 5.7 Autoantibody screening of patient samples using Rth

Anti-human IgG was immobilized on NCD samples and these were incubated with phage complexes and the Rth values were measured in the Rth setups with no buffer flow.

A difference of 2.5 Rth was observed after the removal of the negative complex from the NCD surface. This efect is rather large but can explained by the size of the phage complex that provides a high thermal resistance. Unfortunately, the reproducibility of the measurements was poor and on average only 1 Rth difference (figure 5.7). Nevertheless, the Rth measurements provided interesting results such as an increase in the Rth after binding NCD with the positive complex as compared to the negative complexes. These results were also monitored using light microscopic analysis.

To monitor the presence of phage complexes on the NCD samples at the different experimental steps in Rth measurements, the NCD samples were used in

microscopic analysis. This was done for NCD surfaces before mounting them into the Rth setup and after the Rth measurement has been completed. This way we can characterize the NCD surface and evaluate the presence of the beads that are representative for the complex.
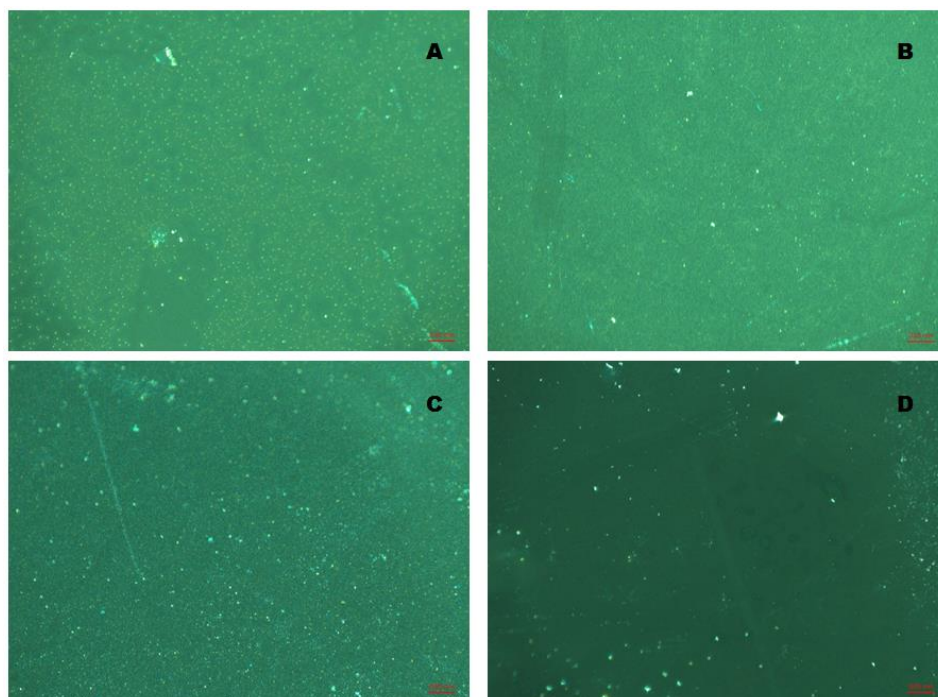
Figure 5.8 Microscopic studies on NCD samples functionalized with phage complexes

Light microscopy images of anti-human IgG immobilized NCD samples, exposed to either positive complexes, or negative complexes, before and after Rth measurements. A) NCD sample incubated with the positive complex before Rth. B) NCD sample incubated with the negative complex before Rth. C) NCD sample incubated with the positive complex after Rth. D) NCD sample incubated with the negative complex after Rth.

Figure 5.8 A and B show that before the Rth measurements the NCD sample treated with the positive complex had more beads than the NCD treated with the negative complex. This suggests the more efficient capture of the positive complex by the covalently bound anti-human IgG on the NCD, due to the presence of the

autoantibodies in the complex that had recognized the displayed UH_RA.21 autoantigenic target. However also non specific capturing or settlement of negative complexes is observed. After Rth (Figure 5.7 C,D) both NCD samples show a decrease in the amount of beads, indicating a certain degree of aspecific binding in both NCD containing positive and negative complexes. However, the NCD treated with the negative showed a significantly lower amount of beads as compared to the positive NCD sample. And once again it proves that the increased specificity of the dual displaying phage after exposure to positive control sera, and hence its ability to discriminate from negative control sera.

5.4 Discussion

Recently, the use of magnetic beads with different functionalities was applied in various sensing platforms. Aytur et al, 2006 have detected the presence of anti-dengue virus antibodies using dengue virus antigen coated magnetic beads in CMOS Hall (Complementary metal oxide semiconductors) sensors. Whiteaker JR et al, 2007 have observed a 10^3 order increase in sensitivity, when performing magnetic bead based sample purification of antibodies and peptides from complex samples. Researchers have also used nano STV magnetic beads functionalised with biotinylated antibodies or peptides and carried sample purification and concentration from stool samples and also observed higher signal in their assays (Soelberg SD et al, 2009). In this novel work, we have exploited an STV coated magnetic bead mediated sample purification of autoantibodies from patients serum samples by forming phage complexes using dual displaying phage constructions. As far as we know, there were no reports available using this kind of complex containing three elements (phage, serum autoantibodies and STV coated magnetic beads).

Dual display phage (SR21) were pre-incubated with positive control serum and negative control serum in order to prepare positive complex and negative complexes respectively. And then we have applied these somplexes onto label free and robust sensors. Using QCM-D, the physical adsorbtion of the anti human IgG to the Au crystals did show a large variablility for each sample. Different factors could be the reason for this such as sample cleaning, stearic hinderance and uneven adsorbtion of the ligand. Nevertheless the different levels of antibody

binding did not alter the efficiency or selective binding of anti human IgG to the autoantibodies in the phage bead serum complex. The positive complex always binds more than the negative complex. Different levels of anti-human IgG immobilized surfaces were used, such as more ligand bound surface for positive complex and less ligand bound surface for negative complex and vice versa. In all these cases, positive complex binds more to the surfaces and shows clear differences in both frequency and dissipation. The negative complex did show little binding and this could be due to the fact that we did not using any blockers. All Δf values for the different overtones were identical indicating a rigid layer is formed. Olsen et al, 2006 suggested a possible attractive force between the gold surface and the phage and of the phage sedimentation on the gold surface as a possible explanation for the binding of the negative complex.

Phage always show higher dissipation when immobilizing them in a vertical format (chapter four) and this is due to the continuous oscillation on the sensor surface. However, the phage used in our approach have a magnetic bead bound to the SBP phage at one end and the autoantibody UH-RA21 from the patient serum at the other end. If these phage complexes are bound to the anti IgG on the sensor surface then the heavy magnetic beads will bring down the phage to the surface and it does not allow the phage to dissipate on the sensor surface. Hence, no larger disspation has been observed. The QCM-D measurements turns out to be highly reproducible and always can discriminate positive serum complex from healthy control negative serum complexes.

The use of phage in SPR biosensor platforms is limited due to its macro size when it is immobilized as a ligand molecule, but theoretically it could be used as an analyte without any problem. The highly sensitive SPR system allows different kinds of functionalization on the chip surfaces. The most commonly used CM5 chips are available with carboxylated functional groups in a three dimensional dextran matrix. Though the binding of positive complex resulted in higher response than the negative complex over the anti-human IgG immobilized surface of CM5 chips, the observed response values are very low when considering the size of the phage complex. This may be due to the three dimensional matrix of the SPR sensor chip that prevents (steric hindrance) the binding of the phage

complex to the immobilized anti human IgG and therefore only 10% of phage complex only could bind (Hengerer A et al, 1999). May be the use of dextran matrix-free surface of the SPR Sensor Chip C1 carboxymethylated surfaces could be a solution. However results could still be compromised because of the low binding capacity of the C1 chips.

Recently, a label-free Rth sensor technique has been applied for different biomolecules such as DNA (Van Grinsven et al, 2012), surface imprinted polymer based cell assays (Eersels et al, 2015) and in measuring phase transition of lipid vesicles (Losada-Perez et al, 2014). In this study we tried for the first time to dsign a phage based assay using the Rth technology. Using the Rth method we could differentiate the positive complex (having autoantibodies) from the negative complex (no autoantibodies present). The initial Rth values of both positive complex and negative complex after binding were almost similar but when flushing with running buffer, the weakly bound negative complexes were easily removed from the NCD surface and a decrease in Rth value has been observed. Due to the final difference in the insulating layer, the Rth goes up to 10°C/W for the positive complex and 8°C/W for the negative. However on average the Rth difference was only 1°C/W. Because of the large insulating potential of the bound phage complexes this observed Rth values was unexpectedly low. Further optimization will be needed such as washing steps, optimized anti-human IgG concentration, repeated using of same NCD samples and blockers to make this method more effective for measuring phage complexes.

Taken together the results demonstrate that the use of a dual phage display system can be succesfully applied in biosensing platforms in order to qualitatively assess the presence of targets such as autoantibodies in patient serum samples. The concept of phage complex formation is usefull in sample purification or preparation from a complex serum or a blood sample or even as a pre-concentrating step. Good reproducible results were achieved using QCM-D as a sensing platform while SPR and Rth platforms need more optimization and modifications as described above in order to get reproducible results.

5.5 Conclusion

In this study we demonstrate a novel methodology for the real time monitoring and the qualitative screening of autoantibodies in patient serum samples by applying our novel dual display phage platform on QCM-D, SPR and Rth biosensing devices. The dual display consists of an SBP expressed at one end and a Rheumatoid Arthritis specific autoantigenic target at the other end of a phage. These dual displaying phage were used to bind to an RA specific autoantibody UH-RA.21 present in patient serum samples and this autoantibody-phage complex was extracted from the patient serum using STV coated magnetic beads. These so called phage complexes can be positive (from patient serum with autoantibodies present) or negative (no autoantibodies present in patient serum). The detection of autoantibodies was done using the anti-human IgG surfaces in biosensor chips. In QCM-D the autoantibodies present in the positive complex specifically bound to the anti-human IgG immobilized surfaces and this resulted into larger frequency and dissipation shifts as compared to the negative complex. In SPR manual competitive binding assays were performed and positive complexes bind more than the negative complexes. In RTH, when flushing with running buffer weakly bound negative complex were washed off from the NCD samples and an Rth gain was obtained. These results have proven that our dual display phage design can be used for the isolating of a protein of interest from complex mixtures and its use in biosensing devices could be a better alternative to the time consuming laborious phage ELISA protocols in qualitatively detecting the presence of autoantibodies in patient serum samples. In the future, this work can be taken as a reference to use this novel type of dual display as a label free diagnostic tool into rapid, highly sensitive sensing platforms for the analysis of patient serum samples.

6

General discussion, Summary
And
Nederlandstalige samenvatting

6.1 General Discussion

Since Dr. Clark presented the first biosensor in 1962, different biosensor platforms have been developed. Biosensors are defined as physicochemical analytical devices that measure the interaction between a ligand molecule and a biological component (bioreceptor). A bioreceptor molecule can be any of the following: an enzyme, an antibody, a nucleic acid, a microorganism or a cell. Bioreceptors are considered as an important component of a biosensor, since the specificity and sensitivity are depending on them. Filamentous M13 bacteriophage has been identified as a good bioreceptor molecule due to its intrinsic properties like stability in harsh environmental conditions and its ability to display target specific peptides on its surface (Mao C et al, 2009, Wu et al, 2011 and Ayela C et al, 2007). In addition, it can be applied onto a sensor surface as a probe. In the high throughput phage display approach, desired peptides could be displayed on the surface of the bacteriophage by cloning a cDNA encoding a peptide in one of the coat protein genes.

At Hasselt University, V. Somers and collaborators have identified a panel of biomarkers (autoantibodies) present in patients suffering from autoimmune diseases such as Multiple Sclerosis (MS) and Rheumatoid Arthritis (RA). These autoantibodies were detected using a pVI displayed cDNA library in M13 phages and a high throughput SAS technology (Somers K et al, 2011 and Somers V et al, 2008). These biomarkers are validated in phage ELISA protocols for disease diagnosis using patient serum samples and subsequent synthetic peptide ELISAs were developed. The above mentioned assays are limited to ELISA protocols and cannot readily be transformed into biosensor platforms. The main goal of this project is to provide a strategy in which phage displaying the relevant biomarkers could be integrated in a sensing platform, generating high sensitivity biosensors. In order to address this, we have developed a dual display phage system displaying a capturing peptide at one end of the phage in an exchangeable cassette structure and an autoantigenic biomarker at the opposite end. In this chapter, the results will be discussed based upon the research questions (problem statement) as mentioned in chapter one.

1) Can biotin like peptides serve as a good capturing peptide?

The selection of a capturing peptide is considered as a critical first step in the oriented immobilization of biomolecules on sensor surfaces and this has been elaborated on in chapter three. The well-known streptavidin (STV)-biotin system is a very strong protein-ligand interaction that is present in nature that has been successfully exploited in a number of applications including the detection of proteins, nucleic acids and lipids as well as protein purification. We used a biotin like peptide called Streptavidin binding peptide (SBP), as a capturing peptide because of its specificity to STV and its small size making it easy to display as a fusion protein (Santala V et al, 2004; Su X et al, 2005 and Kwasnikowski P et al, 2005). The recombinant biotin/ biotin like peptide tags are considered as more effective than providing an enzymatic biotin/ biotin like peptide tags on the phage (Santala V et al, 2004). The expression of SBP was evaluated using phage ELISA, dot blotting and also in label–free sensing platforms such as QCM-D and SPR. SBP displaying phage can elicit a very specific binding with STV molecules. These results make SBP a good candidate as capturing probe and it also allows for displaying phages to be immobilized as a probe onto an STV functionalized sensing platform. Hence, SBP is a good candidate capturing peptide. In order to include the possibility to introduce other capturing probes or peptides in future experiments, the SBP fusion protein is created as an exchangeable cassette like structure flanked with two unique restriction sites.

2) Can a dual display phage successfully be developed, by combining an RA biomarker displaying phagemid and a genetically fused capturing protein displaying system?

High throughput phage display technology has been traditionally designed using a phage vector or a phagemid vector system. The development of end modified dual display phage can provide a way to have phage immobilized in a vertical orientation onto solid surfaces. This way it allows the attachment of a higher number of phage and hence leading to the higher sensitivity for identifying the presence of such a biomarker. It also can be useful in sample purification processes and this objective of dual display phage development is described in chapter three. There are different dual display phage systems that have been

previously reported, Chen L. and coworkers (2004) have displayed an STV binding adapter (SBP like) in the major coat protein and a α_V integrin-targeting sequence on the minor coat protein pIII. This way they have successfully targeted the α_V integrin presence on cells in culture and in tumor-related blood vessels. Guo Y and coworkers (2010) have developed a dual display system in which gold binding peptides were presented on the pVIII coat protein while pIII was modified to display a Single Chain Variable Fragment (ScFv). In both dual display examples major coat proteins were used for the display of substrate binding peptides and minor coat proteins for the target specific peptides. Newton-Northup and coworkers (2009) have developed a dual display phage in a different way. Single displaying phage were modified chemically with a biotin group.

As a proof of principle, we have chosen to use one of the phagemid based pVI displayed autoantigenic target previously identified by the group of V. Somers, which is specific for Rheumatoid arthritis (UH_RA.21) (Somers K et al, 2011). The autoantigenic target is displayed at the coat pVI protein and therefore the display of SBP as a capturing peptide should be achieved on the opposite end of the M13 phage. For this reason pIX or pVII coat proteins are the only candidates for displaying the capturing peptide SBP. We have chosen pVII to display the capturing peptide because from literature it is known that pVII show higher stability than pIX display systems (Kwasnikowski P et al, 2005). Making use of the coat protein pVIII, which is spread all over the phage surface, would lead to the horizontal immobilization of phage over the sensor surface. This approach would occupy more sensor surface and most probably results in the immobilization of less phage and hence the sensitivity might be compromised. As a novel approach we have used a phagemid in combination a helper plasmid system instead of the usual helper phage. According to our knowledge this is the first time that a helper plasmid mediated dual display phage is used modifying pVI and pVII.

The M13cp helper plasmid system as designed by A. Bradbury and his coworkers is easy to work with and it performs the same as helper phage do in phage packaging (Chasteen L et al, 2006). This helper plasmid system contains all of the 11 genes of the M13 phage with the origin of replication (ori) for the double stranded DNA and the ori for the single stranded DNA of a phage. Moreover, it

provides only proteins to the progeny phage but not the genetic material and therefore it produces genetically pure phagemids. A genetically pure phagemid does have a smaller genome hence it produces a smaller phage than the regular phage produced via the phagemid and helper phage system. Since, SBP was introduced in the helper plasmid and the autoantigenic targets present in the phagemids both the helper plasmid and phagemid had to be transformed into the same bacterial host. We have shown that the resultant dual display phage SR21 phage displays both SBP at the pVII and the autoantigenic target at the pVI coat protein of the bacteriophage. Hence, the dual display phage construct was prepared successfully. However both the helper plasmid and phagemid carry gVI genes, resulting in the display of wild type protein coming from the helper plasmid and the autoantigenic target coming from the phagemid. This reduces the displayed copies of the autoantigenic target potentially to only one copy. This may explain why we could not detect the autoantigenic target display in a dot blotting procedure to evaluate dual display phage samples. Also the evaluation of dual displaying phage using high sensitive phage ELISA protocols on an anti-human IgG coated wells was not successful, because of the cross reactivity of the secondary antibodies with the coating antigen. So, a different strategy had to be designed. Therefore, and in view of the importance of sample preparation and purification in most biosensor approaches, we considered the use of phage, serum autoantibodies and STV coated magnetic beads based phage complexes as a good alternative. This is discussed in the following paragraphs.

3) Can we achieve sample purification from complex sample mixtures using dual display phage? Will it provide a higher sensitivity as compared to the conventional single display system?

One of the critical issues with phage based biosensor assays on serum samples is the non-specific binding of different proteins to the sensor surface. So a sample purification step is in most cases essential. Wang F and co-workers (2011) previously combined STV coated magnetic beads based sample purification and amplification of biotinylated FITC reporter molecules by nanoparticles for the fluorescent detection and the rapid identification of *Mycobacterium tuberculosis* in sputum samples. They reported 83 % higher sensitivity and 91 % higher

specificity as compared to the conventional method. In our case the targeted autoantibodies had to be isolated from the complex patient serum samples and the way we performed this is described in the last part of chapter three. This isolation of autoantibodies from the patient serum was achieved by incubating dual displaying phage SR21, carrying on one end the UH-RA.21 autoantigenic marker and on the other end SBP, with autoantibody containing patient serum. Using STV coated magnetic beads, we managed to capture the SBP carrying dual displaying phage, and to isolate the formed (bead-STV-SBP-phage-UH-RA.21-autoantibody) complex. Following this approach we successfully could detect the presence of specific autoantibodies in serum samples. This was further demonstrated using serum from patients with different levels of autoantibodies present. These are called highly positive, moderately positive and borderline positive patient serum samples. It is important to know that the presence and not the levels of anti UH-RA.21 in patient serum has a potential diagnostic value. Therefore it is important to detect autoantibodies in the most sensitive way possible and hence the effect of sample preparation was tested using phage, serum and STV coated magnetic bead based complexes.

Interestingly, the results could significantly distinguish borderline positive samples from the negative control (healthy control), which is not possible using conventional single display phage ELISA procedures. This increase in sensitivity using our approach, most probably is due to the successful sample purification from the complex serum samples containing many proteins, including antibodies. Since the dual display phage show high sensitivity in our new phage ELISA format, the next step was to apply this format into biosensing platforms to achieve a rapid, high sensitivity biosensor approach.

4) Can dual display phage be applied in a label free biosensing platform to detect autoantibodies in patient serum samples?

Although phage ELISA, and certainly the new approach we developed in the previous chapters, is considered to be a sensitive technique, it is time consuming, highly laborious and needs labeling and secondary antibodies. Previously Chen L and co-workers (2004) have successfully applied bifunctional phage displaying

pVIII-SBP like peptides and α_γ integrin targeting sequences on an SPR platform for the qualitative detection of α_γ integrin in cell suspensions. Using such label-free, real-time sensing platforms will reduce the analysis time and also may increase the assay sensitivity. As described in chapter four and five we used three high sensitive label free sensing platforms: SPR (Biacore T200), QCM-D (Q-Sense) and RTH. In parallel with our phage ELISA approach in chapter three, we have applied dual display phage onto the above sensing platforms in 2 different formats. One is comparable to the conventional ELISA approach in which a phage is immobilized on STV functionalized surfaces and the results of this approach are described in chapter four. The second approach is comparable to our new developed dual phage ELISA protocol and makes use of the previous mentioned phage complex (bead-STV-SBP-phage-UH_RA21-autoantibody) that is captured by an anti-human IgG antibody immobilized on the sensor surface. The results of this approach are reported in chapter five.

a) Phage immobilization on STV functionalized sensor surface
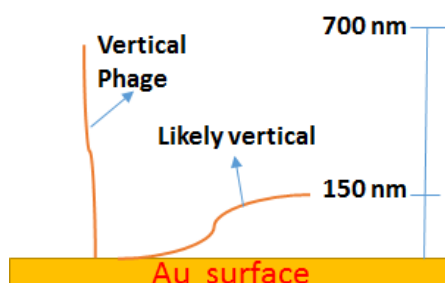
Figure 6.1 Vertical immobilization of dual display phage on a sensor surface

The first approach is comparable to the conventional Phage ELISA setup. The SBP-pVII displaying dual display phage SR21 were immobilized on the sensor surface. Schematically phage are vertically immobilized on a surface as shown on the left side in Figure 6.1 giving a total height of about 700 nm. However it is more likely that phage are oriented in a more realistic vertical orientation as is shown on the right side in Figure 6.1. This results in a phage layer of about 150 nm thickness

in which the biomarker is protruding into the solution (Malmstorm J, 2007; Voinova MV et al, 1997 and Losada-Pérez P et al, 2014). Phage immobilization has been carried on QCM-D as well as on SPR biosensor chips. QCM sensors are used to measure the nanogram level mass change over the piezoelectric quartz crystals in a given voltage and the dissipation measurements allow to study the viscoelastic properties of the biomolecules which is bound to the sensor surface.

b) Phage complex based autoantibody screening
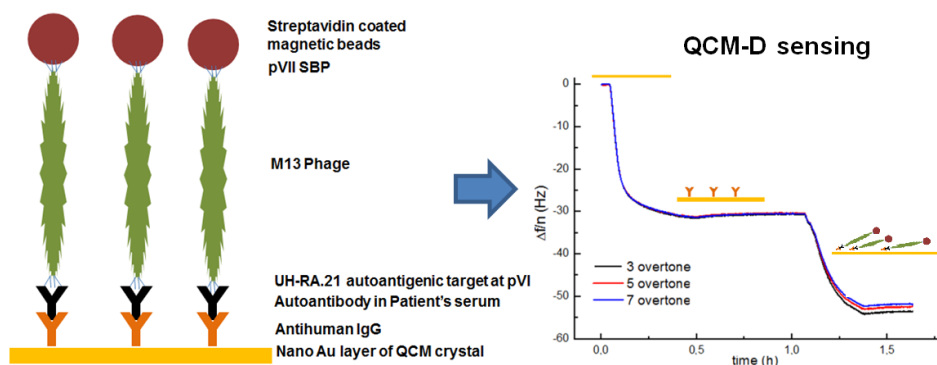
Figure 6.2 Schematic presentation of the proposed phage complex based autoantibody screening

Schematic diagram of the dual display phage sensor and the change in the frequency Δf with time upon binding of anti-human IgG and the phage complex on QCM-D.

Again, comparable to the ELISA setup in chapter three, no reproducible nor significant differences in autoantibody detection were observed between the positive and negative serum samples both in QCM and in SPR sensing devices. In this case this is mainly due to the aspecific binding or sedimentation of serum proteins and antibodies on the sensor surface. Since these sensors are label free, all proteins bound (specific or not) on the sensor surface will generate a sensor signal. As is the case in phage ELISA, also the low display level of phagemid based autoantigenic target (UH_RA21) and steric hindrance of the immobilized phage may explain the low sensitivity of this setup. More specifically, the detection limit

of the SPR system that it can only measure binding events within 200 nm from the Au surface (Tang Y et al, 2010) may decrease sensitivity. The size of the phage itself is 700 nm but it is likely to be immobilized in a layer of about 150 nm as shown in Figure 6.1. (Rajaram K et al, 2015) So the detection of autoantibodies in serum samples is close to the 200 nm limit of the detection of binding events.

Accordingly, the alternative approach developed for phage ELISA (chapter three) using a phage complex of [bead_STV-SBP_phage_UH_RA21-autoantibody] could be a good solution to in sensing platforms as well. The approach we developed is described in chapter five and a cartoon of this setup is shown in Figure 6.2. Using this approach we demonstrated that anti-human IgG adsorbed on plain gold crystals (QCM chip) can capture the phage complexes as prepared from serum samples. A significant and reproducible difference between negative control (Δf= 5 Hz) and positive control serum (Δf= 25 Hz) was observed. Though the difference was less than theoretically expected. According to Olsen and his coworkers (2006), the residual binding of a negative complex (no autoantibodies present) could occur due to the attractive forces of the phage towards Au coated sensor surface, to refractory movements of the phage in suspension due to resonator perturbations, and the tendency of phage to aggregate in solution and also by sedimentation. Besides that and in contrast with the ELISA setup no blocking reagents (e.g.: BSA) were used and also this could lead to the aspecific binding of the negative complex. Nevertheless the positive complex (393 s) binds much faster than the negative complex (713 s) to the anti-human IgG immobilized on the QCM crystals.

Using SPR, the same strategy with phage complexes was applied. Anti-human IgG was immobilized on an SPR CM5 chip and also here, positive complexes resulted in higher binding responses than the negative complexes in relay alternating binding protocols. Also in this case the observed difference in response to negative or positive samples was lower than the expected response. Hengerer et al, 1999 described that the 3D surface of SPR chips may prevent that molecules cannot bind to anti-human IgGs which are deep inside the matrix or may cause steric hindrance in binding large molecules. Also here no specific blocking agents were used in the setup

Recently a label-free biosensor technique called Rth or HTM was developed at Hasselt University (Van Grinsven et al, 2012). Rth is considered as an inexpensive, fast and label-free technology in combination with a high degree of specificity, selectivity and sensitivity. This technology measures the changes in heat-transfer resistance over a functionalized solid−liquid interface. The same approach used in SPR and QCM measurements was also applied in HTM measurements for the detection of autoantibodies in positive control samples using the phage complex based assay. HTM provided two types of results, such as higher initial Rth value for a positive complex (~ 10°C/W) than the negative complex (~ 8°C/W) and washing out of negative complex in the buffer flow from the initial baseline while the positive complex showed a constant Rth. These both types have shown a clear difference between the positive complex and negative complex by forming specific binding between the anti-human IgG and the autoantibodies in the phage complex. The washing steps need to be optimized.

Also using HTM no reproducible results could be obtained which may be partly due to the defects in the NCD samples by repeated use or cleaning and hydrogenation. Hence, a non-uniform covalent coupling of capturing antibodies was observed. On the other hand phage complexes may sediment and stick to the NCD and may interfere with the HTM signal. Additional washing steps did remove most of the sedimented beads but the hard surface of the NCD allows the beads to stay attached. Again, optimization of the protocol is required in order to obtain a reproducible response. Overall, the dual display phage system developed is a useful technological approach that could be applied in label-free sensing platforms for the qualitative screening of autoantibodies in patient serum samples using a phage complex based sample purification step.

Taken together, in this work we have successfully developed dual display phage displaying RA specific autoantigenic target (phagemid based) at one end of the phage and SBP (helper plasmid based) at the other end of phage using a two vector system. SBP served as a very good capturing entity that allows the immobilization of phage on biosensing platforms. It also allows a sample purification process using a magnetic bead based formation of a (bead-STV-SBP-phage-UH_RA21-autoantibody) phage complex. This dual display phage is

constructed as an exchangeable cassette structure and both the displayed autoantigenic target and the capturing peptide can be exchanged easily with other targets/capture sequences. The dual display phage complex provides a higher sensitivity in the newly developed ELISA approach than the conventional single display phage by significantly differentiating borderline positive samples from the healthy control serum samples. Though, it can be applied in different label free sensing platforms such as QCM-D, SPR and HTM, QCM-D served so far as a better approach for the phage based assays with good reproducible results and it also allowed to study the binding kinetics. In all experiments positive complex samples have shown higher response than the negative complexes. Thus, our novel dual display system turns out to be a good tool in the qualitative detection of autoimmune diseases.

In the future, the exchangeable dual display cassette like approach could be extended into different potential biomarkers based on pVI display system. Ultimately the approach of a multi biomarker system (dual display phage displaying different biomarkers) could be used in an array in order to provide complete diagnosis of RA. Also, it is important to consider a pVIII display of SBP to use them in sensing platforms in order to overcome the issues with its size on the SPR sensors. It is also interesting to use biomarkers in a helper plasmid based system instead of a phagemid approach. This will increase the copy number of the biomarker displayed on the phage and hence will increase the sensitivity and eventually this also reduces the size of the phage.

It is also necessary to optimize the protocols for HTM and SPR measurements in order to achieve reproducible autoantibody screening assays. For HTM or Rth based approaches, it may be interesting to apply a temperature gradient to the measurements in order to analyse the aspecificity. At the elevated temperature the weakly bound/sedimented negative complexes could be washed off easily from the NCD surface. In SPR and QCM measurements switching from micron-sized magnetic beads to nano-sized beads could reduce the observed steric hindrance and increase the number of phage complexes attached on the sensor surface. Finally optimizing the protocols is important to apply our novel developed phage

complex approach in order to develop an eventually point of care potential diagnostic tool.

6.2 Summary

Biosensors are bioanalytical devices that detect biochemical events between bioreceptor molecules and analytes on the surface of a sensor chip. There are different types of bioreceptors molecules such as enzymes, antibodies, peptides, whole cells and microorganisms that are used. Phage are considered as good bioreceptor molecules due to their unique property of displaying different target specific peptides as fusion coat proteins on their surface. Phage display has become a valuable high throughput technique in molecular biology, where it allows the display of foreign peptides by inserting cDNA of the peptide of interest in one of the coat proteins genes. Although, this technology was being exploited for displaying biomarkers for different diseases, most of the phage-based assays are carried out using phage ELISA protocols. Therefore, there is a need to develop new strategies to apply phage displaying biomarkers on biosensing platforms in order to achieve fast measuring devices with an increased sensitivity. In order to provide a solution for this, we developed a dual display phage system displaying a disease specific biomarker at one end (pVI) and a capturing protein at the opposite end (pVII) of an M13 phage using helper plasmid and phagemid systems. As a proof of concept, we used an autoantigenic biomarker (UH_RA.21) binding to autoantibodies present in patients with Rheumatoid Arthritis. Streptavidin binding protein (SBP) was used as a capturing protein.

The helper plasmid mimics a helper phage infection, but it provides only the wild type proteins to the progeny phage in the phage packaging process. Hence only recombinant phage genomes are incorporated in the produced phage resulting in genetically pure phagemid. In our dual display system, both the biomarker and the capturing protein are designed to be displayed at the opposite ends of the M13 phage. This is expected to provide a directed orientation of the resulting phage in sensing platforms with protruding biomarker phage ends. This way an increase in the sensitivity of the assay can be achieved. Our results do prove the hypothesis that the proposed dual display system provides higher sensitivity in

phage ELISA protocols when comparing to the conventional single display phage system. Indeed a significant difference between borderline positive patient serum samples and negative control serum samples could be demonstrated, while this is not possible using conventional phage ELISA approaches. Hence, our dual display system is a good alternative tool for the early stage diagnosis of the disease as described in chapter three. The proposed dual display phage based approach has been applied to different biosensing platforms. To achieve this two different strategies were used for the screening of autoantibodies in serum samples. Firstly, the dual display phage is immobilized on the surface of the sensor to capture the autoantibodies present in serum samples. Secondly a phage complex using magnetic beads was isolated from serum samples and these complexes were captured by the biosensor surface using anti-human IgG antibodies. In chapter four, real-time immobilization of phage has been monitored in rapid, label-free and high sensitive sensing platforms such as SPR and QCM-D. In the QCM-D platform STV functionalized plain gold crystals and biotinylated gold crystals were used for the immobilization of phage. In both platforms we demonstrated the efficient binding of SBP displaying phage SR 21 and SB and not the non SBP displayers (CR 21 and CB). Moreover in QCM-D, we have also confirmed that the orientation of the phage on the sensor surface is in a likely vertical orientation as deduced from the viscoelastic properties of the layer. The same pattern of results was obtained for the STV functionalized SA sensor chips on the SPR Biacore T200.

Chapter five deals with the screening of autoantibodies in positive patient serum samples using SPR, QCM-D and heat transfer resistant Rth or HTM setups. Interestingly in all experiments on the QCM-D and SPR platforms, positive patient serum complexes binds significantly more to anti-human IgG coated surfaces than the so called negative complex from negative serum samples. Also in the case of HTM or Rth, the positive complex samples produced initial a higher HTM signal on functionalized NCD as compared to the negative complex. While QCM-D measurements are highly reliable and reproducible, SPR and HTM were less reproducible. Both SPR and HTM approaches require optimization.

In conclusion, we succeeded in constructing a dual display phage system displaying an autoantigenic target at one end and a capturing peptide on the

opposite end using a phagemid and a helper plasmid based approach. The proposed dual display phage have shown high sensitivity in phage ELISA assays, allowing for the detection of autoantibodies in borderline positive patient serum samples that could not be detected in conventional phage ELISA procedures. This way the developed approach is a better alternative for the conventionally used single display based phage ELISA in the qualitative screening for autoantibodies. Since we designed the dual display phage with exchangeable cassette like displaying constructs, the exchange of both displayed peptides (capturing and biomarkers) in the future is easily achieved. Moreover, phage are easy to prepare, are inexpensive as compared to the conventional antibodies and do show a high stability.

The developed dual display phage have been applied successfully in different sensing platforms (QCM-D, SPR and HTM) and all platforms allow to discriminate between autoantibody containing serum and negative control serum samples. However the proposed phage based biosensors are not yet ready for development of a point of care diagnostic tool. But the dual display system we have reported here, can be the method of choice for such a biosensor development because our approach gives smaller than normal phage and it reduces the aspecificity by allowing sample purification from a complex mixtures and gives rise to a significant increase is sensitivity as demonstrated by the identification of borderline positive patient samples. We anticipate that these results could open exciting opportunities for the use of dual display phage in the qualitative screening for autoantibodies in the patient samples.

6.3 Nederlandstalige Samenvatting

Een biosensor is een bioanalytisch toestel dat biochemische reacties detecteert tussen bioreceptormoleculen en een analyt aan het oppervlak van de transducer. Er bestaan verschillende types bioreceptormoleculen zoals enzymen, antilichamen, peptides, ganse cellen en micro-organismen. Recent kwamen fagen onder de aandacht als potentieel goede bioreceptormoleculen aangezien zij verschillende targetspecifieke peptides op hun oppervlak tot expressie kunnen brengen. Faagdisplay wordt beschouwd als een highthroughput techniek in de moleculaire biologie. Allerhande peptides kunnen tot expressie gebracht worden door het inbrengen van cDNA van het peptide van interesse in het genoom van één van de faag manteleiwitten. Deze technologie werd gebruikt om biomerkers voor diverse ziektes tot expressie te brengen, maar de meeste faag gebaseerde testen blijven tot dusver beperkt tot ELISA's. Er is een strategie vereist om ze te integreren in een biosensorplatform met als doel snelle testen met een hoge sensitiviteit te bereiken. Om hier een oplossing voor te bieden, hebben wij in dit werk een dubbel faagdisplay systeem ontwikkeld. Deze presenteert een ziekte specifieke biomerker (pVI) aan het ene uiteinde van de faag en een capture eiwit (pVII) aan het andere uiteinde. Als een proof-of-concept hebben we gebruik gemaakt van het autoantigene target (UH_RA.21) specifiek voor rheumatoïde arthritis, eerder ontwikkeld door Prof. Somers aan de UHasselt als biomerker. Als capture eiwit maken we gebruik van het streptavidine bindend proteïne (SBP). Voor de dubbele faagdisplay werd gebruik gemaakt van een helper plasmide en faagmid systeem.

Het helper plasmide systeem bootst de helper faag na en zorgt tijdens de produktie van fagen enkel voor de aanmaak van de wild-type faageiwitten. Bijgevolg helpt dit helper plasmide systeem bij het maken van een genetisch zuivere faagmid. Bij het dubbele faagdisplay systeem worden de biomerker en het SBP gepresenteerd aan de tegenovergestelde uiteinden van de faag. Hierdoor verwachten we een goede verticale oriëntatie in een biosensor platform, hetgeen het aantal gebonden fagen op het sensoroppervlak verhoogd en bijgevolg ook de gevoeligheid van de sensor kan verhogen.

Zoals verwacht gaf ons dubbel faagdisplay systeem een hogere gevoeligheid in ELISA protocols in vergelijking met de conventionele enkele faagdisplay systemen. Dit werd bevestigd doordat een significant verschil tussen de "*borderline"* positieve serum stalen en de negatieve serum controle kon gemeten worden, hetgeen niet mogelijk is in de conventionele assays. Dit systeem kan bijgevolg gebruikt worden als een goed hulpmiddel voor een vroege opsporing van een ziekte, zoals verder wordt bediscussieerd in hoofdstuk 3. De dubbele faagdisplay biosensor werd gebruikt in combinatie met verschillende detectieplatformen. In hoofdstuk 4 gaat men verder in op de ontwikkeling van een SBP display gebaseerde faag probe. Dit werd gedaan met de *state-of-the-art* methoden SPR en QCM-D. In beide gevallen gaven SBP bevattende fagen SR21 en SB een hogere respons in vergelijking tot de SBP negatieve faagpreparaten CR 21 en CB. De faagbinding werd in *real-time* gemonitord met behulp van de hoger genoemde biosensor opstellingen. Bovendien kon met behulp van de QCM-D tevens de verticale orientatie van een faag op de STV gefunctionaliseerde sensor oppervlakken aangetoond worden. In hoofdstuk 5 werd gescreend voor de aanwezigheid van autoantilichamen in positieve serum stalen van patienten op SPR, QCM-D en in *heat transfer resistance* (Rth) opstellingen. De gevormde positieve serum complexen binden meer aan de anti-mens IgG gecoate oppervlakken in alle experimenten uitgevoerd op QCM-D en SPR. In Rth, produceren de positieve complex gefunctionaliseerde NCDs een hogere initiële respons in vergelijking met de negatieve complexen. De QCM-D resultaten waren in hoge mate reproduceerbaar en dus beter betrouwbaar in vergelijking tot de SPR en Rth data die meer optimalisatie vereisen.

Deze experimenten bevestigen dat de door ons ontwikkelde dubbele faagdisplay gebaseerde biosensor assays een beter alternatief zijn voor de conventioneel gebruikte faag ELISA om autoantilichamen in patiënten serum te screenen. Het dubbele faagdisplay platform zoals voogesteld bestaat uit een cassette structuur die op eenvoudige wijze de uitwisseling van de biomerker(s) en het capture peptide mogelijk maakt. Fagen zijn tevens gemakkelijk aan te maken, budgetvriendelijk in vergelijking met conventionele antilichamen en ze tonen een hogere stabiliteit. De faag gebaseerde sensoren zijn nog niet klaar om gecommercialiseerd te worden of om verder ontwikkeld te worden tot point of

care diagnostische testen. De grootte van de faag en zijn aspecifieke bindingskarakteristieken verlagen de kansen om het te gebruiken als specifieke affiniteitsmoleculen in sensor ontwikkeling. Het systeem dat hier gerapporteerd werd, kan fagen in sensor platformen integreren, ondermeer door het kleiner formaat in vergelijking met een normale faag en het verlaagd risico op aspecifieke binding door de opzuivering uit complexe stalen.

Het dubbele display systeem door ons voorgesteld zou in de toekomst uitgebreid kunnen worden naar verschillende biomerkers gebaseerd op het pVI display systeem. Het is ook belangrijk te overwegen om pVIII display van SBP op te zetten om een beter signaal in een SPR sensor te bereiken. De optimalisatie van de Rth en SPR platformen is nodig voor de screeningsassays van autoantilichamen. Ook zou het interessant kunnen zijn om de biomerkers in een helper plasmide gebaseerd systeem te gebruiken in plaats van een faagmid. Dit kan zorgen voor een verhoogde expressie op de faag, waardoor de gevoeligheid kan verhogen. Uiteindelijk kan een multi-biomerker systeem (dubbel faagdisplay, die verschillende biomerkers presenteert) gebruikt worden in een array voor een complete diagnose van RA.

Reference List

1. Albano SA, Santana-sahagun E, Weisman MH. Cigarette smoking and rheumatoid arthritis. Seminars in arthritis and rheumatism. 2001; 31, 3, 146.

2. Aletaha D, Neogi T, Silman AJ, Funovits J, Felson DT, Bingham CO, Birnbaum NS et al. Rheumatoid arthritis classification criteria: an American College of Rheumatology/European League Against Rheumatism collaborative initiative. Arthritis & Rheumatism. 2010; *62*(9): 2569-2581.

3. Amstutz P, Forrer P, Zahnd A, Pluckthun A. In-vitro display technologies: novel developments and applications. Current opinion in Biotechnology. 2001; 12, 400-405.

4. Arap MA. Phage display technology. Applications and innovations. Genetics and Molecular Biology. 2005;28 (1): 1−9.

5. Ayela C, Roquet F, Valera L, Granier C, Nicu L, Pugniere M. Antibody-antigenic peptide interactions monitored by SPR and QCM-D A model for SPR detection of IA-2 autoantibodies in human serum. Biosensors and Bioelectronics. 2007; 22, 3113-3119.

6. Aytur T, Foley J, Anwar M, Boser B, Harris E, Beatty PR. A novel magnetic bead bioassay platform using a microchip-based sensor for infectious disease diagnosis. Journal of Immunological Methods. 2003; 314, 21-29.

7. Azzazy HME, Highsmith W Jr. Phage Display technology: Clinical applications and recent innovations. Clinical Biochemistry. 2002; 35, 425-445.

8. Balasubramaninan S, Sorokulova IB, Vodyanoy VJ, Simonian AL. Lytic phage as specific and selective probe for detection of *Staphylococcus aureus*-A surface plasmon resonance spectroscopic study. Biosensors and Bioelectronics. 2007; 22, 948-955.

9. Bastings MMC, Helms BA, Baal IV, Hackeng TM, Merkx M, Meijer EW. From phage display to dendrimer display: Insights into multivalent binding. Journal of the American Chemical Society. 2011; 133, 6636-6641.

10. Bennett JC. The infectious etiology of rheumatoid arthritis. Arthritis & Rheumatism. 2005; 21(5): 531-538.

11. Bernal Rv, Miranda ER, Herrera-Perez G. Evolution and Expectations of Enzymatic Biosensors for Pesticides. Imtech. 2012; 12, 329-356.

12. Bers K, Eersels K, van Grinsven B, Daemen M, Bogie J, Hendriks JA, Bouwmans EE et al., Heat-Transfer Resistance Measurement Method (HTM)-Based Cell Detection at Trace Levels Using a Progressive Enrichment Approach with Higly Selective Cell-Binding Surface Imprints. Langmuir. 2014; 30, 3631 –3639.

13. Bhusan B, Kasai T, Kulik G, Barbieri L, Hoffmann P. AFM study of perfluoroalkylsilane and alkylsilane self-assembled monolayers for anti-stiction in MEMS/NEMS. Ultramicroscopy. 2005; 105, 176-188.

14. Bratkovic T. Progress in phage display: evolution of the technique and its applications. Cellular and Molecular Life Sciences. 2010; 67, 749-767.

15. Byrne B, Stack E, Gilmartin N, O'Kennedy R. Antibody based sensors: Prinicples, problems and potential for detection of pathogens and associated toxins. Sensors. 2009; 9, 4407-4445.

16. Carvalho FC, Martins DC, Santos A, Roque-Barreira MC, Beuno PR. Evaluating the equilibrium association constant between ArtnM lectin and

myeloid leukemia cella by impedimetric and piezoelectric labelfree approaches. Biosesnors. 2014; 4(4): 358-369.

17. Chasteen L, Ayriss J, Pavlik P, Bradbury ARM. Eliminating helper phage from phage display. Nucleic Acids Research. 2006; 34, 21, e145.

18. Chen H, Su X, Neoh KG, Choe Ws. QCM-D analysis of binding mechanism of phage particles displaying a constrained heptapeptide with specific affinity to SiO_2 and TiO_2. Analytical Chemistry. 2006; 78, 4872-4879.

19. Chen L, Zurita AJ, Ardelt, PU, Giordano RJ, Arap W, Pasqualini R. Design and validation of a bifunctional ligand display system for receptor targeting. Chemistry and Biology. 2004; 11, 1081-1091.

20. Cheng MS, Ho JS, Lau SH, Chow VT, Toh CS. Impedimetric microbial sensor for real time monitoring of phage infection of *Escherichia coli.* Biosensors and Bioelectronics. 2013; 47, 340-344.

21. Christiaens P, Vermeeren V, Wenmackers S, Daenen M, Haenen K, Nesladek M et al. EDC-mediated DNA attachement to nanocrystalline CVD diamond films. Biosensors and Bioelectronics. 2006; 22, 170-177.

22. Clark LC, Lyons C. Electrode system for continuous monitoring in cardiovascular surgery. Annals of the New York Academy of Science. 1962; 102(1): 29-45.

23. Daugherty PS. Protein engineering with bacterial display. Current Opinion in Structural Biology. 2007; 17, 474-480.

24. Donavan KC, Arter JA, Pilolli R, Cioffi N, Weiss GA, Penner RM. Virus- Poly (3,4-ethylenedioxythiophene) composite films for impedance based biosensing. Analytical Chemistry. 2011; 83, 2420-2424.

25. Dover JE, Hwang GM, Mullen EH, Prorok BC, Suh SJ. Recent advances in Peptide probe-based biosensors for detection of infectious agents. Journal of Microbiological Methods. 2009; 78, 10-19.

26. Dudak FC, Boyaci IH, Orner BP. The discovery of small-molecule mimicking peptides through phage display. Molecules. 2011; 16, 774-789.

27. Dultsev. FN, Speight. RE, Fiorini. MT, Blackburn. JM, Abell. C, Ostanin. OP, Klenerman. D. Direct and quantitative detection of bacteriophage by "Hearing" surface detachment using a quartz crystal microbalance. Analytical Chemistry. 2001; 73, 3935.

28. Eersels K, Van Grinsven B, Khorshid M, Somers V, Peuttmann C, Stein C et al. Heat resistant method based cell culture quality assay through the cell detection by surface imprinted polymers. Langmuir. 2015; 31(6): 2043-2050.

29. Faix PH, Burg MA, Gonzales M, Ravey EP, Baird A, Larocca D. Phage display of cDNA libraries: enrichment of cDNA expression using open reading frame selection. Biotechniques. 2004; 36, 6.

30. Fattahi MJ, Mirshafiey A. Prostaglandins and rheumatoid arthritis. Arthritis. 2012.

31. Frank R, Hargreaves R. Clinical biomarkers in drug discovery and development. Nature. 2003; 2, 566-580.

32. Gao C, Mao S, LO CHL, Wirsching P, Lerner A, Janda KD. Making artificial antibodies: A format for phage display of combinatorial heterodimeric arrays. Proceedings of National Academic Science United States of America. 1999; 6, 6025-6030.

33. Garipcan B, Caglayan MO, Demirel G. New generation biosensors based on Ellipsometry (Book chapter). New perspectives in biosensors technology and application. 2011; 9, 197-214.

34. Georgieva Y, Konthur Z. Design and screening of M13 phage display cDNA libraries. Molecules. 2012; 16, 1667-1681.

35. Gervais L, Gel M, Allain B, Tolba M, Brovka L, Zourob M et al. Immobilization of biotinylated bacteriophages on biosensor surfaces. Sensors and Actuators B. 207; 125, 615-621.

36. Goshal S, Mitra D, Roy s, Majumdar DD. Biosensors and biochips for nanomedical applications: A review. Sensors and Transducers Journal. 2010; 113(2): 1-17.

37. Green RJ, Frazier RA, Shakesheff KM, Davies MC, Roberts CJ, Tendler SJ. Surface plasmon resonance analysis of dynamic biological interactions with biomaterials. Biomaterials. 2000; 21, 1823-1835.

38. Guo Y, Liang X, Zhou Y, Zhang Z, Wie H, Men D, Luo M, Zhang XE. Construction of bifunctional phage display for biological analysis and immunoassay. Analytical Biochemistry. 2010; 396, 155-157.

39. Haes AJ, VanDuyne RP. A nanoscale optical biosensor: Sensitivity and selectivity of an approach based on the localized surface plasmon resonance spectroscopy on triangular silver nanoparticles. Journal of American Chemical Society. 2002; 124, 10596-10604.

40. Hammers CM, Stanley JR. Antibody phage display: Techniques and application. Nature. 2013; 134, e17.

41. Hassan A, Nurunnabi M, Morshed M, Paul A, Polini A, Kulia T et al. Recent Advances in Application of Biosensors in Tissue Engineering. Biomed Research International. 2014; 307519, 1-18.

42. Hengerer A, Decker J, Prohaska E, Hauck S, Koblinger C, Wolf H. Quartz crystal Microbalace (QCM) as a device for the screening of phage libraries. Biosensor and Bioelectronics. 1999; 14, 139-144.

43. Hengerer A, Kossliger C, Decker J, Hauck S, Queitsch I, Wolf H, Dubel S. Determination of phage antibody affinities to antigen by a microbalance sensor system. Biotechniques. 1999; 26, 956-964.

44. Hof D, Cheung K, Roossien HE, Pruijn GJ, Raats JM. A novel substractive Antibody phage display method to discover disease markers. Molecular Cellular Proteomics. 2006; 5(2): 245.

45. Höök F, Rodahl M, Kasemo B, Brzezinski P. Structural changes in hemoglobin adsorption to solid surfaces: Effects of pH, ionic strength, and ligand binding. Proceedings of the National Academy of Science United States of America. 1998; 95(21): 12271−12276.

46. Huang S, Li SQ, Yang H, Johnson M, Wan J, Chen I, Petrenko VA, Barbaree JM, Chin BA. Optimization of phage-based magnetoelastic biosensor performance. Sensors and Transducers. 2008; 3, 87-96.

47. Hwang I. Virus Outbreaks in Chemical and Biological Sensors. Sensors 2014; 14, 13592-13612.

48. Ionescu RE, Cosnier S, Herrmann S, Marks RS. Amperometric immunesensor for the detection of anti-west Nile virus. Analytical Chemistry. 2007; 79, 8662-8668.

49. Iqbal SS, Mayo MW, Bruno JG, Bronk BV, Batt CA, Chambers JP. A review of molecular recognition technologies for detection of biological threats. Biosensors and Bioelectronics. 2000; 15(11-12):549-78.

50. Ivnitski et al. Biosensors for detection of pathogenic bacteria. Biosensors Bioelectronics. 1999; 14, 599-606.

51. Jia J, Tang M, Chen x, Qi L, Dong S. Co-immobilized microbial biosensors for BOD estimation based on sol-gel derived composite material. Biosensors and Bioelectronics. 2003; 18, 1023-1029.

52. Jia Y, Qin M, Zhang H, Niu W, Li X, Wang L et al., Label-free biosensor: A novel phage-modified Light addressable Potentiometric Sensor system for cancer cell monitoring. Biosensors and Bioelectronics. 2007; 22, 3261-3266.

53. Johannesmann D. Viscoelastic, mechanical, and dielectric measurements on complex samples with the quartz crystal microbalance. Physical Chemistry Chemical Physics. 2008; 10, 4516- 4534.

54. Johnson ML, Wan J, Huang S, Cheng Z, Petrenko VA, Kim DJ et al., A wireless biosensor using microfabricated phage-interfaced magnetoelastic particles. Sensors and Actuators A. 2008; 144, 38-47.

55. Kierny MR, Cunningham TD, Kay BK. Detection of biomarkers using recombinant antibodies coupled to nanostructured platforms. Nano Reviews. 2010; 3, 17240.

56. Kim WJ, Choi SH, Rho YS, Yoo DJ. Biofunctionalized gold nanoparticles for surface-plasmon-absorption-based protein detection. Bull Korean chemical society. 2011; 32, 12, 4171-4175.

57. Koivunen E, Arap W, Rajotte D, Lahdenranta J, Pasqualini R. Identification of receptor ligandswith phage display receptor peptide libraries. Journal of Nuclear Medicine. 1999; 40, 883-888.

58. Kwasnikowski P, Kristensen P, Markiewick WT. Multivalent display system on filamentous bacteriophage pVII minor coat protein. Journal of Immunological Methods. 2005; 307, 135-143.

59. Lakshmanan RS, Guntupalli R, Hu J, Petrenko VA, Barbaree JM, Chin BA. Detection of *Salmonella typhimurium* in fat free milk using a phage immobilized magnetoelastic sensor. Sensors and Actuatators B. 2007; 126, 544-550.

60. Lamla T and Erdmann VA. The nano-tag, a streptavidin binding peptide for the purification and detection of recombinant proteins. Protein Expression and Purification. 2004; 33, 39-47.

61. Laricchia-Robbio L, Revoltella RP. Comparison between the surface plasmon resonance (SPR) and the quartz crystal microbalance (QCM) method in a structural analysis of human endothelin-1. Biosensor and Bioelectronics. 2004; 19, 1753-1758.

62. Lee JH, Cha JN. Amplified protein detection through visible plasmon shifts in gold nanocrystal solutions from bacteriophage platforms. Analytical Chemistry. 2011; 83, 3516-3519.

63. Lee JO, So HM, Jeon EK, Chang H, Won K, Kim YH. Aptamers as molecular recognition elements for electrical nanobiosensors. Analytical Bioanalytical Chemistry. 2008; 390, 1023-1032.

64. Liedberg B, Nylander C, Lunstrom I. Surface plasmon resonance for gas detection and biosensing. Sensors and actuators. 1983; 4, 299-304.

65. Lin Z, Wang X , Li ZJ, Ren SQ, Chen GN, Ying XT, Lin JM. Development of a sensitive, rapid, biotin–streptavidin based chemiluminescent enzyme immunoassay for human thyroid stimulating hormone. Talanta. 2008; 75, 965–972.

66. Lindstrom TM, Robinson WH. Biomarkers for Rheumatoid arthritis: making it personal. Scandinavian Journal of Clinical & Laboratory Investigation. 2010; 70(S242): 79-84.

67. Losada-Pérez P, Jiménez-Monroy K, van Grinsven B, Leys J, Janssens SD, Peeters M, Glorieux C, Thoen J, Haenen K, De Ceuninck W, Wagner P. Phase transitions in lipid vesicles detected by a complementary set of methods: heat-transfer measurements, adiabatic scanning calorimetry and quartz crystal microbalance. Physica Status Solidi A. 2014; 211(6): 1377−1388.

68. Losada-Pérez P, Khorshid M, Hermans C, Robijns T, Peeters M, Jiménez-Monroy K, Truong LT, Wagner P. Melittin disruption of raft and non-raft-forming biomimetic membranes: a study by quartz crystal microbalance with dissipation. Colloids and Surfaces B: Biointerfaces. 2014; 123, 938−944.

69. Loset GA, Sandlie I. Next generation phage display by use of pVII and pIX as display scaffolds. Methods. 2012; 58, 40-46.

70. Luong JH, Male KB, Glennon JD. Biosensor technology: Technology push versus market pull. Biotechnological Advance. 2008; 26(5): 492−500.

71. Luppa PB, Sokoll LJ, Chan DW. Immunosensors—Principles and applications to clinical chemistry. Clinical Chimica Acta. 2001; 314(1−2): 1−26.

72. Malmstrom J, Agheli H, Kingshott P, Sutherland DS. Viscoelastic Modeling of Highly Hydrated Laminin Layers at Homogeneous and Nanostructured Surfaces: Quantification of Protein Layer Properties Using QCM-D and SPR. Langmuir. 2007; 23, 9760-9768.

73. Mao C, Liu A, Cao B. Virus-Based Chemical and Biological Sensing. Angewandte Chemie. International Edition. 2009; 48, 6790-6810.

74. Marquette CA, Blum LJ. State of the art and recent advances in immunoanalytical systems. Biosensors and Bioelectronics. 2006; 21(8): 1424–1433.

75. Martínez BC, Amaya-Amaya J, Pineda-Tamayo R, Mantilla RD, H J, Bernal-Macías S, Rojas-Villarraga A, Anaya JM. Gender Differences in Latin-American Patients with Rheumatoid Arthritis. Gender Medicine. 2012; 9(6): 490-510.

76. Marx KA. Quartz crystal microbalance: A useful tool for studying thin polymer films and complex Biomolecular systems at the solution-surface interface. Biomacromolecules. 2003; 4, 5.

77. Mattheakis LC, Bhatt RR, Dower VJ. An in vitro polysome display system for identifying ligands from very large peptide libraries. Proceedings of the National Academy of Sciences of the United States of America. 1994; 91, 9022-9026.

78. Monjezi R, Tey BT, Sieo CC, Tan WS. Purification of bacteriophage M13 by anion exchange chromatography. Journal of chromatography. 2010; 848, 1835-1859.

79. Mu Y, Song D, Li Y, Zhang HQ, Li W, Luo GM, Jin QH. Selection of phage antibodies with GPX activity by combination of phage displayed antibody library with chemical modification and their characterization using a surface plasmon resonance biosensor. Talanta. 2005; 66, 181-187.

80. Nakanishi K, Sakiyama T, Kumada Y, Imamura K, Imanaka H. Recent advances in controlled immobilization of proteins onto the surface of the solid substrate and its possible applications to proteomics. Current Proteomics. 2008; 5(3), 161−175.

81. Nanduri V, Balasubramanian S, Sista S, Vodyanoy VJ, Simonian AL. Highly sensitive phage-based biosensor for the detection of β-galactosidase. Analytical Chimica Acta. 2007; 589, 166-172.

82. Nanduri V, Sorokulova IB, Samoylov AM, Simonian AL, Petrenko VA, Vodyanoy VJ. Phage as a molecular recognition element in biosensors immobilized by physical adsorption. Biosensors and Bioelectronics. 2007; 22, 986-992.

83. Nanduri V, Bhunia AK, Tu S, Paoli GC, Brewster JD. SPR biosensor for the detection of L. monocytogenes using phage-displayed antibody. Biosensors and Bioelectronics. 2007; 23, 248.

84. Nelson JL, Ostensen M. Pregnancy and rheumatoid arthritis. Rheumatic disease clinics of North America. 1997; 23(1): 195-212.

85. Newton-Northup JR, Figueroa SD, Quinn TP, Deutscher SL. Bifunctional phage –based pretargeted imaging of human prostate carcinoma. Nuclear Medicine and Biology. 2009; 36, 789-800.

86. Olsen E, Iryna B. Sorokulova b, Petrenko VA, Chen IH, Barbaree JM, Vodyanoy VJ. Affinity-selected filamentous bacteriophage as a probe for acoustic wave biodetectors of Salmonella typhimurium. Biosensors and Bioelectronics. 2006; 21, 1434 -1442.

87. Owen TW, Al-Kaysi RO, Bardeen CJ, Cheng Q. Microgravimetric immunosensor for direct detection of aerosolized influenza A virus particles. Sensors and Actuators B. 2007; 126, 691-699.

88. Park JW, Jung HS, Lee HY, Kawai T. Electrical recognition of label free oligonucleotides upon streptavidin modified, surfaces. Biotechnology and Bioprocess Engineering. 2005; 10(6): 505-509.

89. Park MK, Wikle III HC, Chai Y, Horikawa S, Shen W, Chin BA. The effect of incubation time for Salmonella Typhimurium binding to phage-based magnetoelastic biosensors. Food Control. 2013; 26, 539-545.

90. Pedura Hewa TM, Tannock GA, Mainwaring DA, Harrison S, Fecondo JV. The detection of influenza A and B viruses in clinical specimens using a Quartz crystal microbalance. Journal of virological Methods. 2009; 162(1-2): 14-21.

91. Peeters M, Csipai P, Geerets B, Weustenraed A, van Grinsven B, Gruber J, De Ceuninck W et al., Heat-Transfer-Based Detection of L-Nicotine, Histamine, and Serotonin Using Molecularly Imprinted Polymers as Biomimetic Receptors, Analytical and Bioanalytical Chemistry. 2013; 405, 6453 – 6460.

92. Petrenko VA. Landscape phage as a molecular recognition interface for detection devices. Microelectronics Journal. 2008; 39(2): 202−207.

93. Prasek J, Trnkova L, Gablech I, Businova P, Drbohlavova J, Chomoucka J et al. Optimization of planar three electrode system for three electrode system detection. International Journal Electrochemical Science. 2012; 7, 1785 – 1801.

94. Pulli. T, Hoyhtya. M, Soderlund. H, Takkinen. K. One-Step homogeneous immunoassay for small analytes. Analytical chemistry. 2005; 77, 2637.

95. Putzbach W, Ronkinen NJ. Immobilization technique in the fabrication of Nanomaterials-based electrochemical Biosensors: A review. Sensors. 2013; 13, 4811-4840.

96. Qi H, Lu H, Qiu HJ, Petrenko V, Liu A. Phagemid vectors for phage display: properties, characteristics and construction. Journal of Molecular Biology. 2012; 417, 129-143.

97. Rajaram K, Vermeeren V, Somers K, Somers V, Michiels L. Construction of a helper plasmid-mediated dual-display phage for autoantibody screening in serum. Applied Microbiology and Biotechnology. 2014; 98(14): 6365−6373.

98. Rapp BE, Gruhl FJ, Länge K. Biosensors with label free detection designed for diagnostic applications. Analytical and Bioanalytical Chemistry. (2010); 398, 2403-2412.

99. Redeker ES, Ta DT, Cortens D, Billen B, Guedens W, Adriaensens P. Protein engineering for directed immobilization. Bioconjugate Chemistry. 2013; 24, 1761-1777.

100. Reynolds F, Panneer N, Tutino CM, Wu M, Skrabal WR, Moskaluk C, Kelly KA. A functional proteomic method for biomarker discovery. Plos ONE. 2011; 6(7): e227471.

101. Rich RL, Myszka DG. Higher-throughput, label-free, real-time molecular interaction analysis. Analytical Biochemistry. 2007; 36(1): 1−6.

102. Rickert J, Weiss T, Kraas W, Jung G, Gopel W. A new affinity biosensor: Self assembled thiols as selective monolayer coatings of quartz crystal microbalances. Biosensors and Bioelectronics. 1996; 11(6/7): 591-598.

103. Roy MD, Stanley SK, Zmis EJ, Becker ML. Identification of a highly specific Hydroxyapatite-binding peptide using phage display. Advanced Materials. 2008; 20, 830-1836.

104. Saerens D, Huang L, Bonroy K, Muyldermans S. Antibody fragments as probe in Biosensor development. Sensors. 2008; 8, 4669-4686.

105. Sagle LB, Ruvuna LK, Ruemmele JA, Van Duyne RP. Advances in localized surface plasmon resonance spectroscopy biosensing. Nanomedicine. 2011; 6(8): 1447-1462.

106. Sandberg T, Carlsson J, Ott MK. Interactions between human neutrophils and mucin-coated surfaces. Journal of Material Science and Materials in Medicine. 2009; 20(2): 621−631.

107. Santala V, Lamminmäki U. Production of a biotinylated single chain antibody fragment in the cytoplasm of *Escherichia coli*. Journal of Immunological Methods. 2004; 284, 165-175.

108. Sauerbrey G. The use of oscillators for weighing thin layers and microweighing. Zeitschrift für Physik. 1959; 155 (2): 206-222.

109. Scott JK, Smith GP. Searching for peptide ligands with an epitope library. Science. 1990; 249, 386-390.

110. Serizawa T, Matsunao H, Sawada T. Specific interfaces between synthetic polymers and biologically identified peptides. Journal of Materials Chemistry. 2011; 21, 10252.

111. Sheets. MD, Amersdorfer. P, Finnern R, Sargent. P, Lindqvist. E, Schier. R, Hemingsen. G, Wong. C et al. Efficient construction of a large nonimmune phage antibody library: The production of high-affinity human single-chain antibodies to protein antigens. Proceedings of the National Academy of Sciences of the United States of America. 1998; 95, 6157.7.

112. Sidhu SS. Engineering M13 for phage display. Biomolecular Engineering. 2001; 18, 57-63.

113. Sidhu SS. Phage display in pharmaceutical biotechnology. Current Opinion in Biotechnology. 2000; 11, 610-616.

114. Simon BP, Saint C, Voelcker NH. Electrochemical biosensor featuring oriented antibody immobilization via electrografted and self-assembled hydrazide chemistry. Analytical Chemistry. 2014; 86(3): 1422–1429.

115. Singh A, Somayyeh P, Evoy S. Recent advances in bacteriophage based biosensors for food-borne pathogen detection. Sensors. 2013; 13(2): 1763−1786.

116. Smolen JS, Steiner G. Therapeutic strategies for rheumatoid arthritis. Nature Reviews Drug Discovery. 2003; 2(6): 473-488.

117. Soelberg SD, Stevens RC, Limaye AP, Furlong CE. Surface plasmon resonance (SPR) detection using antibody –linked magnetic particles for analyte capture purification, concentration and signal amplification. Analytical Chemistry. 2009; 81(6): 2357-2363.

118. Soendegaard M, Newton-Northup JR, Palmier MO, Deutscher SL. Peptide phage display for discovery of novel biomarkers for imaging and therapy of cell subpopulations in ovarian cancer. Journal of Molecular Biomarkers and Diagnosis. 2011; S2:004.

119. Somers K, Geusens P, Elewaut D, De Keyser F, Rummens JL, Coenen M, Blom M, Stinissen P, Somers V. Novel autoantibody markers for early and seronegative rheumatoid arthritis. Journal of Autoimmunity. 2011; 36, 33–46.

120. Somers K, Govarts C, Stinissen P, Somrs V. Multiplexing approaches for autoantibody profiling in multiple sclerosis. Autoimmunity reviews. 2009; 8(7), 573-579.

121. Somers K, Stinissen P, Somers V. Optimization of high throughput autoantibody profiling for the discovery of novel antigenic targets in Rheumatoid arthritis. Annals of the New York Academy of Sciences. 2009; 1173, 92–102.

122. Somers V, Govarts C, Hellings N, Hupperts R, Stinissen P. Profiling the autoantibody repertoire by serological antigen selection. Journal of Autoimmunity. 2005; 25, 223-228.

123. Somers V, Govarts C, Somers K, Hupperts R, Medaer R, Stinissen P. Autoantibody profiling in multiple sclerosis reveals novel antigenic candidates. The Journal of Immunology. 2008; 180, 3957-3963.

124. Sorensor AE, Askin SP, Schaeffer PM. In-gel detection of biotin-protein conjugates with a green fluorescent streptavidin probe. Analytical methods. 2015; 7, 2087-2092.

125. Stoler E, Warner JC. Non-Covalent Derivatives: Cocrystals and Eutectics. Molecules. 2015; 20, 14833-14848.

126. Su X, Wu YJ, Robelek R, Knoll W. Surface plasmon resonance spectroscopy and Quartz Crystal Microbalance study of streptavidin film structure effects on biotinylated DNA assembly and target DNA hybridization. Langmuir. 2005; 21, 348-353.

127. Swann MJ, Peel LL, Carrington S, Freeman NJ. Dual-polarization interferometry: an analytical technique to measure changes in protein structure in real time, to determine the stoichiometry of binding events, and to differentiate between specific and nonspecific interactions. Analytical Biochemistry. 2004; 329, 190–198.

128. Neufeld. T, Mittelman. AS, Buchner. V, Rishpon. J. Electrochemical Phagemid Assay for the Specific Detection of Bacteria Using Escherichia coli TG-1 and the M13KO7 Phagemid in a Model System. Analytical Chemistry. 2005; 77, 652.

129. Tang Y, Zeng X, Liang J. Surface plasmon resonance: An introduction to a surface spectroscopy technique. Journal of Chemical Education. 2010; 87 (7): 742-746.

130. Tolba M, Minikh O, Brovko LY, Evoy S, Griffiths MW. Oriented immobilization of bacteriophages for biosensor applications. Applied Environmental Microbiology. 2010; 76(2): 528−535.

131. Tothill IE. Biosensors for cancer markers diagnosis. Seminars in Cell & Developmental Biology. 2009; 20, 55–62.

132. Turner APF. Biosensors: Sense and sensibility. Chemical Society Reviews. 2013, 42(8): 3175-3648.

133. Turner APF. Biosensors: Sense and sensitivity. Science. 2000; 290, 5495, 1315.

134. Ulman A. Formation and structure of self-Assembled monolayers. Chemical Review. 1996; 96, 1533-1554.

135. Uttenthaler E, Schraml M, Mandel J, Drost S. Ultrasensitive quartz crystal microbalance sensors for detection of M13-Phages in liquids. Biosensors and Bioelectronics. 2001; 16 (9-12): 735-743.

136. Van Grinsven B, Vanden Bon N, Strauven H, Grieten L, Murib M, Jiménez Monroy et al. Heat-Transfer Resistance at Solid–Liquid Interfaces: A Tool for the Detection of Single-Nucleotide Polymorphisms in DNA. ACS Nano. 2012; *6*(3): 2712-2721.

137. Velappan N, Fisher HE, Pesavento E, Chasteen L, Angelo SD, Kiss C, Longmire M, Pavlik P, Bradbury ARM. A comprehensive analysis of filamentous phage display vectors for cytoplasmic proteins: an analysis with different fluorescent proteins. Nucleic Acids Research. 2010; 38, 4, e22.

138. Vithayathil R, Hooy RM, Cocco MJ, Weiss GA. The scope of phage display for membrane proteins. Journal of Molecular Biology. 2011; 414, 499-510.

139. Voinova MV, Jonson M, Kasemo B. Dynamics of viscous amphiphilic films supported by elastic solid substrates. Journal of Physics and Condensed Matter. 1997; 9(37): 7799−7808.

140. Wan J, Johnson ML, Guntupalli R, Petrenko VA, Chin BA. Detection of *Bacillus anthracis* spores in liquid using phage-based magnetoelastic micro-resonators. Sensors and Actuators B. 2007; 127, 559-566.

141. Wang H, Zhao C, Li F. Rapid identification of *Mycobacterium tuberculosis* complex by a novel hybridization signal amplification method based on self-assembly of DNA-Streptavidin nanoparticles. Brazilian Journal of Microbiology. 2011; 42, 964-972.

142. Wang KC, Wang X, Zhong P, Luo PP. Adapter directed display: A modular design for shuttling display on phage surface. Journal of Molecular biology. 2009; 395, 1088-1101.

143. Weissmann G. The pathogenesis of rheumatoid arthritis. Bulletin-hospital for Joint Diseases New York. 2006; 64(1/2): 12.

144. Whitaker JR, Zhao L, Zhang HY, Feng LC, Piening BD, Anderson L, Paulovich AG. Antibody-based enrichment of peptides on magnetic beads for mass-spectrometry-based quantification of serum biomarkers. Analytical Biochemistry. 2007; 362, 44-54.

145. Williams OR. What Have We Learned about the Pathogenesis of Rheumatoid Arthritis from TNF-Targeted Therapy? ISRN Immunology. 2012; 652739.

146. Wu J, Cropek DM, West AC, Banta S. Development of a Troponin I. Biosensor Using a Peptide Obtained through Phage Display. Analytical Chemistry. 2010, 82, 8235–8243.

147. Xing Y, Chaudry Q, Shen C, Kong KY, Zhau HE, Chung LW et al. Bio-conjugated quantum dots for multiplexed and quantitative immunohistoche- mistry. Nature protocols. 2007; 2(5): 1152-1165.

148. Yang. LMC, Diaz. JE, McIntire. TM, Weiss. GA, Penner. RM. Covalent virus layer for mass-based biosensing. Analytical Chemistry. 2008; 80, 933.

149. Yao L, Hajj-Hassan M, Ghafar-Zadeh E, Shabani A, Chodavarapu V, Zourob M. CMOS Capacitive Sensor System for Bacteria Detection using Phage Organisms. Proceedings of IEEE Canadian Conference on Electrical and Computer Engineering, Niagara Falls, ON, Canada. 2008; 877-880.

150. Yogeswaran U, Chen SM. A review on the electrochemical sensors and biosensors composed of nanowires as sensing material. Sensors. 2008; 8, 290-313.

151. Yoo EH, Lee SY. Glucose Biosensors: An Overview of Use in Clinical Practice. Sensors. 2010; 10, 4558-4576.

152. Zhu H, White IM, Suter JD, Fan X. Phage based label free biomolecule detection in an opto fluidic ring resonator. Biosensors and Bioelectronics. 2008; 24, 461-466.

Curriculum vitae
Academic qualifications

Kaushik Rajaram completed his higher secondary school (1995-2001) at SVV Higher secondary School, Kullursandai, India. He attended Thiagarajar College, Madurai, India, affiliated to the Madurai Kamarajar University from 2002-2005 and 2005-2007 and obtained bachelors in Industrial Microbiology and Masters in Microbiology in the respective years. He pursued his master thesis under the guidance of Prof. Dr. A. Arun and the thesis entitled as "Optimization study on production of Lovastatin (anti-cholesterol agent) from *Aspergillus terreus* and Basidiomycetes fungi".

He started his career as a project assistant at the Indian Institute of Science, Bangalore, India, under the supervision of principal research scientist Dr. HN. Vasan in the department of Solid State Structural Chemistry (2008-2010). He carried out two different research projects there, such as Antimicrobial activity of nanoparticles and E-DNA biosensor preparation for the diagnosis of filariasis. He, also completed a certificate course on proteomics at the Indian Institute of Science in the year 2009.

In 2010, he started his PhD, at Hasselt University, Belgium in the School of Life Science and Medicine under the supervision Prof. Dr. Luc Michiels. It was completed in 2014, with a PhD thesis entitled "Construction of dual display phage system and its applications on real-time label-free biosensing platforms".

Bibliography

Publications related to this dissertation

Real time analysis of dual display phage immobilization and autoantibody screening using quartz crystal microbalance with dissipation monitoring. **Kaushik Rajaram,** Patricia Losada-Pérez, Veronique Vermeeren, Baharak Hossenikhani, Patrick Wagner, Veerle Somers, Luc Michiels. ***International journal of nanomedicine***. (IF- 4.38)

Construction of a helper plasmid-mediated dual-display phage for autoantibody screening in serum. **Kaushik Rajaram**, Veronique Vermeeren, Klaartje Somers, Veerle Somers and Luc Michiels ***Applied Microbiology and Biotechnolology.* 2**014; 98(14): 6365−6373. (IF 3.8)

Conference paper

Real-time analysis of dual display phage immobilization and qualitative screening for Rheumatoid Arthritis specific autoantibodies in serum sample Using QCM-D sensor platform. **Biomedica Summit 2015, Genk, Belgium. Kaushik Rajaram,** Patricia Losada-Perez, Veronique Vermeeren, Baharak Hossenikhani, Patrick Vagner, Veerle Somers, Luc Michiels.

Other publications

Optical, Field-Emission, and Antimicrobial Properties of ZnO Nanostructured Films Deposited at Room Temperature by Activated Reactive Evaporation D Yuvaraj, **R Kaushik,** and K. Narasimha Rao. ***ACS Appl. Mater. Interfaces***, 2010, 2(4), pp1019−*1024* (IF 6.2)

Antimicrobial activity of highly stable silver nanoparticles embedded in agar–agar matrix as a thin film. S. Ghosh, **R. Kaushik**, K. Nagalakshmi , S. L. Hoti , G. A. Menezes, B. N. Harish , H. N. Vasan. ***Carbohydrate Research*** *345 (2010) 2220–2227* (IF 2.8)

Optimisation of an asymmetric polymerase chain reaction assay for the amplification of single-stranded DNA from *Wuchereria bancrofti* for electrochemical detection Vasuki V, Sugeerappa L H, Nagalakshmi K, Somnath G, **Kaushik** R. ***Mem Inst Oswaldo Cruz***, **Rio de Janeiro**, Vol. *108*(6): 804-807, September 2013 (IF 1.7)

Antimicrobial activity of recombinant defensin BBD126 while induced sitedirected mutation at different cysteine positions. Fernando NM, **Kaushik R**, Kieran M, Ken M, Cliona OF. Under preparation

Poster presentations

Real-time analysis of dual display phage immobilization and qualitative screening for Rheumatoid Arthritis specific autoantibodies in serum sample Using QCM-D sensor platform. Biomedica Summit 2015, Genk, Belgium**.**

Kaushik Rajaram, Patricia Losada-Perez, Veronique Vermeeren, Baharak Hossenikhani, Patrick Vagner, Veerle Somers, Luc Michiels.

Dual display phage construct for the diagnosis of rheumatoid arthritis" in Label free technologies congress 2012, Amsterdam, The Netherland.

Kaushik Rajaram, Veronique Vermeeren, Klaartje Somers, Veerle Somers and Luc Michiels.

Bifunctional phage sensor in the diagnosis of multiple sclerosis" in Biomedica summit 2012, Liege, Belgium.

Kaushik Rajaram, Veronique Vermeeren, Klaartje Somers, Veerle Somers and Luc Michiels.

Antimicrobial activity of highly stable silver nanoparticles embedded in agar-agar thin film" on the felicitation of SSCU Unit Day 2008 at IISc, Bangalore, India.

Kaushik Rajaram, Somnath Ghosh, Nagalakshmi Kamaraj, Subash Lakshmana Hoti, Hasan Narasimma Vasan.

Acknowledgement

It is a moment of being thankful and pride to look back with a deep sense of fulfillment and gratitude at the long path I have come across. I would like to capture some of the golden moments, to be able to thank the infinite number of people whose love and blessing have made this day possible for me.

"Motivation is what gets you started. Habit is what keeps you going." --

Jim Ryun-

Here, I remember my mother who sow seeds of motivation in me and my family who made me to achieve those. Here, I pay tributes to the almighty and thy representatives, my family and teachers for showering their infinite bounties, graces and mercies upon me and for lifting me up till this phase of life. I revere them for their love, trust, patience and support, and of course, for bearing all kind of stresses, they could, to make me what I am. I owe everything to them.

I would like to convey my sincere thanks to my research promoter Prof. Dr. Luc Michiels for spending his valuable time to impart me the gains of his knowledge. He guided my efforts to maintain a focus on critical thinking that directed my interest in scientific research. His insights, careful attention to details and experience has helped to maintain the level of quality of my work. His active guidance helped me to develop skills and insight in research procedures, scientific writing and communication. His caring attitude always enlightened the way during my research. Unconditional support in purchasing materials for the research, indeed helped me to design my work in SPR and QCM. It was a great experience to have worked under his apt and sound guidance. It has been an honor to be his student.

Here by, I privileged to thank my co-promoter Prof.Dr. Veerle Somers for her sincere supervising and giving freedom in phage lab to explore myself. I have got expertise in phage display technology and which helped me in getting my first job before finishing my PhD. I have learned good laboratory practice (GLP) from the phage lab.

I take this opportunity to sincerely thank Dr. Veronique Vermeeren, who is my supervisor and being so nice with me, spent lot of time with my every abstracts, multiple versions of my manuscripts, posters and helped me in designing the work. And I always remember your visits to my home and you gave a letter for my parents to visit me in Belgium. Dr. Klaartje Somers, you are so good in answering my questions and you have helped me in planning my work. In a way, they have been the driving force behind the endeavor.

I sincerely thank all the faculty members of BIOMED and IMO-IMECH especially Prof. Dr. Patrick Wagner, who is so kind with me and allowing me to his labs and asking his students to help me in every experiments I carried out in IMO-IMECH. Dr. Patricia, Dr. Mohammed, Prof. Bart and Ms. Kathiya you guys are wonderful, you helped me a lot. Especially Dr. Patricia, because of you I could have achieved some good results in QCM. And the technicians of BIOMED, especially Mrs. Igna Rutten a wonderful human being, she helped me a lot in the labs, and you are the encyclopedia of BIOMED and you are awesome. And Mrs. Regine, Ms. Lotte for their help in the lab.

I would like to express the deep sense of reverence for the members of Biosensors group who shares the lab and office room, Dr. Natalie Vonden Bon, Dr. Karoline Deprez, Dr. Katrijn Vanschonbeek, Ms. Evi Vanoppan and Dr. Jeroen Vanbrabant,

Revathy, Soren, Dr. Baharak you guys made every moment very pleasant and lively. The discussions we made in group meetings and in informal discussions at the office and lab helped a lot in shaping the talent I acquired. Also, I thank phage display group colleagues Hung Anh, Myrthe, Liesbeth, Laura, Ilse, Nile, Dr. Wendy and Dr. Judith for their support and sharing of reagents with me. All non-teaching/ research staff especially Agnes, Ilse, Veronique, Rani, and Hilde for extending help and co-operation.

It will not be complete if I miss Yaso, Sathya, Babu, Ambili, Anurag, Gopala, Priya, Sankaran, Meena, Revathy, Heman, Laxmana and Sujitha who created my home in a foreign land. My time in Belgium was happy in large part due to many friends I shared my life with. I am especially thank Yaso, Babu, Sathya and Ganapathy you guys took care of me from the day one to till date, no words to express my gratitude. I am remembering major students Theophilus, Mehran and Josephin who helped me in lab and the conversations we made in the cafeteria of BIOMED every day.

I take this opportunity to sincerely thank the foreign colleagues of BIOMED Hung Anh, Stelios, Ariel, Pia, Ambili, Anurag, Giovanni and Derbhaila with whom, I spent many of my parties and weekends. You guys gave me a wonderful time all these years. My vocabulary fells short to expresses my gratitude towards Mr Sudhakar and family. You are awesome, the support and help provided by you are incredible. And my Torenstraat housemates Lien, Wim, Jan, Jonathan, Barbara, Alesandra, Jarno who shared food, house and friendship.

In the end, I am wordless to express my heartfelt feelings for my better half, Vidhya, who was with my side whenever I had tough times and gave her shoulders to push me up. The unconditional support, motivation and inspiration what you gave are the driving force to achieve this level. My dear baby Shravika you are my energy tonic, whenever I see you, I felt so light, a relieved from my stress.

I would like to express my sincere gratitude to my advisor Prof. Dr. Luc Michiels for the opportunity he gave me. It has been an honor to be his PhD student. He gave me continuos support and more importantly, inspiration. A big thanks that he allowed me to join in an another job before I finished my PhD. I thank him for the freedom to develop our scientific project and interesting scientific discussions. I also thank for his valuable time that he invested in correcting my manuscripts and valuable suggestions and guidance throughout my PhD.

I thank Hasselt University, and the people of Belgium for the funding for my PhD and wonderful supportive life in Belgium. I also thank VIB for providing different training programs to excel my skills.

I should thank Prof. Dr. Cliona O'Farrelly of Trinity college Dublin, Ireland for accepting me in her lab and allowing me to learn different techniques in a short span of time. Current and past members of Biosensors group, forensic team and phage display group at Biomedical research institute UHasselt have been a source of friendship and collaboration.

I thank all the members of the jury who critically read my manuscript and provided insightful comments. Lastly I would like to thank my family for their love and

support. I especially thank my parents who raised me with love for knowledge, perseverance and hard work. This helped me to move on during my PhD.

Thank you

Kaushik

March, 2016